Techniques for solving two-loop massive Feynman integrals

Dissertation
zur Erlangung des Grades
“Doktor
der Naturwissenschaften"
am Fachbereich Physik, Mathematik und Informatik
der Johannes Gutenberg-Universität
in Mainz

Ekta
Geboren in Siswa Gopal

Mainz, 19th August 2019

Supervisor:

2nd supervisor:

Date of dissertation: **24th October 2019**

ABSTRACT

The Large Hadron Collider (LHC) is dedicated to the task of performing high energy scattering collisions. The success of the physics program at the LHC also demands high precision of theoretical predictions. We need to calculate multi-loop scattering amplitudes in perturbative quantum field theory to obtain precise theoretical predictions. Feynman integrals are the building blocks for scattering amplitudes and therefore the calculation of scattering amplitudes at higher orders in perturbation theory also requires a deep understanding of multi-loop Feynman integrals. Now is the age when we need to evaluate two-loop corrections to processes with massive particles, like the top quark and the electroweak bosons. The calculation of two-loop Feynman integrals with masses, using the available tools, often turns out to be a difficult task. The algebraic structure of the Feynman integral has proven to be a great help in computing these integrals. In practice, we use the method of differential equations to solve a particular Feynman integral. We can exploit the properties of dimensionally regulated integrals to find a basis of integrals which we call the master integrals. Solving these master integrals correspond to solving the Feynman integral. The use of a particular 'canonical form' makes the solution of the differential equation for the master integrals simpler and lets us immediately write them down in terms of iterated integrals at all orders in the dimensional regularization parameter. In the case of mostly massless processes, the integrals are known to evaluate to a special class of functions known as the multiple polylogarithms. This is not true starting from two loops. The simplest single scale example for this case is given by the very famous sunrise integral which is known to contain an elliptic curve and needs elliptic generalizations of multiple polylogarithms in order to write down the solution.

In this work, we present two examples of Feynman integrals which depend on multiple scales. The first one is the planar double box integral with a closed top loop, which is required for the top-pair production. This integral enters the next-to-next-to-leading order (NNLO) contribution for the process $pp \to t\bar{t}$ and was a bottleneck for a long time. The system of differential equations for the double box integral is governed by three different elliptic curves, which originate from different sub-topologies. In order to solve the differential equation satisfied by the master integrals in this case, we use the factorization properties of the Picard–Fuchs operator associated with the 'elliptic' topologies to bring down the system of differential equation to the one coupled in blocks of sizes 2×2 at worst, at order ϵ^0. We also use the linear form for the differential equation in order to solve the system as iterated integrals in the dimensional regularization parameter conveniently. The other example presented is that of the two-loop master integrals relevant to mixed QCD-EW corrections to the decay $H \to b\bar{b}$ through a $Ht\bar{t}$ coupling. This has been done keeping full dependence on the heavy particle masses (m_t, m_H and m_W), but neglecting the b-quark mass. In this case, the system of differential equations for the master integrals can be brought to the canonical form and the master integrals can be expressed entirely in terms of multiple polylogarithms.

Publication-list on which this work is based

List of journal publications:

1. **Simplifying Differential Equations for Multiscale Feynman Integrals beyond Multiple Polylogarithms**
   L. Adams, E. Chaubey and S. Weinzierl,
   Phys. Rev. Lett. **118** (2017) no.14, 141602

2. **Planar Double Box Integral for Top Pair Production with a Closed Top Loop to all orders in the Dimensional Regularization Parameter**
   L. Adams, E. Chaubey and S. Weinzierl,
   Phys. Rev. Lett. **121** (2018) no.14, 142001

3. **Analytic results for the planar double box integral relevant to top-pair production with a closed top loop**
   L. Adams, E. Chaubey and S. Weinzierl,
   JHEP **1810** (2018) 206

4. **Two-loop master integrals for the mixed QCD-electroweak corrections for $H \to b\bar{b}$ through a $Ht\bar{t}$-coupling**
   E. Chaubey and S. Weinzierl,
   *JHEP***1905** (2019) 185

List of conference proceedings:

1. **From elliptic curves to Feynman integrals**
   L. Adams, E. Chaubey and S. Weinzierl,
   PoS LL **2018** (2018) 069

2. **Differential equations for Feynman integrals beyond multiple polylogarithms**
   L. Adams, C. Bogner, E. Chaubey, A. Schweitzer and S. Weinzierl,
   PoS RADCOR **2017** (2017) 015

Contents

1 Introduction

Contents

> "The world" is something like a great chess game being played by the Gods, and we are observers of the game. We do not know what the rules of the game are; all we are allowed to do is to watch them playing. Of course if we watch long enough, we may eventually catch on to a few of the rules. The rules of the game are what we mean by fundamental physics. -Richard Feynman.

Our most ambitious and organized efforts to understand what the world around us is made up of has given us the best candidate for particle physics: "The Standard Model (SM)" which has been verified to all extent by our present-day experiments. It has been able to predict the existence of several particles, the most recent one to be confirmed was the infamous Higgs boson. However, we have now also come to the conclusion that this cannot be the ultimate model as it lacks many important aspects. There exist very significant signals that the SM is incomplete. The most concrete evidence comes from astrophysical and cosmological observations. The vacuum energy density crisis, presence of too many fundamental parameters, the inability of incorporation of the most fundamental interaction, namely gravitation, and the matter-antimatter asymmetry are few of the most famous problems which point to further deficiencies of the SM. More evidence comes from the results confirming the existence of dark energy and dark matter, some other intriguing manifestations of physics beyond the Standard Model (BSM).

Deviations from SM prediction is believed to be a strong signal for the existence of BSM physics. The Large Hadron Collider (LHC) at Cern is dedicated to the task of performing precision measurements of high energy scattering of particles, which may be sensitive to BSM physics.

The experimental signals are not able to distinguish BSM physics with the SM mediated scattering processes. Experimentally, a way to handle this situation is the inference of signals based on statistical analysis, by measuring an excess of events with respect to the predicted frequency of occurrence by SM. On the theoretical side, a successful interpretation of precision measurements requires accurate predictions of SM contributions of observable quantities in scattering processes, for example, cross sections and decay rates. Therefore performing calculations using the SM gives us a very good basis to start our future efforts on.

The most robust theoretical framework for particle physics is provided by the relativistic quantum field theory (QFT). The possible interactions in quantum field theory are governed by few basic principles: locality, symmetry, and renormalization group flow which make QFT the most concrete framework for the interaction of particles: given a set of fields there is very often an almost unique way to couple them together. The term “Standard Model" basically stands for a quantum field theory based on the gauge group $SU(3)\otimes SU(2)\otimes U(1)$. $SU(3)$ is the gauge group for the Quantum Chromodynamics (QCD) whereas $SU(2)\times U(1)$ is the symmetry group under which the gauge transformations of unified electromagnetic and weak interactions (EW) remain invariant. The full symmetry, in this case, has to be broken by the Higgs mechanism down to the electromagnetic gauge symmetry in order to give masses to the $W^{\pm}$, Z bosons. The minimal formulation, which is the SM, requires a single Higgs field which is a doublet under $SU(2)$. Since we are interested in scattering processes at high energy, a scale at which all coupling constants are small, perturbation theory presents itself as a valuable tool to obtain predictions from the theory systematically. In this framework, observables are expanded as a series in powers of small coupling constants, with individual orders expressed in terms of a bunch of Feynman diagrams.

1.1 Road map of the thesis

Computing scattering processes to higher orders in perturbation theory requires a deeper understanding of ‘multi-loop Feynman integrals’ and further refinement of the mathematical techniques used to evaluate them. The thesis discusses the innovative ideas to tackle complicated multi-scale Feynman integrals along with shedding light upon the wonderful breakthroughs in the field of multiple-loop calculations going beyond the class of integrals which evaluate to a well-known class of function: the multiple polylogarithms (MPLs).

The thesis is divided into 7 chapters with each chapter being informative and complete on its own. In the very first chapter, we briefly discuss the connection of scattering amplitude computations in quantum field theory with Feynman integrals. We also try to cover the beautiful structure of Feynman integrals and various famous methods to evaluate them. In chapter 2 we take a small detour from the evaluation to Feynman integrals to getting an overview of techniques of evaluating scattering amplitudes and physical observables, like cross section and decay rates, along with learning about the state of the art and the hindrances and bottlenecks of the field. This puts the important and technical world of multi-loop Feynman integral computations into the bigger framework of scattering amplitudes. MPLs have proven to be an amazingly successful class of functions to describe many scattering processes [9–11]. However, MPLs do not exhaust the space of functions to which Feynman integrals evaluate. It has now been known from decades that starting from two loops, not all Feynman integrals evaluate to MPLs [13, 14] and we need elliptic generalizations to span the function space of these integrals. Elliptic obstructions were already registered during the evaluation of massive Feynman diagrams more than 50 years ago by Sabry [110]. In physics community, the study of elliptic integrals started to gain momentum with

the work of Laporta and Remiddi [15], where they presented the result of the sunrise diagram as complete elliptic integrals of the first kind with suitable arguments. Bloch and Vanhove in 2013 [16] further revolutionized this field by expressing the sunrise integral through a generalization of the dilogarithm to an elliptic curve. This study revolutionized the field of evaluation of Feynman integrals containing elliptic curves. We have seen a lot of progress in the study of such Feynman integrals since then, which led us to some very fascinating results, some of which can be found in [17–26]. Some of the results involve new classes of transcendental functions, related either to elliptic generalizations of MPLs [27] or iterated integrals of modular forms [73]. Chapter 3 carries the intention of introducing us to the mathematical world of elliptic curves and modular forms, apart from fixing up the convention and setting up the stage for the mathematical objects that appear in the rest of the thesis. It is well known that Feynman integrals satisfy differential equations in the external kinematic variables [29–31]. In chapter 4, we study the method of differential equations in great detail and learn about the 'canonical form' for Feynman integrals which makes our task of 'solving' the integrals easier along with hinting us about its structure [35]. In the two chapters following this, we present two cases of evaluation of multi-scale Feynman integrals at two-loops, which apart from using all the concepts from the chapters preceding this, shows explicitly the problems we face while tackling such complicated diagrams along with giving us information about the route to tackle them. Chapter 5 carries the example of the so-called 'topbox' which contributes to the process $pp \to t\bar{t}$ and contains three different elliptic curves, which made this diagram a bottleneck for a long time. Solving such a diagram for the very first time gives the motivation to deal with more complicated cases and also hinted the need of more mathematical study for the class of functions arising in these diagrams. Chapter 6, on the other hand, presents the case of an integral which contains the hints for being 'elliptic', and hence more complicated in nature, but turns out to be evaluating to simpler mathematical entities. This again shows us that guessing the structure of a massive Feynman integral by predicting the objects it evaluates to, is far from obvious. In order to make the evaluation and the techniques of both these cases more understandable and comparable, we choose a specific pattern for both these chapters. The structure of both chapter 5 and chapter 6 is as follows:

1. Physical importance and state of the art,
2. set-up and master integrals,
3. choice of co-ordinate system,
4. elliptic curves (if any),
5. transformation for the master integrals,
6. differential system (and integration kernels),
7. singularities and boundary conditions,
8. numerical results,
9. conclusions.

At the end of chapter 6, we also briefly sketch how we can use the master integrals in the corresponding case for computing an actual observable, particularly the decay rate of the Higgs boson into a pair of bottom quarks. Chapter 7 concludes the thesis. In the appendix, we collect all the other useful information that could be helpful to understand this thesis in a clearer way. We

hope that the meaning of the word Feynman integral is clear from the context, however, we try to make this as obvious as possible.

1.2 From scattering amplitudes to Feynman diagrams

We are interested in physical quantities such as scattering cross sections and decay width. A simple 2-to-n particle scattering process is given as

$$(p_1) + (p_2) \to (p_{1'}) + ... + (p_{n'}).$$

Pictorially, it can be visualized by

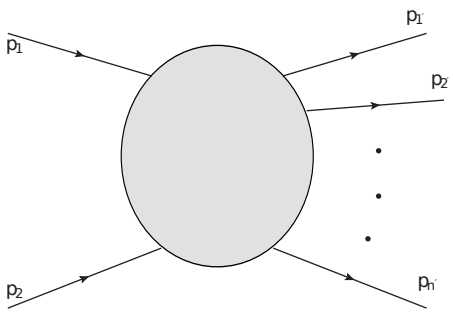

Figure 1.1. A 2-to-n scattering process.

Here, p_1 and p_2 are momenta of the initial two particles while $p_{1'}, p_{2'}, ...p_{n'}$ are momenta of the final n particles. The observables quantities, which allows the straight-forward comparison between theory and experiment, are the scattering cross section $\sigma(1 + 2 \to 1' + 2' + ... + n')$ and the decay width $\Gamma(1 \to 1' + 2' + ... + n')$. Usually, we wish to measure not only what the final-state particles are, but also the momenta of those, and hence we are interested in the differential cross sections, $d\sigma/(d^3 p_{1'} ... p_{n'})$. The outgoing momenta are not independent but constrained by 4-momentum conservation. The theoretical expression for the differential cross section is given as

$$d\sigma = \frac{1}{2E_1 2E_2 |v_1 - v_2|} \left(\prod_f \frac{d^3 p_f}{(2\pi)^3 2E_f} \right) |\mathcal{M}(p_1, p_2 \to \{p_f\})|^2 \, (2\pi)^4 \delta^4 \Big(p_1 + p_2 - \sum_f p_f \Big)$$

where $|v_1 - v_2|$ is the relative velocity of the two beams viewed from the lab frame, E_i is the energy of the $i-$th particle, and $\{p_f\} = p_{1'}, p_{2'}, ..., p_{n'}$. The scattering amplitude is denoted by $\mathcal{M}$. To actually compute the scattering amplitude, in practice, we need a set of Feynman rules that associate the factors with elements of the Feynman diagram. For completion, we write down the Feynman rules for QCD and EW theories in appendix 8. The methodology we acquire is the following: we expand a scattering amplitude in the small parameter g and calculate the first few terms. For instance, an amplitude A_n having n external partons (quarks and gluons) can be written as a perturbative expansion:

$$A_n = g^{n-2} \Big(A_n^{(0)} + g^2 A_n^{(1)} + g^4 A_n^{(4)} + g^6 A_n^{(3)} + ... \Big).$$

In order to calculate $A_n^{(l)}$ we first draw all the Feynman diagrams with the given number of external particles and l loops and then translate each of these graphs into a mathematical formula

with the help of above mentioned Feynman rules. The sum of all such diagrams, at a specific loop, is given by $A_n^{(l)}$. To be kept in mind that here we have not specifically mentioned the corresponding gauge group to the coupling constant, as at high energies all of the three coupling constants are small and this technique can be carried out. In practice, to draw all the possible graphs we can use tools like FeynArts [78] and Qgraph [79] and then carry out the translated mathematical formula for the Feynman graphs using a computer algebra system (CAS) like FORM [84]. It is a theoretical challenge to describe scattering events with many jets (narrowly collimated bundles of hadrons), as well as to increase the precision of the predictions by including higher-order perturbative corrections, which is required to match higher precision in experimental physics. We will discuss more regarding scattering amplitudes in chapter 2. We will also learn in chapter 4 that these Feynman integrals can be reduced to a set of basis integrals, namely the master integrals. Reducing the amplitude to a set of master integrals is done by exploiting the (generalized) unitarity or recurrence relations, for instance, integration by parts relations. The evaluation of these master integrals is often a non-trivial task, even bottlenecks for some of the cases. For the rest of this chapter, we move on to the very fascinating part of scattering amplitudes: the Feynman integrals.

1.3 Feynman integrals

We now know that to calculate an amplitude in QFT one has to take into account various graphs that contribute to a given process. The number of graphs however greatly increase with the increasing number of loops. Feynman amplitude is represented as a sum of Feynman graphs, where these graphs are written as Feynman integrals over loop momenta, due to the Feynman rules. In general, a Feynman integral also contains several Lorentz indices. The calculation of Feynman integrals mainly consists of three difficulties: tensor decomposition of integrals, reduction of scalar integrals to a set of basis integrals, termed as the master integrals, and the evaluation of these scalar basis integrals. The standard way to handle the tensor quantities is to perform a tensor reduction that enables us to write the given quantity as a linear combination of tensor monomials with scalar coefficients. The systematic method for one-loop case was worked out by Passarino and Veltmann [7], whereas for higher loops, concrete methods are presented in [45, 46]. We discuss the tensor reduction in a bit more detail in the appendix. The reduction of scalar integrals into a set of master integrals can be carried out comfortably, thanks to the various identities fulfilled by dimensional regulated integrals. The most powerful of these identities goes by the name 'integration by parts (IBP) identities' and is explained in detail in chapter 5. Consequently, we can imply that we deal with scalar Feynman integrals. The evaluation of these scalar master integrals remains the focus of this thesis and some explicit computations of master integrals corresponding to two-loop Feynman integrals containing massive particles in the loop is presented in the last two chapters.

Let us consider a scalar Feynman graph I with n internal lines in general D dimensions. The associated scalar l-loop integral is given by

$$I = \int \prod_{r=1}^{l} \frac{d^D k_r}{i\pi^{\frac{D}{2}}} \prod_{j=1}^{n} \frac{1}{(-q_j^2 + m_j^2)^{\nu_j}}, \tag{1.3.1}$$

where we raise each propagator having mass m_j by integer power ν_j. Our task is to be able to do this integration in order to write it down in terms of basic (mathematical) objects, for example, the hypergeometric functions. There are broadly two ways to calculate these integrals. The first one

is the analytic method where we can express the result in terms of analytic functions, usually as an expansion in the dimensional regularization parameter ϵ, where $D = 4 - 2\epsilon$. Or we can choose to calculate these integrals numerically where each coefficient of each term in the Laurent series in ϵ is just a number. To carry out the analytic evaluation, we may adopt many methods. Direct integration in Feynman parameter space is the most straightforward option, but for multi-scale integrals this quickly becomes very cumbersome. Another method is to transform the integral to a Mellin-Barnes representation [8]. However, the most successful method nowadays to obtain analytic results is by using the differential equation method. We also present a review of the few famous options for numerical evaluation at the end of this chapter.

1.3.1 Feynman parametrization

An example of very commonly used parametrization is given by the Feynman parametrization. The trick we use in this case is to write down Feynman integrals occurring in any loop integration in terms of a master formula. We can combine the denominators d in the eq. (1.3.1), using the formula:

$$\frac{1}{d_1^{\nu_1} d_2^{\nu_2} ... d_n^{\nu_n}} = \frac{\Gamma\left(\sum_{i=1}^n \nu_i\right)}{\prod_{i=1}^n \Gamma(\nu_i)} \int_0^1 \Pi_{i=1}^n dx_i x_i^{\nu_i - 1} \frac{\delta\left(1 - \sum_{j=1}^n x_j\right)}{\left(x_1 d_1 + x_2 d_2 + ... + x_n d_n\right)^{\sum_{i=1}^n \nu_i}}$$

the parameters x_i are called the Feynman parameters. Using the Feynman parameters in 1.3.1, we obtain the form

$$I = \frac{\Gamma(\nu - lD/2)}{\prod_{j=1}^n \Gamma(\nu_j)} \int_{x_j \geq 0} d^n x\, \delta\left(1 - \sum_{i=1}^n x_i\right) \left(\prod_{j=1}^n dx_j x_j^{\nu_j - 1}\right) \frac{\mathcal{U}^{\nu - (l+1)D/2}}{\mathcal{F}^{\nu - lD/2}} \tag{1.3.2}$$

Here $\mathcal{U}$ and $\mathcal{F}$ depend on the Feynman polynomials.

We can also look at these $\mathcal{U}$ and $\mathcal{F}$ polynomials from a graph theoretical view [61]. Let there be a connected graph G for the integral presented above, having n internal lines and r number of vertices. Let $\{d_1, d_2, ..., d_n\}$ denote the set of internal edges and l be the number of loops (Betti number in mathematical terminology). We have then

$$l = n - r + 1.$$

For disconnected graphs, the corresponding formula for l is $n - r + k$, where k is the number of connected components. Let T be the spanning tree for G, then it can be obtained from G by deleting l edges. A given graph G has several spanning trees. If F is a spanning k-forest for G, it can be obtained from G by deleting $l + k - 1$ edges. Consider an example of the diagram shown below.

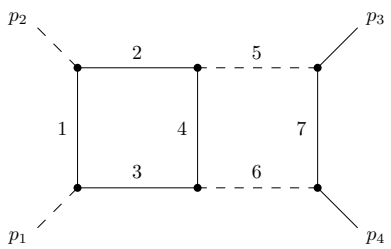

Figure 1.2. The double-box graph.

Let P_{T_i} denote the set of external momenta attached to the connected components, T_i of a k-forest. For the component T_1 for this graph, we have $P_{T_1} = \{p_2, p_3\}$ whereas for the component T_2, we get $P_{T_2} = \{p_1, p_4\}$. The $\mathcal{U}$ and $\mathcal{F}$ polynomials can be expressed very conveniently in terms of these spanning trees and forests as:

$$\mathcal{U} = \sum_{T \in \mathcal{T}_1} \prod_{e_i \notin T} x_i, \tag{1.3.3}$$

$$\mathcal{F} = \sum_{(T_1,T_2)\in\mathcal{T}_2} \Big(\prod_{e_i \notin (T_1,T_2)} x_i \Big) \Big(\sum_{p_j \in P_{T_1}} \sum_{p_k \in P_{T_2}} \frac{p_j \cdot p_k}{\mu^2} \Big) + \mathcal{U} \sum_{i=1}^{n} x_i \frac{m_i^2}{\mu^2}. \tag{1.3.4}$$

The sum is over all spanning trees or $\mathcal{U}$, and all spanning 2-forests in the first term of the formula for $\mathcal{F}$. The first formula says that $\mathcal{U}$ is the sum of all the monomials obtained from all spanning trees. The formula for $\mathcal{F}$ has two parts, the first part is related to the external momenta and the other part involves the masses. These $\mathcal{U}$ and $\mathcal{F}$ polynomials carry a lot of information about the Feynman integral it derives from. They can be used to get knowledge of the divergence of a Feynman graph, which is often taken as a guiding principle in order to solve a particular integral (for example the sunrise graph). There is also another parametrization known as the Schwinger parametrization which one can adopt.

In order to do a direct evaluation, we choose any convenient parametrization. We see a very simple example of direct integration of a Feynman integral in section ⟨1.3.4⟩. The choice of the parametrization and the order of the integration over Feynman parameters is very important. The method of direct integration is convenient, however, it is highly impractical when we need to go to higher orders. Managing the algebraic computations become very cumbersome as the size of the expressions become very large.

1.3.2 Divergences

It has been known from the early days of QFT that Feynman integrals suffer from divergences. Let us consider a very standard example of a one-loop graph $I(q)$ in 4-dimension, to understand the concept of divergence,

$$I(q) = \int \frac{d^4k}{(2\pi)^4} \frac{1}{(k^2 - m_1^2)\left((q-k)^2 - m_2^2\right)}. \tag{1.3.5}$$

Here q is the momentum flowing into the graph, k is the momentum of the first line and m_i is the mass of the particle i. Note that we took a different pre-factor here in order to keep things simple here and to smoothly connect later on to the notation in the eq. (1.3.1). This is done in section ⟨1.3.4⟩.

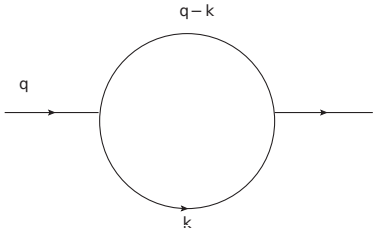

Figure 1.3. One loop self-energy diagram.

To perform a simple power counting, we introduce spherical coordinates $k = r\hat{k}$ in the eq. (1.3.5), where $\hat{k}$ is on the unit sphere and is expressed by the means of three angles. If we do a simple power counting of the propagators, we obtain a logarithmically divergent integral given by $\int_\Lambda^\infty dt\, t^{-1}$, in the limit of large t. For a general diagram G, we get three contributions for the power counting. The first one is from the Jacobian that arises when one introduces generalized spherical coordinates in the $(4\times l)$-dimensional space of l loop four-momenta and is given by $4l-1$ at large values of the loop momenta. The other two contributions are from the powers of the propagators and the degrees of its polynomials. Overall, this leads to an integral $\int_\Lambda^\infty dr\, r^{\omega-1}$, where

$$\omega = 4l - 2n + \sum_a p_a,$$

where p_a denotes the degree of the polynomials in the numerator depending on loop momenta k_i and n is the number of internal lines in a graph. The quantity ω is often called the degree of divergence (DOD) of a graph. Ultra-violet (UV) divergences arise from the region where all loop momenta become large. From DOD, we see that a Feynman integral is UV convergent if the DOD is negative. We say that the integral has a logarithmic, linear, quadratic, ... overall divergence when $\omega = 0, 1, 2, ...$ respectively. For massive fields, we have only UV divergences for an integral. However, In the zero-mass limit, there exists another type of divergence for the small momenta, known as the *infrared* (IR) divergence. The figure 1.3 is also a typical example of such divergence if one of the lines has a second power for the propagator which gives a factor $(k^2)^2$ in the integrand if the mass of this line becomes zero. Here k is chosen as the momentum of this line. In this case as well, we use the spherical coordinates and perform power-counting at small k to get a divergent behaviour $\int_0^\Lambda drr^{-1}$ but this time at small values of r.

These types of divergences are unavoidable in almost every attempt of calculating corrections beyond the leading order. The concept we follow is simply that as long as we are computing measurable quantities the answer has to come out finite. In practice, we adopt the following methodology to calculate physical observables: we "shove these divergences under a rug", i.e. instead of computing a physical observable all along, we deform the theory so that it depends on some regulating parameter, in such a way that the integrals come out finite. When we put all the integrals together, the answer we get for the observable is independent of the regulator, and therefore the regulator can be removed. However, we still need to deal with divergent integrals in the intermediate stage which we require to be mathematically manageable. Therefore we also need to choose a renormalization scheme to absorb infinities in the intermediate stages of perturbative calculations. The divergences drop out from the final physical answer irrespective of the renormalization program we choose.

1.3.3 Dimensional regularization

The procedure of making divergent integrals tentatively finite by introducing a suitable convergence device, i.e. a regulator, is called *regularization*. Also, it is a purely mathematical procedure and has no physical consequences. Dimensional regularization is not a unique procedure and we can adopt any other regularization scheme. Some famous examples of regularization schemes apart from dimensional regularization are momentum cut-off, Pauli-Villars, and analytic regularization. We now briefly discuss the dimensional regularization (DR) [4].

Within DR we replace the 4 dimensional integral over the loop momentum by a D dimensional integral, where D can be a non-integer or even a complex number. The integration is treated as a

function of D. We have several reasons to choose DR over the other options. Some of them are as follows: DR preserves all symmetries of the theory, particularly, the gauge symmetry. It allows an easy identification of the divergences as the divergence usually appears as a pole in the regulator when expanded in a series (when D approaches 4). In practice, we separate the part of the integral which is finite in the limit of D approaching 4 from the part which is not. This procedures we may choose to carry out this separation goes by the name subtraction schemes. DR suggests a minimal subtraction scheme (MS) in a natural way, which greatly simplifies the calculations. DR regularizes both UV as well as IR-divergences in massless theories at the same time.

The D-dimensional integration has to fulfil the standard laws for integration: Linearity:

$$\int d^D k\, (af(k) + bg(k)) = a \int d^D k\, f(k) + b \int d^D k\, g(k),$$

translation invariance:

$$\int d^D k\, f(k+p) = \int d^D k f(k),$$

for any vector p, and scaling law:

$$\int d^D k\, f(\lambda k) = \lambda^{-D} \int d^D k\, f(k).$$

In addition, the D-dimensional integral is rotationally invariant:

$$\int d^D k f(\Lambda k) = \int d^D k f(k),$$

where Λ belongs to the Lorentz group $SO(1, D-1)$ of the D-dimensional vector space (assuming this vector space has the metric diag(+1,-1,-1,-1)). In practice, we can always arrange the terms in the integral, for instance, by completing the square in the denominator, such that every function is rotationally invariant when we integrate over D dimensions, i.e. a function of k^2. While using the Feynman or Schwinger parametrization, for example, after this change of variables for the diagonalization, we have a polynomial in the Feynman or Schwinger parameters and the loop momentum k in the numerator. The integrals with odd powers of loop momentum in the numerator vanish by symmetry. We can deal with the even powers and reduce the integral into scalar integral following the method outlined in appendix. All the other useful techniques for handling Feynman integrals, like Wick rotations, can also be combined with DR. There are other useful properties of DR, which we refrain from mentioning here and one may refer to any standard QFT book for the same.

We now try to understand how DR works in handling the divergences. Let us take an example of a logarithmically divergent UV integral (no IR divergence). From the power counting we can see that it be convergent if the real part of D is smaller than 4. Therefore we can consider $Re(D) < 4$, by taking $D = 4 - 2\epsilon$ where $\epsilon > 0$, in order to compute this integral as a function of D. Later we can analytically continue to the whole complex plane. This result of this integral will exhibit a pole at $D = 4$. Similarly, for an IR divergent integral (no UV divergence), the integral converges for $Re(D) > 4$. We can follow the same procedure in this case as well. We compute it in $Re(D) > 4$ by taking $D = 4 + 2\epsilon$, and continue the result to $D = 4$. This will give us a double pole at $D = 4$. It is also possible to regulate both types of divergences simultaneously. In this case, we can use dimensional regularization for the UV-divergences while using a second regulator for the IR-divergences. Some possible option for regulating the IR-divergences are as follows. We can keep all external momenta off-shell, introduce small masses for all massless particles or raise the original propagators to some power. Then we perform the loop integration in the

domain where the integral is UV-convergent to obtain a result which we can analytically continue to the whole complex D-plane. Then we can remove the additional regulator which makes the IR-divergences regulated by DR and the IR divergences will also show up as poles at $D = 4$. For the sufficiently inclusive (IR safe) observables, the IR singularities cancel between real and virtual quantum corrections at the same order in perturbation theory, according to the KLN theorem [5,6].

Computationally speaking, we would like to express the final result of this D dimensional integrals in terms of known functions. To perform analytic continuations to the physical regions (where our external invariants and variables are well defined), we require good analytical behaviour of the functions used. Practical calculations force us to find a solution as a Laurent expansion in ϵ. Residues for a given power of the poles can be expressed in terms of known functions. We know that an important role in mathematical physics is played by hypergeometric functions since they are related to a wide class of special functions appearing in a large variety of fields. The connection between multi-loop calculations of Feynman amplitudes and generalized hypergeometric functions and polylogarithms has been known for quite some time.

1.3.4 Direct integration of Feynman integrals

Let us now look at evaluating the D-dimensional loop integrals. Considering any integral constructed from the Feynman rules we find out that they are only convergent because of the small imaginary part i. Moreover, the square of space-time is not positive semi-definite. We perform a Wick rotation, i.e. we substitute $t = i\tau$, to circumvent both these problems. Now our vectors become Euclidean and their square is strictly non-negative. The integral in this case will remain convergent even without i, given that it was convergent before. We can analytically continue to Minkowski space to obtain physical results.

Consider a D-dimensional one-loop integral:

$$\int \frac{d^D k}{(2\pi)^D} \frac{1}{\left(k^2 - M + iO\right)^2}$$

From the power counting we can see that the integral is divergent only if $D \geq 4$, whereas for $D < 4$, it converges. We have an integral over D-dimensional Euclidean space, where the integrand depends only on the magnitude of k. Therefore, it is natural that we introduce spherical coordinates.

$$\int d^D k = \int d\Omega_D \int k^{D-1} dk,$$

where $d\Omega_D$ denotes the differential solid angle of the $D-$dimensional unit sphere.

$$d\Omega_D = sin^{D-2}(\phi_{D-1}) sin^{D-3}(\phi_{D-2}) ... sin(\phi_2)\, d\phi_1 ... d\phi_D - 1,$$

where ϕ_i is the angle to the $i-th$ axis. Therefore, we have,

$$\Omega_D = 2\pi \prod_{n=2}^{D-1} \left(\int_0^{\pi} d\phi_n sin^{n-1} \phi_n \right) = 2\pi^{D/2} \frac{1}{\Gamma(\frac{D}{2})}.$$

The integral over Euclidean k_e is straightforward:

$$\int dk_e \frac{k_e^a}{(k_e^2 + M)^b} = M^{(a+1)/2-b} \frac{\Gamma(\frac{a+1}{2})\, \Gamma(b - \frac{a+1}{2})}{2\Gamma(b)}.$$

We can use the above formula to get the result of our integral:

$$\int \frac{d^D k}{(2\pi)^D} \frac{1}{(k^2 - M + iO)^2} = \frac{i}{(4\pi)^{D/2}} \frac{1}{M^{2-\frac{D}{2}}} \Gamma\Big(\frac{4-D}{2}\Big). \tag{1.3.6}$$

Observe the occurrence of Gamma functions in the evaluation of Feynman integral, as already hinted before. The factors i and $(4\pi)^{D/2}$ are amongst the recurring factors in the integration of Feynman integrals. Therefore we can already include them in the prefactor, as in the eq. (1.3.1), which we recall here

$$I = \int \prod_{r=1}^{l} \frac{d^D k_r}{i\pi^{\frac{D}{2}}} \prod_{j=1}^{n} \frac{1}{(-q_j^2 + m_j^2)^{\nu_j}}, \tag{1.3.7}$$

to get rid of the repeating appearances. In practice, we also multiply the overall Feynman integral by a factor of $e^{2\gamma_E \epsilon} \, (\mu^2)^{\nu - lD/2}$ where γ_E is the Euler-Mascheroni constant, μ is an arbitrary scale which makes the Feynman integral dimensionless, l is the number of loops in the integral and ν is the sum of powers of the propagators, i.e. $\nu = \sum_i^n \nu^i$.

Let us again look at the singularity structure of a Feynman integral. First of all the Gamma-function in the eq. (1.3.6), which for general ν, l and D is $\Gamma(\nu - lD/2)$ can give rise to a (single) pole if the argument of this function is close to zero or to a negative integer value. This divergence is the UV divergence explained before. Now, we consider the polynomial $\mathcal{U}$. Depending on the exponent $\nu - lD/2$ of $\mathcal{U}$ the vanishing of the polynomial $\mathcal{U}$ in some part of the integration region can lead to poles in ϵ after integration. These poles resulting from the vanishing of $\mathcal{U}$ is related to UV sub-divergences. Lastly, let us consider the $\mathcal{F}$ polynomial. In the Euclidean region (where all the invariants are negative or zero and all internal masses are positive or zero), the polynomial $\mathcal{F}$ can only vanish on the boundary of the integration region, which is the same as for $\mathcal{U}$, and these may again lead to poles in ϵ after integration. These poles are related to IR divergences. If we do not restrict the kinematics to the Euclidean region, the vanishing of $\mathcal{F}$ may result in divergences after integration which are called the Landau singularities. In this way, we observe that the graph polynomials $\mathcal{U}$ and $\mathcal{F}$ give us a lot of information about the graph it comes from. In chapter 4, we explicitly see how we can utilize the structure of the graph polynomial in the context of differential equations, particularly to use the dimensional shift relations as well as to set up the differential equations for our Feynman integrals.

1.3.5 Mathematical structure

Apart from the physical motivation for performing Feynman integral calculations, the mathematical structure of these Feynman integrals has brought us to a whole new area of research. In the last few years, we have seen a lot of coordination between mathematicians and physicists in this area, which has given us some wonderful results. Understanding the mathematical structure of Feynman integrals is not only interesting on its own but also helps us solving a particular integral more efficiently. A better understanding of the analytic structure of a Feynman diagram also often aids multi-scale generalizations.

Feynman integrals are blessed with beautiful mathematical structure. They give interesting results in terms of typical transcendental constants like zeta and multiple zeta values [85]. An algebraic variety is defined as the set of solutions of a system of polynomial equations over the real or complex numbers. Algebraic variety of dimension one are called algebraic curves and algebraic

varieties of dimension two are called algebraic surfaces. Feynman integrals are related to periods of these algebraic varieties. As an example, in the case of the family of kite integrals, the non-trivial algebraic variety is an elliptic curve [58]. We talk more about this in detail in chapter 3. We now shortly go through some of the nice mathematical properties of Feynman integrals, without diverging from our main goal which is to solve these Feynman integrals, preferably as a series expansion in the dimensional regulator.

1.3.5.1 Periods

The definition of a period is a follows: A period is a complex number whose real and imaginary parts are values of absolutely convergent integrals of rational functions with rational coefficients, over domains of absolutely convergent integrals of rational functions with rational coefficients, over domains in $\mathbb{R}^n$ given by polynomial inequalities with rational coefficients [87]. The number of periods is a countable set. Any rational and algebraic number is a period, but there are also transcendental numbers which are periods. For example, the number π, which can be expressed through the integral

$$\pi = \iint_{x^2+y^2\leq 1} dxdy$$

is a period. On the other hand, it is also conjectured that natural logarithm e and Euler's constant γ_E are not periods. There are uncountably many numbers which are not periods.

Let us consider a loop integral in the Euclidean region (where all the masses are positive or zero and all invariants are negative or zero). Let us also assume that all ratios of invariants and masses are rational. A general Feynman graph written as a Laurent series expansion in the dimensional regularization parameter is given by,

$$I = \sum_{j=-2l}^{\infty} c_j \epsilon^j,$$

where l denotes the number of loops. The coefficient c_j in this equation are shown to be numerical periods [86]. This feature strongly restricts the class of functions that can appear in multi-loop integral calculations.

1.3.5.2 Shuffle algebras

Feynman integrals written as iterated integrals satisfy the shuffle algebra. We now discuss the shuffle algebra and how they fit into the world of Feynman integrals. Let us consider a set of letters A, which is also called the alphabet. A word is an ordered sequence of letters:

$$W = l_1 l_2 ... l_k,$$

where l_i denotes a particular letter. The word of length zero is denoted by e. Let us consider the vector space of words over a field K. A shuffle algebra on the vector space of words is defined by

$$(l_1 l_2 ... l_k) \cdot (l_{k+1} ... l_r) = \sum_{shuffles\ \sigma} l_{\sigma(1)} l_{\sigma(2)} ... l_{\sigma(r)},$$

where the sum runs over all permutations σ, which preserve the relative order of $1, 2, ..., k$ and of $k+1, ..., r$. It is similar to shuffling a deck of cards: If we split a deck of cards into two parts and

shuffle, the relative ordering between the two individual parts remains the same, hence the name 'shuffle' for this algebra. The unit of this algebra is the empty word e:

$$e \cdot W = W \cdot e = W.$$

The shuffle product is defined recursively by

$$(l_1 l_2 ... l_k) \cdot (l_{k+1...l_r}) = l_1[(l_2 ... l_k).(l_{k+1...l_r})] + l_{k+1}[(l_1 l_2 ... l_k) \cdot (l_{k+2} ... l_r)].$$

Feynman integrals expressed as iterated integrals belong to the category of shuffle algebras. Let $[a,b]$ be a segment of the real line and $f_1, f_2, ..$ functions on this interval. Let us denote by I the following iterated integral:

$$I(f_1, f_2, ..., f_k; a, b) = \int_a^b dt_1 f_1(t_1) \int_a^{t_1} dt_2 f_2(t_2) ... \int_a^{t_{k-1}} dt_k f_k(t_k).$$

For fixed a and b we have a shuffle algebra:

$$I(f_1, f_2, ..., f_k; a, b) \cdot I(f_{k+1}, ..., f_r; a, b) = \sum_{shuffles\ \sigma} I(f_{\sigma(1)}, f_{\sigma(2)}, ..., f_{\sigma(r)}; a, b),$$

where the sum runs over all permutations σ, which preserves the relative the order of $1, 2, ..., k$ and $k+1, ..., r$. Shuffle algebra is a commutative Hopf algebra. Feynman integrals satisfying the shuffle algebra plays a very crucial role in fast computations of the integrals. This will also become clear in chapter 3. As a side remark, the symbol calculus is also an active part of research in the field of Feynman integral calculations.

1.3.6 Numerical tools

We now discuss some aspects of the numerical calculations of Feynman integrals and different numerical tools that we use in our computations.

Sector Decomposition: We begin by the very well known technique for numerical evaluation of divergent multi-loop integrals, known as the sector decomposition. It is a method operating in Feynman parameter space which is useful to extract singularities regulated by dimensional regularisation, by converting the integral into a Laurent series in ϵ. It can be used to calculate virtual and real corrections to processes at higher orders. The basic idea is to decompose the integration region into sectors with simple singularity structure, expanding in the regularization parameter ϵ and finally integrating the finite coefficients numerically. Some of the famous implementations of this technique are as follows:

1. Binoth, Heinrich: SecDec [62], which is based on a heuristic algorithm, where the number of sectors is small and infinite recursion is possible.
2. Bogner, Weinzierl: Sector Decomposition [63], which is based on Hironaka's polyhedra game, where the number of sectors is large however infinite recursion is not possible.
3. Smirnov, Tentyukov: FIESTA [64], which is a hybrid of the above of algorithms, where again, the number of sectors is small and infinite recursion is not possible.

4. Kaneko, Ueda , a geometric method of sector decomposition [65], in which case, the recursion capabilities are the same as those of FIESTA.

Ginac. GiNaC is an iterated and recursive acronym for GiNaC is Not a CAS, where CAS stands for Computer Algebra System [66]. It is an open framework for symbolic computation within the C++ framework. It uses the CLN library for implementing arbitrary-precision arithmetic. Symbolically, it can do multivariate polynomial arithmetic, factor polynomials, compute GCDs, expand series, and compute with matrices. Therefore it is a very efficient tool which we use to numerically evaluate Feynman integrals to very high precision. It is also equipped to handle certain non-commutative algebras which are extensively used in theoretical high energy physics: Clifford algebras, SU(3) Lie algebras, and Lorentz tensors.

PSLQ algorithm. The PSLQ algorithm [70, 71] is another one of the important techniques for efficient computations. This algorithm is useful, for example, when we want to evaluate a Feynman integral in expansion in ϵ. Let us suppose that, in a given order of expansion in ϵ, we know the transcendental numbers which can appear in the result and that we can obtain the result numerically with high accuracy. For example, in the finite part of $\epsilon-$expansion in two loops we can expect at least $x_{i-1} = \zeta(i)$ with $i = 2,3,4$ or, equivalently, $x_1 = \zeta(2)$, $x_2 = \zeta(3)$ and $x_3 = \pi^4$. Then we can use the PSLQ algorithm. Here, it gives the possibility to estimate whether or not a given number x, can be expressed linearly as $x = c_1x_1 + c_2x_2 + c_3x_3$ with rational coefficients c_i. In practice, we assign a weight -1 to ϵ and therefore, at a given order in ϵ, we are interested in the coefficients of all the possible transcendental constants having the same weight. A set of basis of these transcendental constants (up to weight 22 for multiple zeta values) can be found from [109].

PSLQ is an example of an 'integer relation algorithm'. If $x_1, x_2, ..., x_n$ are some real numbers, it gives the possibility to find the n integers c_i such that $c_1x_1 + c_2x_2 + ... + c_nx_n = 0$ or provide bounds within which this relation is impossible. More formally, suppose that x_i is given with the precision of ν decimal digits. Then we have an integer relation with the normal bound N

$$|c_1x_1 + ... + c_nx_n| < \delta, \tag{1.3.8}$$

provided that $max\ |c_i| < N$, where $\delta > 0$ is a small number, of order $10^{-\nu}$. With a given accuracy ν, a detection threshold δ and a norm bound N as an input, the PSLQ algorithm enables us to find out the relation exits or not at some confidence level.

The numerical checks for the multi-scale Feynman integrals evaluated in chapters 5 and 6, use the techniques and implementations mentioned above extensively.

2 Scattering Amplitudes

Contents

The lesson from the previous chapter was the following:

$$\text{Feynman diagrams} \overset{\text{Feynman rules}}{\longrightarrow} \text{scattering amplitude} \longrightarrow \text{observables.}$$

This chapter presents the techniques and an overview of general ideas to compute scattering amplitudes for perturbative calculations. As already motivated in the previous chapter, theoretical predictions based on the SM are one of the most important ingredients for the interpretation of collider data. Perturbative calculations at parton level or in combination with parton showers, embedded into the well-established factorization picture for hadronic collisions is used by the vast majority of experimental analyses. The level of experimental precision at LHC demands an equally precise theoretical calculation. Precise theoretical predictions demand a long chain of various tools and methods, all of which require highly technical computations. The current processes of interest include final states involving the Higgs boson, electroweak gauge bosons, jets and heavy quarks [88].

In a nut-shell this is what we do: at a particular loop l, the scattering amplitude is decomposed into a basis of integrals together with rational coefficients,

$$A^{l}_{2\to n} = \sum \text{Feynman diagrams} \to \sum_{i} (\text{coefficients})_i \, (\text{integrals})_i,$$

and we must then remove the infrared singularities to obtain a finite cross-section prediction of order k,

$$d\sigma_{2\to n}\text{N}^k\text{LO} = \text{IR}_k\left(A^{k}_{2\to n}, A^{k-1}_{2\to n+1}, ..., A^{0}_{2\to n+k}\right),$$

where the function IR_k represents an infrared subtraction technique. UV renormalization should also be performed but this is not a problem in analytic approaches. Let us now look at the technicalities we need to take care of in amplitude calculations in perturbative calculations.

2.1 Calculation of scattering amplitudes

The short distance cross section is built out of scattering amplitudes. In the 1960s the scattering amplitudes were built directly from the analytic properties, which is termed as the “on-shell" method. With the rise of QCD and Feynman rules in the 1970s, this analyticity fell out of favor. Later it was again resurrected for computing amplitudes in perturbative QCD as an alternative to Feynman diagrams. Now perturbative information assists analyticity and the multi-loop amplitudes can be generated from Feynman diagrams and other unitarity-inspired techniques. **The complexity of a scattering amplitude calculation grows very fast with the number of loops and the number of legs**.

At one loop, the last two decades saw huge progress in the construction of automated tools [78–83] to generate amplitudes and reduce them to a small set of building blocks in order to evaluate them. At one loop, we have the following factors to our benefit:

- Scattering amplitudes computations makes us deal with tensor integrals, apart from the scalar integrals (i.e. integrals having no vectors with free indices in the numerator)

$$I^{\mu_1 \ldots \mu_n} = \int d^D k \frac{k^{\mu_1} \ldots k^{\mu_n}}{P_1 \ldots P_N},$$

  where P_i denote the denominators and μ_i are the indices in the numerator. At one-loop, reduction of tensor integrals to scalar integrals have been worked out for a long time now and it is known by the *Passarino-Veltman reduction* [7]. We can perform a tensor reduction that enables us to write a given quantity as a linear combination of tensor monomials with scalar coefficients. At one loop, all tensor integrals are reducible, which means that integrals with loop momenta in the numerator can always be expressed in terms of integrals with trivial numerators.

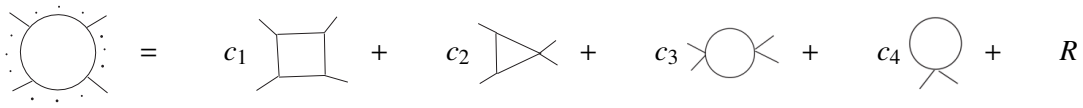

Figure 2.1. Basis integrals for one-loop amplitude.

  where the c_i and R are rational functions of external kinematic invariants.

- The integrals we need to know explicitly, in this case, have maximally $N = 4$ external legs. Integrals with $N > 4$ can be expressed in terms of boxes, triangles, bubbles and tadpoles (in the case of massive propagators). The analytic expressions for these “master integrals" are well-known. The most complicated analytic functions which can appear at one loop are dilogarithms.

We can say that the next-to-leading order (NLO) calculations are well established. Unfortunately, we are stuck at two loops. Beyond one loop, the integrals can have irreducible numerators, and the function class the amplitude lives in is not necessarily known. However, we know that there a large class of amplitudes where the function class is the well studied multiple polylogarithms. With the inclusion of masses in the internal particle, the integrals quickly become elliptic and hence requires

further study in order to tackle them. The state of the art amplitude computation is $2 \to 3$ processes. The amplitude calculations at NNLO generates large expressions, containing integrals with loop momenta in the numerator, contracted with external momenta and/or polarization vectors. It is not feasible to perform the evaluation of each one of these diagrams separately. To some rescue these diagrams are not all independent and there exist algebraic identities, like the *integration-by-parts* (IBP) identities and Lorentz identities, between these integrals, which we can use to bring them down to a set of basis integrals, called the master integrals, solving which corresponds to solving the whole set of integrals they span.

Apart from using these 'indirect methods' to carry out the computations, calculating multi-loop integrals numerically remains one of the most efficient ways to calculate integrals with a rather large number of kinematic scales. However, extending the current multi-loop methods to higher multiplicity still represents a serious challenge. The trending method to obtain the functional form of the amplitude is the use of generalized unitarity methods. Let us now discuss briefly some unitarity based methods for solving loop amplitudes and the growth in the techniques that are useful at the present state of the art.

Unitarity based methods. We can use unitarity to determine the functional form of the amplitudes. Scattering amplitude exhibit branch cut singularity when the particles in the loop can be produced as real particles. The basic concept of using unitarity methods for amplitude calculation is as follows: if we cut an amplitude in two all particles will be exchanged in the cut channel. It is just a statement about probabilities summing to one. The imaginary part for $\mathcal{M}$ is non-zero only when the virtual particles in the diagram go on-shell. Therefore, the appearance of an imaginary part of $\mathcal{M}(s)$ always requires a branch cut singularity. We first derive the optical theorem which explicitly shows how one can employ the imaginary of amplitudes into the computations of cross sections.

The initial state particles are related to the final state particles through an abstract scattering matrix, called the S-matrix, which avoids any reference to the intermediate states. The unitarity of the S-matrix, acts as a constraint on the analytic structure of amplitudes.

$$S^\dagger S = \mathbf{1}.$$

In a theory without any interactions, the S-matrix is simply the identity matrix $\mathbf{1}$. We can therefore write

$$S = \mathbf{1} + iT, \tag{2.1.1}$$

where T is called the transfer matrix and describes deviations from the free theory. From the unitarity of the S matrix it follows that

$$-i(T - T^\dagger) = T^\dagger T \tag{2.1.2}$$

Let $|k_i\rangle$ denote a state with momentum k of $i-$th particle. For a scattering process of $2 \to 2$ particles having initial momentum p_1 and p_2 and final momentum k_1 and k_n, we can write

$$\langle p_1 p_2 | T^\dagger T | k_1 k_2 \rangle = \sum_n \Big(\prod_{i=1}^{n} \int \frac{d^3 q_i}{(2\pi)^3} \frac{1}{2E_i} \Big) \langle p_1 p_2 | T^\dagger | \{q_i\} \rangle \langle \{q_i\} | T | k_1 k_2 \rangle$$

where we used the completeness of states $|q_i\rangle$ in the form of inserting a $\mathbf{1}$. We express the T-matrix element as the invariant matrix element $\mathcal{M}$ times 4-momentum conserving delta functions. Using eq. (2.1.2) we get,

$$-i\Big[\mathcal{M}(k_1k_2 \to p_1p_2) - \mathcal{M}^*(p_1p_2 \to k_1k_2)\Big] = \sum_n \Big(\prod_{i=1}^{n} \int \frac{d^3q_i}{(2\pi)^3 2E_i}\Big)\mathcal{M}^*(p_1p_2 \to \{q_i\})\mathcal{M}(k_1k_2 \to \{q_i\}) \times (2\pi)^4\delta^{(4)}(k_1 + k_2 - \sum_i q_i))),$$

with overall momentum conservation. Let us clean up this equation a little. The factors $\left(\prod_{i=1}^{n} \int \frac{d^3q_i}{(2\pi)^3 2E_i}\right)$ along with the overall delta function constraint can be written as Π_{LIPs} where LIPS stands for Lorentz invariant phase space. To make things compact, let us just denote the initial state by the state $|p\rangle$ and final state by $|k\rangle$. Using these we can write,

$$\Big[\mathcal{M}(k \to p) - \mathcal{M}^\dagger(p \to k)\Big] = -i\sum_X \int \Pi^{(X)}_{LIPS}(2\pi)^4\delta^4(p_k - p_X)\ \mathcal{M}(k \to X)\ \mathcal{M}^\dagger(X \to p), \quad (2.1.3)$$

the sum runs over all possible sets of X of final state particles. We can note here that the left-hand side denotes the matrix elements, however, the right-hand side is matrix elements squared. That means that at a particular order g^2 in the coupling the left-hand side must be a loop to match a tree-level calculation on the right-hand side. Thus, the imaginary parts of loop amplitudes can be determined completely by tree-level amplitudes.

For forward scattering amplitudes, initial and final states are the same, hence we can set $|k\rangle = |p\rangle = |A\rangle$, where A is some state. In this case we obtain

$$2i\ \mathrm{Im}\mathcal{M}(A \to A) = -i\sum_X \int \Pi^{(X)}_{LIPS}(2\pi)^4\delta^4(p_k - p_X)\ |\mathcal{M}(A \to X)|^2. \quad (2.1.4)$$

In particular, when $|A\rangle$ is a one particle state, then the decay rate is given by

$$\Gamma(A \to X) = \frac{1}{2m_A}\int \Pi^{(X)}_{LIPS}|\mathcal{M}(A \to X)|^2, \quad (2.1.5)$$

which gives us,

$$\mathrm{Im}\mathcal{M}(A \to A) = m_A\sum_X \Gamma(A \to X). \quad (2.1.6)$$

In this case, $\mathcal{M}(A \to A)$ is just a 2-point function. Therefore the imaginary part of the propagator is equal to the sum of decay rates into every possible particle. The cross section for a 2-particle state $|A\rangle$ is given by

$$\sigma(A \to X) = \frac{1}{2E_{CM}|\vec{p}_{CM}|}\int \Pi^{(X)}_{LIPS}|\mathcal{M}(A \to X)|^2. \quad (2.1.7)$$

Using this we obtain the standard form of the optical theorem,

$$\mathrm{Im}\ M(A \to A) = 2E_{CM}\vec{p}_{CM}\sum_X \sigma(A \to X), \quad (2.1.8)$$

where E_{CM} $\vec{p}_{CM}$ denote the energy and momentum in the center of mass frame respectively. This equation states that the imaginary part of the forward scattering amplitude is proportional to the

total scattering cross section. There are different ways to apply the optical theorem. One of them is what we just saw, that is to obtain a total cross section by computing the complete amplitude in forward scattering kinematics and taking the imaginary part of the full result at the very end. Doing this, we trade the computation of different squared amplitudes and their integration over different phase spaces, with the computation of the related imaginary parts of the forward scattering amplitude. We see a sketch of such a calculation at the end of chapter 6.

Cutkowsky presented the rules [89] which one can use to calculate the discontinuity of a Feynman amplitude with respect to an external invariant. Cutkowsky rules state:

- Cut a particular diagram in all possible ways, such that the cut propagators can be put on-shell.
- Replace each cut by a delta function by substituting

$$\frac{1}{q^2 - m^2 + i\epsilon} \to 2\pi i \delta(q^2 - m^2).$$

- Sum the contribution of all possible cuts.

Using these rules, the discontinuity of the amplitude is given as a sum of cut diagrams which feature on-shell intermediate particles. The use of these rules allows for a diagrammatic interpretation. The cut propagators dissect a diagram into two parts. Each of these parts is connected to either all incoming or all outgoing legs. Computation of the contribution of an individual cut of a single diagram is also closely related to the computation of a phase space integrals. Let us now see an example of how one can use cuts to exchange evaluation of phase space integrals in with the evaluation of multi-loop integrals.

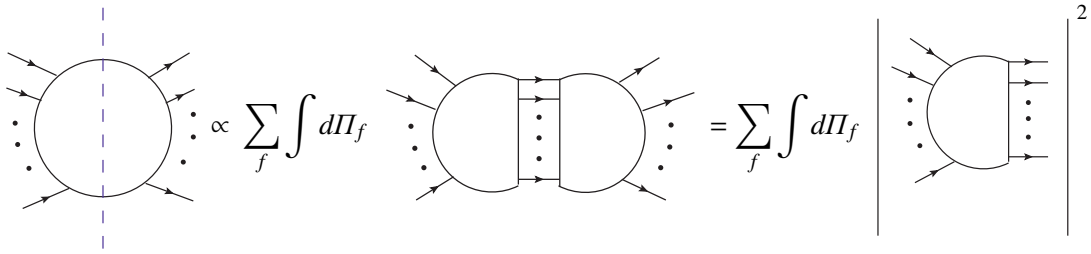

Figure 2.2. Exchanging phase space integral evaluation with evaluation of multi-loop integrals.

Here the blue dashed line represents imaginary parts (cuts) associated with states, which are intermediate in the forward scattering amplitude, but final for the squared modulus of the production amplitudes. We replaced each delta function in the final state phase with the difference of two propagators with an opposite prescription for their imaginary parts. Doing so, we get the forward scattering diagram and hence we exchange the square of a Born amplitude with a two-loop diagram, in contrast to the usual application of the Cutkowsky rules. In this way, the phase-space integrals can then be evaluated in the same algorithmic fashion as the multi-loop integrals.

We now present a short overview of how unitarity has been used as a guiding principle in amplitude calculations. The idea that one-loop amplitudes can be reconstructed from their

unitarity cuts was put forward by Bern, Dixon and Kosower in the 1990s [90] and was used in several phenomenological calculations. Britto, Cachazo and Feng [91] observed that the coefficients of the four-point functions, obtained when one-loop amplitudes are reduced to scalar integrals, are products of on-shell tree scattering amplitudes evaluated at complex momenta, and Ossola, Papadopoulos and Pittau (OPP) [92] discovered a simple algebraic method for reducing tensor integrals to scalar master integrals. All this revived the use of unitarity method in amplitude calculations. It was realized that replacing any number of intermediate states by on-shell particles probes deeper into the structure of scattering amplitudes. This extension is called the generalized unitarity which involves cutting amplitudes several times. In the end, we replace a loop amplitude on the cut with products of tree amplitudes which are known and much simpler than the actual loop amplitude. This concept made the computation of one-loop amplitudes in $N = 4$ super Yang-Mills theory feasible and led to the BCFW recursion relations for tree-level gluon amplitudes and caused a revolution in the computation of one-loop QCD amplitudes [72]. Interestingly, while unitarity cuts of Cutkowsky do consist of a physical interpretation, generalized unitarity not so much. The D-dimensional generalized unitarity cuts algorithm [93] has been extended to multi-loop integrands using integrand reduction [94, 95].

2.2 Cross sections

After discussing the techniques of computing amplitude and the advancements so far let us now switch briefly to see how we can compute cross sections using these amplitudes. This section focuses on the computations of cross sections in high energy physics by considering the parton model as an example. At short distances, quarks and gluons (partons) in a proton behave as almost free particles due to the phenomena called 'asymptotic freedom' in QCD. In proper circumstances, the cross section may be decomposed as a partonic cross section multiplied by the probabilities of finding partons of the prescribed momenta:

$$\sigma_{hadronic} = \sum_{ij} \int dx_1 dx_2 f_i(x_1) f_j(x_2)\, d\hat{\sigma}_{partonic}.$$

The probability that a parton of type i carries a fraction of the incident particle's momentum that lies between x_1 and $x_1 + dx_1$ is $f_i(x_1)dx_1$ and similarly for partons in the other incident particle. Hence the cross section is a convolution of a long-distance component, the parton distribution function (PDF) $f_i(\xi)$ for a parton of type i, and a short distance component, the partonic hard scattering cross section $\hat{\sigma}$. It basically separates the *short-distance* effects, which are calculable in perturbative theory, from *long-distance* effects, which belong to the domain of non-perturbative QCD and have to be modeled and fitted from data. Now we discuss shortly the perturbative calculations for the partonic cross section.

The perturbative short-distance cross section is given by

$$\hat{\sigma}(\alpha_s, \alpha) = [\alpha]^{n_\alpha}\Big[\underbrace{\hat{\sigma}^{(0)}}_{LO} + \underbrace{\left(\frac{\alpha_s}{2\pi}\right)\hat{\sigma}^{(1)}}_{NLO} + \underbrace{\left(\frac{\alpha_s}{2\pi}\right)^2\hat{\sigma}^{(2)}}_{NNLO} + \left(\frac{\alpha}{2\pi}\right)\hat{\sigma}^{NLO}_{EW}\ldots\Big]. \tag{2.2.1}$$

In general, the theoretical estimates of the cross section based on computations through to the next-to-leading order (NLO) in perturbative QCD, turns out to be insufficient. The leading-order (LO)

cross section exhibits a strong dependence on the choice of the renormalization scale. Including the $O(\alpha_s)$ corrections decreases the scale dependence. We need at least NLO to obtain reliable predictions whereas NNLO QCD provides the first serious estimate of the theoretical uncertainty. We can say that at the moment **we live in the world of NNLO computations**. NLO EW is naively similar in size to NNLO QCD and it is also important at high energies and near resonances.

In general the NNLO corrections to any given partonic cross section with m particles in the final state contains three different contributions

$$d\hat{\sigma}_{NNLO} = \int_{d\Phi_{m+2}} d\hat{\sigma}^{RR}_{NNLO} + \int_{d\Phi_{m+1}} d\hat{\sigma}^{RV}_{NNLO} + \int_{d\Phi_m} d\hat{\sigma}^{VV}_{NNLO}. \tag{2.2.2}$$

The double-virtual corrections $d\hat{\sigma}^{VV}_{NNLO}$ are constructed with two-loop amplitudes interfered with the corresponding Born matrix element, and with one-loop amplitudes squared. The mixed real-virtual contributions $d\hat{\sigma}^{RV}_{NNLO}$ are built from the interference of one-loop amplitudes with an additional real radiated parton and the corresponding tree-level matrix element. The double-real radiation corrections are constructed from tree-level matrix elements squared with two real partons added to the corresponding basic LO process. The phase-space integration is done with the help of Monte Carlo integrations after divergences are eliminated.

In the calculation of the various pieces of eq. (2.2.2), we have to deal with UV and IR divergences. In the double-virtual corrections, the divergences arise from the integration with respect to the loop momenta. In the real-virtual part, we have an overlapping of the divergences arising from the integration with respect to the one-loop momentum and the integration of the phase space of the additional unresolved gluon or photon. In the double-real part, the matrix element is finite and the divergences arise from the integration of the phase space of the two unresolved photon and gluon in the final state. We use DR to regularize the divergences. The IR divergences are removed after the three cross-sections are added together and the remaining initial state collinear divergences are re-absorbed in the re-definition of the PDF with which we have to convolute the $\hat{\sigma}$ in order to have the hadronic cross section.

3 Mathematical preliminaries

Contents

3.1 Iterated path integrals

Let k be the real or complex numbers and M be a smooth manifold over k. Let $\gamma : [0,1] \to M$ be a piece-wise smooth path on M and let $\omega_1, ..., \omega_n$ be smooth k-valued 1-forms on M. Let use write

$$\gamma^* \omega_i = f_i(t)dt \tag{3.1.1}$$

for the pull backs of the form ω_i to the interval $[0,1]$. The ordinary line integral is given by

$$\int_\gamma \omega_1 = \int_{[0,1]} \gamma^*(\omega_1) = \int_0^1 f_1(t_1)dt_1. \tag{3.1.2}$$

and does not depend on the choice of parametrization of γ.

Definition: The iterated integral of $\omega_1, ..., \omega_n$ along γ is defined by

$$\int_\gamma \omega_1 ... \omega_n = \int_{0 \le t_1 \le ... \le t_n \le 1} f_1(t_1)dt_1 ... f_n(t_n)dt_n. \tag{3.1.3}$$

More generally, an iterated integral is any $k-$linear combination of such integrals. The empty iterated integral (when $n = 0$) is defined to be the constant function 1.

Proposition : Iterated integrals satisfy the following first properties:

1. The iterated integral $\int_\gamma \omega_1 ... \omega_n$ does not depend on the choice of parametrization of the path γ.

2. If $\gamma^{-1}(t) = \gamma(1-t)$ denotes the reversal of the path γ, then

$$\int_{\gamma^{-1}} \omega_1 ... \omega_n = (-1)^n \int_\gamma \omega_n ... \omega_1 \tag{3.1.4}$$

3. If $\alpha, \beta : I \to M$ are two paths such that $\beta(0) = \alpha(1)$, then let $\alpha\,\beta$ denote the composed path obtained by traversing first α and then β. Then

$$\int_{\alpha\beta} \omega_1 ... \omega_n = \sum_{i=0}^{n} \int_\alpha \omega_1 ... \omega_i \int_\beta \omega_{i+1} ... \omega_n, \tag{3.1.5}$$

   where again the empty iterated integral is the constant function 1.

4. There is a shuffle product formula

$$\int_\gamma \omega_\gamma \omega_1 ... \omega_r \int_\gamma \omega_{r+1} ... \omega_{r+s} = \sum_{\sigma \in \Sigma(r,s)} \int_\gamma \omega_{\sigma(1)} ... \omega_{\sigma(r+s)}, \tag{3.1.6}$$

   where $\Sigma(r,s)$ is the set (r,s) shuffles.
   $\Sigma(r,s) = \{\sigma \in \Sigma(r+s) : \sigma^{-1}(1) < ... < \sigma^{-1}(r) \text{ and } \sigma^{-1}(r+1) < ... < \sigma^{-1}(r+s)\}$

3.2 Transcendental functions

The mathematical point of view of loop calculations reveal interesting algebraic structures. The knowledge of the class of functions belonging to the Feynman integral aids the computation. In higher order in perturbation theory, there are a class of mostly massless processes, where the virtual corrections can be entirely expressed in terms of multiple polylogarithms. However, starting from two-loops there are integrals which cannot be expressed in terms of these 'simple' functions and we need to go beyond multiple polylogarithms. Guessing the class of functions sufficient for the loop integrals is an active part of research. In this section, we discuss the various transcendental functions which we encounter, mainly at two-loops.

3.2.1 Multiple polylogarithms (MPLs)

Let us start with generalizing the basic transcendental functions we know from high school, to the class of functions we have so far referred to as the MPLs. The logarithm is defined by:

$$Li_1(x) = -\ln(1-x) = \sum_{i=1}^{\infty} \frac{x^i}{i} \tag{3.2.1}$$

and the dilogarithm is defined by

$$Li_2(x) = \sum_{i=1}^{\infty} \frac{x^i}{i^2} \tag{3.2.2}$$

Generalizing it to any value of n gives us the classical polylogarithm:

$$Li_n(x) = \sum_{i=1}^{\infty} \frac{x^i}{i^n} \tag{3.2.3}$$

The obvious generalization of the classical polylogarithm will bring us to the MPLs [11] [12]. The MPLs are defined by the power series expansion:

$$Li_{n_1,...,n_k}(x_1,...,x_k) = \sum_{i_1>i_2>...>i_k>0} \frac{x_1^{i_1}}{i_1^{n_1}} ... \frac{x_k^{i_k}}{i_k^{n_k}}. \tag{3.2.4}$$

Here $w = n_1 + ... + n_k$ is called the weight and k the depth. Some of the several subclasses of MPLs are as follows:

1. Multiple-zeta values are obtained by substituting ($x_1 = ... = x_k = 1$):

$$\zeta(n_1,...,n_k) = \sum_{i_1>i_2>...>i_k>0} \frac{1}{i_1^{n_1} i_2^{n_2} ... i_k^{n_k}}. \tag{3.2.5}$$

2. Harmonic polylogarithms are denoted as:

$$H_{m_1,...,m_k}(x) = Li_{m_1,...,m_k}\Big(x, \underbrace{1,...,1}_{k-1}\Big). \tag{3.2.6}$$

3. Nielsen's polylogarithms are denoted as

$$S_{n,p}(x) = Li_{n+1,1,...,1}\Big(x, \underbrace{1,...,1}_{p-1}\Big). \tag{3.2.7}$$

MPLs also enjoy representation in terms of iterated integrals. For $z_k \neq 0$, integral representation of MPLs is given by:

$$G(z_1,...,z_k;y) = \int_0^y \frac{dt_1}{t_1 - z_1} \int_0^{t_1} \frac{dt_2}{t_2 - z_2} ... \int_0^{t_{k-1}} \frac{dt_k}{t_k - z_k}. \tag{3.2.8}$$

We observe that one variable is redundant due to the following scaling relations:

$$G(z_1,...,z_k;y) = G(xz_1,...,xz_k;xy). \tag{3.2.9}$$

In addition, the trailing zeroes in the eq. (3.2.8) are taken care of with the definitions:

$$G(\underbrace{0,...,0}_{k};y) = \frac{1}{k!}(\ln(y))^k, \tag{3.2.10}$$

$$G(z_1,...,z_k;y) = \int_0^y \frac{dt}{t - z_1} G(z_2,...,z_k;t). \tag{3.2.11}$$

There exist a relation between the two representation for the MPLs. We can introduce a short hand notation:

$$G_{m_1,...,m_k}(z_1,...,z_k;y) = G(\underbrace{0,...,0}_{m_1-1}, z_1,...,z_{k-1}, \underbrace{0,...,0}_{m_k-1}, z_k;y). \tag{3.2.12}$$

Then the relation is given by

$$Li_{m_1,...,m_k}(x_1,...,x_k) = (-1)^k G_{m_1,...,m_k}\Big(\frac{1}{x_1}, \frac{1}{x_1 x_2}, ..., \frac{1}{x_1 ... x_k}; 1\Big). \tag{3.2.13}$$

Convergence. The series expansion for $Li_{m_1,...,m_k}(x_1,...,x_k)$ is convergent, if $|x_1x_2...x_j| \leq 1$ for all $j \in \{1,...,k\}$ and $(m_1,x_1) \neq (1,1)$. Therefore the function $G_{m_1,...,m_k}(z_1,...,z_k;y)$ has a convergent series representation if $|y| \leq |z_j|$ for all j.

MPLs exhibit several nice algebraic properties. The other beautiful aspects of the MPLs are that they satisfy Hopf algebras. MPLs satisfy two Hopf algebra. The first one is referred to as “shuffle algebra" and is related to the integral representation. An example of this multiplication is:

$$G(z_1;y)\,G(z_2;y) = G(z_1,z_2;y) + G(z_2,z_1;y).$$

The second algebra is called the “quasi-shuffle algebra" and is related to the series representation. An example is given by:

$$Li_{m_1}(x_1)\,Li_{m_2}(x_2) = Li_{m_1,m_2}(x_1,x_2) + Li_{m_2,m_1}(x_2,x_1) + Li_{m_1+m_2}(x_1x_2).$$

All these properties of MPLs allow a wide class of Feynman integrals to be computed systematically to all orders in ϵ. Shuffle algebras satisfied by MPLS are especially useful for numerically evaluating these functions. On the mathematical side, MPLs are very closely related to punctured Riemann surfaces of genus zero.

3.2.2 Elliptic Polylogarithms

The appearance of objects beyond MPLs also required generalization to a class of function related to genus one. A generalization of the classical polylogarithm depending on three variables x,y,q and two (integer) indices n, m:

$$ELi_{n;m}(x;y;q) = \sum_{j=1}^{\infty}\sum_{k=1}^{\infty}\frac{x^j}{j^n}\frac{y^k}{k^m}q^{jk}.$$

The two summations in this equation are coupled through the variable q. Further generalization to include any values of n, m, x and y gives us [19]:

$$\mathrm{ELi}_{n_1,...,n_l;m_1,...,m_l;2o_1,...,2o_{l-1}}(x_1,...,x_l;y_1,...,y_l;q) = \sum_{j_1=1}^{\infty}...\sum_{j_l=1}^{\infty}\sum_{k_1=1}^{\infty}...\sum_{k_l=1}^{\infty}\frac{x_1^{j_1}}{j_1^{n_1}}..\frac{x_l^{j_l}}{j_l^{n_l}}\frac{y_1^{k_1}}{k_1^{m_1}}..\frac{y_l^{k_l}}{k_l^{m_l}}\frac{q^{j_1k_1+...+j_lk_l}}{\Pi_{i=1}^{l-1}(j_ik_i+...+j_lk_l)^{o_i}}. \quad (3.2.14)$$

This formula is a special generalization to include both the genus one and the genus zero cases. We now shift our attention to elliptic curves and later come back to applying them in Feynman integrals.

3.3 Elliptic Curves

Elliptic curves have been an active part of the research for pure mathematicians for many years now. However, only in the past few decades, we saw theoretical physics benefiting heavily from the rich structure of elliptic curves. In this section, we first start with a small introduction of elliptic curves, which by no means is meant to be extensive. Then we explain the mathematical structure and the properties of elliptic curves which make them a powerful candidate for studying various aspects of Feynman integrals.

Elliptic integrals originally arose in the context of finding the arclength of an ellipse, from where the name "elliptic curve" derives. Let K be a general field (not of characteristic 2), and $f \in K[x]$ denote a cubic polynomial with coefficients in K, which has distinct roots. Here x and y are in the algebraic closure of K. The definition of an elliptic curve is then given as the locus of points satisfying

$$y^2 = f(x),$$

for any cubic or quartic polynomial $f(x)$. After a change of variables (using a K-rational point), the equation takes the simpler form

$$y^2 = x^3 + Ax + B,$$

where the values x, y, A and B belong to a field (which we may take to be $\mathbb{C}$). This form is called the Weierstrass form.

In addition to the points (x, y) on the elliptic curve, there is a very important 'point at infinity' that we like to consider on the curve, in the same way as we add a point at infinity in addition to the points on the complex plane to form the 'Riemann sphere' in complex variable theory. The condition that the roots are distinct implies that the curve is smooth everywhere. In this way, we find the formal definition of an elliptic curve: *An elliptic curve is a smooth projective algebraic curve of genus one having a specified point O*. The specified point O, often the point at infinity, is the location of the identity element for the group addition. Let us now understand the concept of the projective spaces in a bit more detail.

Projective space and the point at infinity. We know that parallel lines meet at infinity. Using the concept of projective spaces we can make more sense of this statement and use it to interpret the point at infinity on an elliptic curve. Let K be a field. Two-dimensional projective space P^2_K over K is given by the equivalence class of triples (x, y, z) with $x, y, z \in K$ and at least one of x, y, z non-zero. The triple (x_1, y_1, z_1) is said to be equivalent to another triple (x_2, y_2, z_2) if there exists a non-zero element $\lambda \in K$ such that

$$(x_1, y_1, z_1) = (\lambda x_2, \lambda y_2, \lambda z_2). \tag{3.3.1}$$

We denote this as $(x_1, y_1, z_1) \sim (x_2, y_2, z_2)$, i.e. the equivalence class of a triple only depends on the ratios of x to y to z. Hence it is denoted by $(x : y : z)$. If $(x : y : z)$ is a point with $z \neq 0$, then $(x : y : z) \sim (x/z : y/z : 1)$. These are the "finite" points in P^2_K. However, if $z = 0$, then dividing by z can be thought of as giving ∞ in either the x or y coordinate, and therefore the points $(x : y : 0)$ are called the "points at infinity" in P^2_k. Before we discuss any further, let us define the term genus which often occurs in this chapter.

Genus. An algebraic curve is the set of points satisfying a polynomial equation. The genus of an algebraic curve is roughly the number of holes it has. In topology, the classical result on the classification of two-dimensional manifolds tells us the following: any orientable, connected two-dimensional compact manifold is homeomorphic to a sphere with handles. The number of handles, g, is called the *genus* and it is a basic topological invariant. For an orientable compact surface, $g = 0$ yields a sphere, $g = 1$ a torus, and $g = 2$ a double torus.

3.3.1 Elliptic curves over the complex numbers

The elliptic curves can be formulated as the embedding of a torus in the complex projective plane. This follows straightforwardly from the Weierstrass's elliptic functions. An elliptic curve over the

complex numbers is obtained as a quotient of the complex plane by a lattice L spanned by two fundamental periods ω_1 and ω_2. This section aims to discuss this concept in more detail and to establish the connection between the torus and the complex projective space $\mathbb{P}^2_C$ more concretely.

Lattices and the fundamental parallelogram. Let us first discuss lattices in order to define elliptic curves over the complex numbers. Let ω_1 and ω_2 be two complex numbers, which are linearly independent over the real numbers. Then the lattice L is defined to be

$$L = \{m\omega_1 + n\omega_2 | m, n \in Z\}.$$

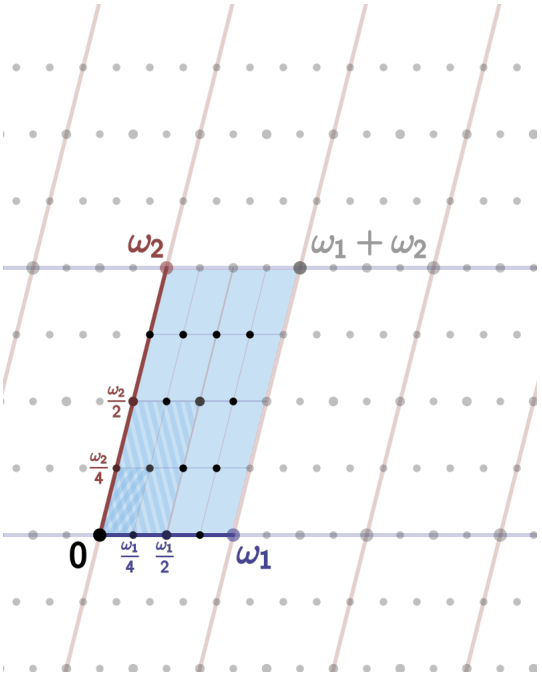

Figure 3.1. A parallelogram with two sides ω_1 and ω_2. Figure from [74].

Also, (ω_1, ω_2) will define the same lattice if and only if they differ by $GL_2(\mathbb{Z})$ action, but to preserve positive imaginary part, we can restrict ourselves to $SL_2(\mathbb{Z})$. Let us also consider the fundamental parallelogram for this lattice which is given by,

$$\Pi = \alpha + \{a\omega_1 + b\omega_2 | 0 \leq a \leq 1,\ 0 \leq b \leq 1\}.$$

where we can set α to be equal to 0 without any loss of generality.

We are looking for periodic functions on $\mathbb{C}/L$. The functions we get are doubly periodic. Let us also recall that the Riemann sphere is just the complex numbers $\mathbb{C}$ plus the point at infinity.

Doubly periodic functions. With the lattice L and ω_i, we can now define a meromorphic function f from the complex numbers to the Riemann sphere, such that

$$f(z + \omega_i) = f(z); \quad z \in \mathbb{C}.$$

We see that ω_1 and ω_2 are the two periods of this function, therefore the function f becomes doubly periodic. These doubly periodic, meromorphic functions are called elliptic. If we glue the opposite edges of the fundamental parallelogram together, we can think of it as a torus.

Complex torus. A complex torus can be obtained as follows: if we consider a lattice L in $\mathbb{C}^n$ as a real vector space; then the quotient group $\mathbb{C}^n/L$ is a compact complex manifold. This is shown in figure 3.1.

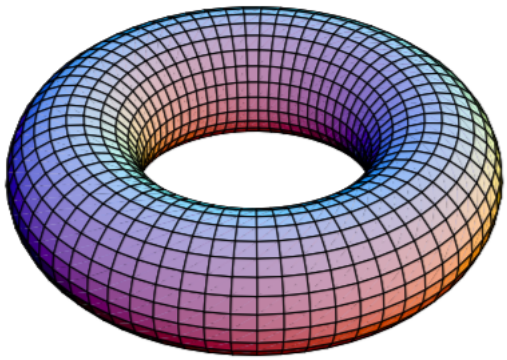

Figure 3.2. Torus obtained after identifying the opposite sides of the fundamental parallelogram; $\mathbb{T}:=\mathbb{C}/L$. Figure from [75].

Let us also briefly consider some properties of this elliptic function, f.

1. If f has no poles on the boundary $\partial\Pi$, then the sum of the residues in Π is 0. This is evident if we consider the residue theorem, $2\pi i \sum Res f = \int f$ over $\partial\Pi$. The integrals on the opposite sides of $\partial\Pi$ cancel, since f is doubly periodic, and we get the sum as 0.

2. If f has no poles in the interior of the fundamental parallelogram Π, then f is constant. This is clear from the Liouville's theorem. Since Π is a compact domain, f is bounded on Π, and since f is doubly periodic, it is bounded in all $\mathbb{C}$. Since f is a bounded meromorphic function over $\mathbb{C}$, it is constant by Liouville's theorem.

3. If f has no poles or zeroes on the boundary of Π, and $\{s_i\}$ represents the singular points of f in Π, with f having an order m_i at s_i, then $\sum m_i = 0$. This follows again using the residue theorem. If f is an elliptic function, then f' and f'/f are also elliptic. Using the residue theorem, we then get $0 = \int f'/f = 2\pi i \sum Res f = 2\pi i \sum m_i$.

After getting familiar with the main properties of an elliptic function, let us now discuss some specific examples for the same. Since we are mainly interested in periodic functions, an example is that of a simple lattice generated by the period $\omega = 2\pi i$ which generates the periodic function $exp(z)$. The inverse function in this case (i.e. $x = exp(z)$) is given by

$$z = ln(x).$$

We may also define functions whose input is a lattice in $\mathbb{C}$. The most natural of these are the Eisenstein series. For a lattice L and $k > 1$, consider

$$G_{2k}(L) = \sum_{\omega \in L}{}' \frac{1}{\omega^{2k}}, \tag{3.3.2}$$

where the prime on the sum means to exclude $\omega = 0$. It is to be noted that the sum is zero if the exponent is odd and hence contains only even exponents. By the above correspondence, this gives rise to a function on the upper half plane, defined by $G_{2k}(\tau) = G_{2k}(\mathbb{Z}\tau + \mathbb{Z})$, also called the Eisenstein series.

Weierstrass $\wp$-function. A very important example of a non-constant elliptic function in $\mathbb{C}$ is given by the Weierstrass $\wp$-function, which is defined with respect to the lattice L as follows:

$$\wp(z) = \wp(z;\, L) = \frac{1}{z^2} + \sum_{\omega \in \Lambda}{}' \Big[\frac{1}{(z-\omega)^2} - \frac{1}{\omega}\Big]. \tag{3.3.3}$$

Here $\sum'$ again denotes 0 not being included in the sum. It is very easy to see that $\wp(z)$ is an elliptic function on the lattice and its only pole is a double pole at each lattice point. For any fixed $l \in L$, the function $\wp(z) - (z-l)^{-2}$ is continuous at $z = l$ (we are not going to prove this here!). Therefore, $\wp(z)$ is a meromorphic function with a double pole at all lattice points and no other poles. Also, the right-hand side of the eq. (3.3.3) remains unchanged if we replace z by $-z$ and l by $-l$. But summing over $l \in L$ is the same as summing over $-l \in L$, therefore $\wp(z) = \wp(-z)$, i.e. the Weierstrass function is even. Next, we consider the term-by-term differentiation of eq. (3.3.3) to obtain,

$$\wp'(z) = -2 \sum_{l \in L} \frac{1}{(z-l)^3}. \tag{3.3.4}$$

If we replace z by $z + l_0$ for some fixed $l_0 \in L$, it merely rearranges the term in the sum in eq. (3.3.4), therefore it is obviously doubly periodic. This proves that $\wp'(z)$ is an elliptic function. In order to prove $\wp(z)$ is also an elliptic function on the lattice L, it suffices to prove that $\wp(z + \omega_i) = \wp(z) = 0$ for $i = 1, 2$. Let us prove this for $i = 1$, the case for $i = 2$ identically follows. Since the derivative of the function $\wp(z + \omega_1) - \wp(z)$ is $\wp'(z + \omega_1) - \wp'(z) = 0$, we have $\wp(z + \omega_1) - \wp(z) = \mathrm{C}$ for some constant C. If we substitute $z = \frac{-1}{2}\omega_1$ and use the fact that $\wp(z)$ is an even function, we conclude that $\mathrm{C} = \wp(\frac{1}{2}\omega_1) - \wp(\frac{-1}{2}\omega_1) = 0$.

One of the main properties of the Weierstrass function is that they are sufficient to recover all elliptic functions as every elliptic function can be written as a rational function in $\wp$ and $\wp'$. All the higher derivatives of $\wp$ are polynomials in $(\wp, \wp')$, for eg:

$$\wp''(z) = \frac{1}{6}\wp(z)^2 - \frac{1}{2}g_4.$$

The set of all elliptic functions forms a field and therefore we can identify the field of elliptic functions with the field of rational functions in $(\wp, \wp')$.

Now, we wish to relate the $\wp$ function to elliptic curves. We find that for a lattice L, the associated function $\wp$ satisfies the differential equation,

$$\wp'(z)^2 \;=\; 4\wp(z)^2 - g_4\wp(z) - g_6 \;=\; 4(\wp - e_1)(\wp - e_2)(\wp - e_3) \tag{3.3.5}$$

where $g_4 = 60G_4(L)$ and $g_6 = 140G_6(L)$ and e_i depend on the two periods ω_1 and ω_2. The differential eq. (3.3.5) has an elegant and basic geometrical interpretation. Suppose we take the function from the torus $\mathbb{C}/L$ to the complex projective space $\mathbb{P}^2_C$ defined by

$$\begin{aligned} &z \mapsto (\wp(z), \wp'(z), 1) \quad \text{for } z \neq 0\,; \\ &0 \mapsto (0, 1, 0). \end{aligned}$$

The image of any nonzero point z of $\mathbb{C}/L$ is a point whose complex coordinate satisfies the relation $y^2 = f(x)$. In this way, we see that every point z is mapped to a point on the elliptic curve $y^2 = f(x)$ in $\mathbb{P}^2_{\mathbb{C}}$. This map is a one-to-one correspondence between $\mathbb{C}/L$ and the elliptic curve (including the point at infinity).

The inverse function to Weierstrass' elliptic function $x = \wp(z)$ is an elliptic integral given by

$$z = \int_x^\infty \frac{dt}{\sqrt{4t^3 - g_4 t - g_6}}$$

where

$$g_4 = 60 \sum_{(m,n)\neq(0,0)} \frac{1}{(m\omega_1 + n\omega_2)^4}, \quad g_6 = 140 \sum_{(m,n)\neq(0,0)} \frac{1}{(m\omega_1 + n\omega_2)^6}.$$

In both examples for the periodic functions presented in this section, we can observe the periods can be expressed as integrals involving only algebraic functions. For the first example,

$$2\pi i = 4i \int_0^1 \frac{dt}{\sqrt{1-t^2}}$$

For the second example, let us assume g_4 and g_6 are the two given algebraic numbers. The periods are expressed as

$$\omega_1 = 2\int_{e_1}^{e_2} \frac{dt}{\sqrt{4t^3 - g_4 t - g_6}}, \quad \omega_2 = 2\int_{e_3}^{e_2} \frac{dt}{\sqrt{4t^3 - g_4 t - g_6}}$$

where e_i are the roots of the cubic equation $4t^3 - g_4 t - g_6 = 0$.

The j-invariant. Let us consider an elliptic curve given by $y^2 = 4x^3 - g_4 x - g_6$ via the Weierstrass elliptic functions. Then the $j-$invariant is defined as

$$j(\tau) = 1728\frac{g_4^3}{\Delta} \tag{3.3.6}$$

where the *modular* discriminant Δ is given by

$$\Delta = g_4^3 - 27g_6^2 \tag{3.3.7}$$

which is non-zero by the assumption that geometrically the graph has no cusps, self-interactions, or isolated points. The j-invariant tells us when two curves are isomorphic over an algebraically closed field. However, while working with non-algebraically closed field K, it is possible that two curves have the same j-invariant that cannot be transformed into each other using rational functions with coefficients in K. If two different elliptic curves defined over a field K have the same j-invariant, then we can say that the two curves are *twists* of each other.

3.4 Elliptic curves and Feynman integral

After getting acquainted with the formal definition of an elliptic curve, we now shift our focus to actually identifying the presence of an elliptic curve in a Feynman integral. Methods of algebraic geometry are often very helpful in the study of Feynman integrals. We have many interesting

examples in the literature where the integral was related to an elliptic curve [17,18,22,24], recently even more than one elliptic curve [48]. In this section, we explain the use of maximal cut in extracting an elliptic curve from a Feynman integral.

In order to detect the presence of an elliptic curve in our calculations, we search for Feynman integrals, whose maximal cuts are periods of an elliptic curve. We can analytically continue the momenta of a Feynman integral to complex values and replace the integration over space-time by contour integrals (contour $\mathbb{C}$) around poles of the integrand. Let us consider an integral of the form

$$I_{\nu_1\nu_2\ldots\nu_n}(D) = (\mu^2)^{\nu - lD/2} \int \frac{d^D k_1}{(2\pi)^4} \ldots \frac{d^D k_l}{(2\pi)^4} \prod_{j=1}^{n} \frac{1}{P_j^{\nu_j}},$$

where ν_i denotes the power of the propagator P_i, D denotes the dimension, l denotes the number of loops, μ is an arbitrary scale which makes the integral dimensionless and ν is the sum of powers of the propagators. By calculating the maximal cut, mathematically, we mean taking the $n-$fold residue at

$$P_1 = \ldots = P_n = 0$$

of the integrand over the remaining $(lD-n)$ variables along a contour C. Let us take the example of the two-loop sunrise integral with equal masses in D- dimensions, with momentum k_1 and k_2 flowing in the loop [19].

$$I_{1001001}(D, p^2, m^2\mu^2) = (\mu^2)^{3-D} \int \frac{d^D k_1}{i\pi^{\frac{D}{2}}} \frac{d^D k_2}{i\pi^{\frac{D}{2}}} \frac{1}{(-k_1^2+m^2)(-k_2^2+m^2)((-(p-k_1-k_2))^2+m^2)}. \tag{3.4.1}$$

p^2 denotes the momentum squared (in the Minkowski metric).

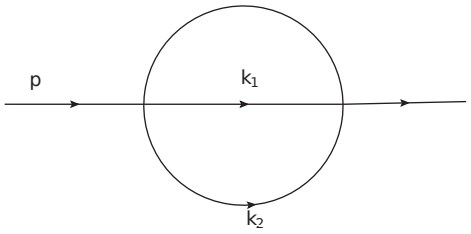

Figure 3.3. The sunrise graph, $I_{1001001}$.

The elliptic curve of the sunrise graph can be obtained using the maximal cut method,

$$MaxCut_C\, I_{1001001}(2-2\epsilon) = \frac{\mu m^2}{\pi^2} \int_C \frac{dP}{(P-t)^{\frac{1}{2}}(P-t+4m^2)^{\frac{1}{2}}(P^2+2m^2P-4m^2t+m^4)^{\frac{1}{2}}} + O(\epsilon). \tag{3.4.2}$$

In this equation P is the propagator variable left after carrying out all the delta integrations, m is the mass of the particle in the loop and $t = p^2$, is the Mandelstam variable.

Employing the method of calculation of a maximal cut to extract the elliptic curve, in practice, we aim for an integral representation having a square root of a quartic polynomial in the denominator along with a constant in the numerator. This defines the elliptic curve. We can integrate between any pair of roots of this polynomial, which gives us the period of the elliptic curve present in

our topology. Since we have only two independent periods, the result for any choice of integration contour may be expressed as a linear combination of these periods. The maximal cuts are solutions of the homogeneous differential equation satisfied by an integral. An extensive discussion about maximal cuts is presented in section ⟨4.2⟩.

In order to obtain the elliptic curve for the sunrise graph, we may also use information from the graph polynomial. The graph polynomial introduced in the section ⟨1.3.2⟩ can be viewed as a polynomial in the Feynman parameters x_1, x_2, x_3 with parameters t and m^2. We can define an elliptic curve from the graph polynomial $\mathcal{F}$ polynomial as

$$\mathcal{F} = 0 \tag{3.4.3}$$

along with the choice of a rational point as an origin [48]. Substituting x for p^2 and putting m equal to one in eq. (3.4.1), we get the following expressing for the elliptic curve using $\mathcal{F} = 0$,

$$-x_1x_2x_3x + (x_1 + x_2 + x_3)(x_1x_2 + x_2x_3 + x_3x_1) = 0.$$

Feynman integrals are known to satisfy differential equations in the external kinematic variable. The knowledge of the algebraic structure is often a guiding principle in the computations. For instance, for the sunrise graph, the order of the ordinary linear differential equation for an integral follows from the dimension of the first cohomology group of the corresponding elliptic curve (which is two). The two solutions of the homogeneous differential equation are the periods, say ψ_1 and ψ_2, of the elliptic curve. We now shift to leaning the differential operators useful for the periods of an elliptic curve.

3.5 Elliptic curve and the Picard–Fuchs operator

In this section, we define the Picard-Fuchs operator for the periods of the elliptic curves we obtain from Feynman integrals. Let us consider a general quartic form for the elliptic curve:

$$E : \omega^2 - (z - z_1)(z - z_2)(z - z_3)(z - z_4). \tag{3.5.1}$$

The variables z_1, z_2, z_3 and z_3 are the roots of eq. (3.5.1) and they may depend on variables $x = (x_1, ..., x_n)$.

$$z_j = z_j(x), \quad j \in [1, 2, 3, 4].$$

We set

$$Z_1 = (z_3 - z_2)(z_4 - z_1), \quad Z_2 = (z_2 - z_1)(z_4 - z_3), \quad Z_3 = (z_3 - z_1)(z_4 - z_2).$$

Not that $Z_1 + Z_2 = Z_3$. The modulus k and the complementary modulus $\tilde{k}$ are given by

$$k = \sqrt{\frac{Z_1}{Z_3}}, \quad \tilde{k} = \sqrt{1 - k^2} = \sqrt{\frac{Z_2}{Z_3}} \tag{3.5.2}$$

There are six possibilities of defining k^2. Our standard choice for the periods ψ_1, ψ_2 is

$$\psi_1 = \frac{4K(k)}{Z_3^{\frac{1}{2}}}, \quad \psi_2 = \frac{4iK(\tilde{k})}{Z_3^{\frac{1}{2}}}.$$

Let us also define quasi periods as

$$\phi_1 = \frac{4[K(k) - E(k)]}{Z_3^{\frac{1}{2}}}, \quad \phi_2 = \frac{4iE(\bar{k})}{Z_3^{\frac{1}{2}}}.$$

where $K(x)$ denotes the complete elliptic integral of the first kind. Our lattice is generated by the two periods we obtain from the elliptic curve, $L = m\psi_1 + n\psi_2 | m, n \in \mathbb{Z}$. The ratio of the two periods and the nome is given by

$$\tau = \frac{\psi_2}{\psi_1}, \quad q = exp(2i\pi\tau). \tag{3.5.3}$$

The Dedekind's η-function is given by

$$\eta(\tau) = e^{\frac{\pi i \tau}{12}} \prod_{n=1}^{\infty}(1 - e^{2\pi i n \tau}) = q^{\frac{1}{12}} \prod_{n=1}^{\infty}(1 - q^{2n}).$$

The periods of an elliptic curve satisfy the first order system of differential equations

$$d\begin{pmatrix} \psi_i \\ \phi_i \end{pmatrix} = \begin{pmatrix} -\frac{1}{2}d\ln Z_2 & \frac{1}{2}d\ln\frac{Z_2}{Z_1} \\ -\frac{1}{2}d\ln\frac{Z_2}{Z_3} & \frac{1}{2}d\ln\frac{Z_2}{Z_3^2} \end{pmatrix}\begin{pmatrix} \psi_i \\ \phi_i \end{pmatrix}, \quad i \in \{1,2\}, \tag{3.5.4}$$

where we use the notation

$$df(x) = \sum_{i=1}^{n}\left(\frac{\partial f}{\partial x_i}\right)dx_i.$$

The periods also satisfy the Legendre relation,

$$\psi_1\phi_2 - \psi_2\phi_1 = \frac{8\pi i}{Z_3} \tag{3.5.5}$$

We also have from the eq. (3.5.3)

$$2\pi i d\tau = d\ln q = \frac{2\pi i}{\psi_1^2}\frac{4\pi i}{Z_3}d\ln\frac{Z_2}{Z_1}. \tag{3.5.6}$$

Similar to the what we did in the section on iterated integrals let us consider a path $\gamma : [0,1] \to \mathbb{C}^n$ such that $x_i = x_i(\lambda)$ parametrized by the parameter λ. A specific choice is the path, $\gamma_\alpha : [0,1] \to \mathbb{C}^n$, indexed by $\alpha = [\alpha_1 : ... : \alpha_n] \in \mathbb{CP}^{n-1}$ and given explicitly by

$$x_i(\lambda) = x_i(0) + \alpha_i\lambda, \quad 1 \le i \le n. \tag{3.5.7}$$

We may view the periods ψ_1 and ψ_2 as a function of the variable λ. *The periods of an elliptic curve satisfy the Picard–Fuchs equation*. We can write the differential equations for the periods in terms of Z_i as :

$$\left[\frac{d^2}{d\lambda^2} + p_{1,\gamma}\frac{d}{d\lambda} + p_{0,\gamma}\right]\psi_i = 0, \quad i \in \{1,2\}, \tag{3.5.8}$$

where,

$$\begin{aligned} p_{1,\gamma} &= \frac{d}{d\lambda}\ln Z_3 - \frac{d}{d\lambda}\ln\left(\frac{d}{d\lambda}\ln\frac{Z_2}{Z_1}\right), \\ p_{0,\gamma} &= \frac{1}{2}\left(\frac{d}{d\lambda}\ln Z_1\right)\left(\frac{d}{d\lambda}\ln Z_2\right) - \frac{1}{2}\frac{\left(\frac{d}{d\lambda}Z_1\right)\left(\frac{d^2}{d\lambda^2}Z_2\right) - \left(\frac{d^2}{d\lambda^2}Z_1\right)\left(\frac{d}{d\lambda}Z_2\right)}{Z_1\left(\frac{d}{d\lambda}Z_2\right) - Z_2\left(\frac{d}{d\lambda}Z_1\right)} \\ &\quad + \frac{1}{4Z_3}\left[\frac{1}{Z_1}\left(\frac{d}{d\lambda}Z_1\right)^2 + \frac{1}{Z_2}\left(\frac{d}{d\lambda}Z_2\right)^2\right]. \end{aligned} \tag{3.5.9}$$

This gives us the Picard-Fuchs operator along the path γ:

$$L_\gamma = \frac{d^2}{d\lambda^2} + p_{1,\gamma}\frac{d}{d\lambda} + p_{0,\gamma}. \tag{3.5.10}$$

The Wronskian is defined by

$$W_\gamma = \psi_1 \frac{d}{d\lambda}\psi_2 - \psi_2 \frac{d}{d\lambda}\psi_1 = \frac{4\pi i}{Z_3}\frac{d}{d\lambda}\ln\frac{Z_2}{Z_1}. \tag{3.5.11}$$

The variation of the Wronskian along the path λ is given by

$$\frac{d}{d\lambda}W_\gamma = -p_{1,\gamma}W_\gamma, \tag{3.5.12}$$

$$2\pi i d\tau = \frac{2\pi i W_\gamma}{\psi_1^2} d\lambda. \tag{3.5.13}$$

It is also to be remembered that our choices for the periods is not unique. Any other choice related to the original one by a Möbius transformation generates the same lattice.

$$\begin{pmatrix}\psi_2' \\ \psi_1'\end{pmatrix} = \begin{pmatrix} a & b \\ c & d\end{pmatrix}\begin{pmatrix}\psi_2 \\ \psi_1\end{pmatrix}, \qquad \begin{pmatrix} a & b \\ c & d\end{pmatrix} \in \mathrm{SL}(2,\mathbb{Z}). \tag{3.5.14}$$

It can be seen in the figure 3.1. In terms of τ and $\tau' = \psi_2'/\psi_1'$, the transformation reads

$$\tau' = \frac{a\tau + d}{c\tau + d}.$$

In the case when the roots z_j depend only on a single variable x, we may exchange the variable x for the variable τ and study our problem as a function of τ. We discuss the Picard–Fuchs operator in more detail in chapter 4, in section ⟨4.4⟩, where we eventually learn how to use the factorization properties of Picard–Fuchs operator in Feynman integral calculations.

3.6 Modular Forms

For the Feynman integral connected to elliptic integrals, often we can use modular forms to express the results as iterated integrals. In this section, we discuss the properties of modular form. A modular form is a function on the complex upper half plane that satisfies certain transformation conditions and holomorphy conditions. Let τ be a complex number with $Im(\tau) > 0$. Then a modular form necessarily has a Fourier expansion,

$$f(\tau) = \sum_{n=0}^{\infty} a_n(f)\, e^{2\pi i n\tau}, \quad a_n(f) \in \mathbb{C} \text{ for all } n. \tag{3.6.1}$$

The modular group is the group of 2×2 matrices with integer entries and determinant 1.

$$\mathrm{SL}_2(\mathbb{Z}) = \left\{ \begin{bmatrix} a & b \\ c & d \end{bmatrix} : a,b,c,d \in \mathbb{Z},\ ad - bc = 1 \right\}. \tag{3.6.2}$$

The modular group is generated by the two matrices

$$\begin{bmatrix} 1 & 1 \\ 0 & 1 \end{bmatrix} \text{ and } \begin{bmatrix} 0 & -1 \\ 1 & 0 \end{bmatrix}. \tag{3.6.3}$$

The group of transformations defined by the modular group is generated by the matrix described by the two matrix generators, $\tau \to \tau + 1$ and $\tau \to -1/\tau$. The upper half plane is

$$\mathcal{H} = \{\tau \in \mathbb{C} : \mathrm{Im}(\tau) > 0\}. \tag{3.6.4}$$

Definition: Let k be an integer. A meromorphic function $f : \mathcal{H} \to \mathbb{C}$ is weakly modular of weight k if

$$f(\gamma(\tau)) = (c\tau + d)^k f(\tau) \quad \text{for } \gamma = \begin{bmatrix} a & b \\ c & d \end{bmatrix} \in \mathrm{SL}_2(\mathbb{Z}) \text{ and } \tau \in \mathcal{H} \tag{3.6.5}$$

If this transformation law holds when γ is each one of the generators $\begin{bmatrix} 1 & 1 \\ 0 & 1 \end{bmatrix}$ and $\begin{bmatrix} 0 & -1 \\ 1 & 0 \end{bmatrix}$ then it holds for all $\gamma \in \mathrm{SL}_2(\mathbb{Z})$. It means that f is weakly modular of weight k if $f(\tau + 1) = f(\tau)$ and $f(1/\tau) = \tau^k f(\tau)$.

Defintion: Let k be an integer. A function $f : \mathcal{H} \to \mathbb{C}$ is a modular form of weight k if

1. f is holomorphic on $\mathcal{H}$.
2. f is weakly modular form of weight k.
3. f is holomorphic at ∞.

The set of modular forms of weight k is denoted $M_k\mathrm{SL}_2(\mathbb{Z})$. $M_k\mathrm{SL}_2(\mathbb{Z})$ forms a vector space over $\mathbb{C}$. The zero function on $\mathbb{H}$ is a modular form of every weight, and every constant function on $\mathcal{H}$ is a modular form of weight 0. Now two non-trivial examples of modular forms follow.

Let $k > 2$ be an even integer and we define the Eisentein series of weight k to be a 2-dimensional analogue of Riemann zeta function $\zeta(k) = \sum_{d=1}^{\infty} 1/d^k$,

$$G_k(\tau) = \sum_{(c,d)}{}' \frac{1}{(c\tau + d)^k}, \quad \tau \in \mathcal{H}, \tag{3.6.6}$$

where the primed summation sign means to sum over nonzero integer pairs $(c, d) \in \mathbb{Z}^2 - \{0, 0\}$ (note that we saw this already in eq. (3.3.2)). It is a typical example of a modular form.

Definition: A cusp form of weight k is a modular form of weight k whose Fourier expansion has leading coefficient $a_0 = 0$, i.e.

$$f(\tau) = \sum_{n=1}^{\infty} a_n q^n, \quad q = e^{2\pi i \tau} \tag{3.6.7}$$

The set of cusp forms is denoted $S_k(\mathrm{SL}_2(\mathbb{Z}))$.

3.6.1 Iterated integral of modular forms

It was shown in [73] that the family of Feynman integral for the sunrise and the kite graph can be expressed as iterated integrals of modular form for a congruence subgroup Γ. In this subsection, we review the basic concepts from the reference.

Let $f_1(\tau), f_2(\tau), ..., f_n(\tau)$ be a set of modular form for a congruence subgroup Γ. The standard congruence subgroups of the modular group $SL_2(\mathbb{Z})$ are defined by

$$\Gamma_0(N) = \left\{ \begin{pmatrix} a & b \\ c & d \end{pmatrix} \in \mathrm{SL}_2(\mathbb{Z}) : c \equiv 0 \bmod N \right\},$$
$$\Gamma_1(N) = \left\{ \begin{pmatrix} a & b \\ c & d \end{pmatrix} \in \mathrm{SL}_2(\mathbb{Z}) : a, d \equiv 1 \bmod N,\ c \equiv 0 \bmod N \right\},$$
$$\Gamma(N) = \left\{ \begin{pmatrix} a & b \\ c & d \end{pmatrix} \in \mathrm{SL}_2(\mathbb{Z}) : a, d \equiv 1 \bmod N,\ b, c \equiv 0 \bmod N \right\}.$$

The weight of the modular form $f_i(\tau)$ is denoted by k_i. The $n-$fold iterated integral of these modular forms is given by

$$I(f_1, f_2, ..., f_n; \tau, \tau_0) = (2\pi i)^n \int_{\tau_0}^{\tau} d\tau_1 \int_{\tau_0}^{\tau_1} d\tau_2 ... \int_{\tau_0}^{\tau_{n-1}} d\tau_n f_1(\tau_1) f_2(\tau_2) ... f_n(\tau_n). \tag{3.6.8}$$

Using eq. (3.6.7) we may write

$$I(f_1, f_2, ..., f_n; \tau, \tau_0) = \int_{q_0}^{q} \frac{dq_1}{q_1} \int_{q_0}^{q_1} \frac{dq_2}{q_2} ... \int_{q_0}^{q_{n-1}} \frac{dq_n}{q_n} f_1(\tau_1) f_2(\tau_2) ... f_n(\tau_n). \tag{3.6.9}$$

For the special case when the first (n-1) modular forms are the constant function 1, we have

$$F(1, ..., 1, f_n; \tau, \tau_0) = \int_{q_0}^{q} \frac{dq_1}{q_1} \int_{q_0}^{q_1} \frac{dq_2}{q_2} ... \int_{q_0}^{q_{n-1}} \frac{dq_n}{q_n} f_n(\tau_n). \tag{3.6.10}$$

Introducing the short-hand notation for the repeated letters

$$\{f_i\}^j = \underbrace{f_i, f_i, ..., f_i}_{j}, \tag{3.6.11}$$

we get in the eq. (3.6.10)

$$F(\{1\}^{n-1}, f_n; \tau, \tau_0) = I(\underbrace{1, ..., 1}_{n-1}, f_n; \tau, \tau_0). \tag{3.6.12}$$

The zero-fold iterated integral is defined as usual:

$$F(; \tau, \tau_0) = 1 \tag{3.6.13}$$

Here *depth* is defined as the number of iterated integrations. In the case of MPLs, the depth is often referred to as the weight. However, here we use the word “depth". It is also to be kept in mind that depth and modular weight are two different notions. Depth is the number of iteration of iterated integrals, whereas, modular weight is associated to the individual modular forms $f_1, ..., f_n$. F satisfies all the other properties of an iterated integral for example the shuffle product.

Let us further assume that $f_k(\tau)$ vanishes at the cusp $\tau = i\infty$. We define the k-fold iterated integral by

$$F(f_1, f_2, ..., f_k; q) = (2\pi i)^k \int_{i\infty}^{\tau} d\tau_1\, f_1(\tau_1) \int_{i\infty}^{\tau_1} d\tau_2\, f_2(\tau_2) ... \int_{i\infty}^{\tau_{k-1}} d\tau_k\, f_k(\tau_k), \qquad q = e^{2\pi i \tau}.$$

The case where $f_k(\tau)$ does not vanishes at the cusp $\tau = i\infty$ is discussed in [73, 77] and is similar to trailing zeros in the case of MPLs. This is easily seen by changing the variable from τ to q:

$$2\pi i \int_{i\infty}^{\tau} d\tau_1 \, f(\tau_1) = \int_0^q \frac{dq_1}{q_1} \, f(\tau_1(q_1)), \qquad \tau_1(q_1) \, = \, \frac{1}{2\pi i} \ln q_1$$

Modular forms have a Fourier expansion around the cusp $\tau = i\infty$:

$$f_j(\tau) = \sum_{n=0}^{\infty} a_{j,n} \, q^n.$$

$f_j(\tau)$ vanishes at $\tau = i\infty$ if $a_{j,0} = 0$. Using the Fourier expansion and integrating term-by-term one can obtain the q-series of the iterated integral of modular forms corresponding to eq. (3.6.1):

$$F(f_1, f_2, ..., f_k; q) = \sum_{n_1=0}^{\infty} ... \sum_{n_k=0}^{\infty} \frac{a_{1,n_1}}{n_1 + ... + n_k} ... \frac{a_{k-1,n_{k-1}}}{n_{k-1} + n_k} \frac{a_{k,n_k}}{n_k} \, q^{n_1 + ... + n_k}.$$

4 Differential equations for Feynman integrals

Contents

> "Differentiating is an operation easier than integrating!"

The direct integration of Feynman integrals suffers from several problems, for example, integration of elementary or special functions, expansion in and summation of infinite series. Kotikov, while dealing with the evaluation of 2- and 3- point functions, realized that a given unknown integral can be considered to be a function of one of the propagator masses, and one can write a differential equation for the integral in that variable [29, 30]. Using differential equations thus allowed obtaining results for massive diagrams without calculating complicated D-space Feynman integrals. This novel idea was soon realized to be very effective and generalized later on by Remiddi [31], who then proposed the differentiation with respect to any other kinematics invariants formed by the external momenta.

4.1 Relation between different master integrals

The set of diagrams we get after differentiating a Feynman integral can in principle be related to each other by one or more identities. We can use these relations to our aid for solving these sets of Feynman integrals efficiently. In this section, we discuss the various relations that we observe between the set of Feynman integrals, in the context of differential equations.

1. **Integration by parts (IBP) identities:** Integration by parts identities are one of the most remarkable properties of dimensionally regularized integrals [32, 33]. These equations follow from the Poincare' invariance of the integrals, which is preserved in dimensional regularization. It is basically the extension to D-dimensional spaces of Gauss' theorem. For each integral I, we can write,

$$\int \frac{d^D k}{(2\pi)^D} \cdots \frac{d^D k_l}{(2\pi)^D} \frac{\partial}{\partial k_i^\mu} v^\mu \prod_{j=1}^{n} \frac{1}{(q_j^2 - m_j^2)^{\nu_j}} = 0. \tag{4.1.1}$$

where q contains any combination of scalar products and loop momentum vectors, v is any loop momenta or external momenta and $\{\nu_j\}$ denotes set of indices of the propagators. For a two loop integral, for example, these identities take the form:

$$\int \frac{d^D k_1}{(2\pi)^d} \frac{d^D k_2}{(2\pi)^D} \frac{\partial}{\partial k_i^\mu} v^\mu F(k_1, k_2, p_j) \quad i = 1, 2, \tag{4.1.2}$$

where F denotes the integrand of the integral I.

2. **Lorentz invariance identities:** Another class of identities we can obtain by exploiting the nature of the integrals as Lorentz scalars are the Lorentz invariance identities.

   Under an infinitesimal Lorentz transformation, $p_i \to p_i + \delta p_i$, where $\delta p_i = \omega_{\mu\nu} p_{i,\nu}$ with $\omega_{\mu\nu}$ a totally antisymmetric tensor, we get,

$$I(p_i + \delta p_i) = I(p_i).$$

   We can have the relation

$$I(p_i + \delta p_i) = I(p_i) + \sum_n \frac{\partial I(p_i)}{\partial p_{n,\mu}} = I(p_i) + \omega_{\mu\nu} \sum_n p_{n,\nu} \frac{\partial I(p_i)}{\partial p_{n,\mu}}$$

   and using the antisymmetry of $\omega_{\mu\nu}$, we get the relation,

$$\sum_n \left(p_{n,\nu} \frac{\partial}{\partial p_{n,\mu}} - p_{n,\nu} \frac{\partial}{\partial p_{n,\nu}} \right) I(p_i) = 0.$$

   This equation can be contracted with all possible antisymmetric combinations of the external momenta $p_{i,\mu} p_{j,\nu}$ to obtain other identities for the considered integrals. It has been shown in [111] that the Lorentz invariance identities are not linearly independent of the IBP relations and therefore not strictly necessary for the reduction of the integrals to a set of master integrals. Nevertheless, they can be used to speed up the reduction process.

3. **Symmetry relations:** The integrals can be further related to each other in the sense that the value of the integral does not change if we redefine the loop momenta, but the integrand transforms into a combination of different integrands. We can impose the condition that both the integrals (original and the combination of integrals after shifted momentum) are equal and get another relation. In order to understand it in a better way, let us consider the sunrise graph which we have already mentioned a lot of times before.

$$I_{1001001}(D, p^2, m^2\mu^2) = (\mu^2)^{3-D} \int \frac{d^D k_1}{i\pi^{\frac{D}{2}}} \frac{d^D k_2}{i\pi^{\frac{D}{2}}} \frac{1}{(-k_1^2 + m^2)(-k_2^2 + m^2)((-(p - k_1 - k_2))^2 + m^2)}.$$

We consider the three members family of diagrams belonging to the sunrise graph, which we obtain after raising the three propagators by a power one by one. We get the following integrals:

$$I_{2001001}(D,p^2,m^2\mu^2) = (\mu^2)^{3-D}\int \frac{d^Dk_1}{i\pi^{\frac{D}{2}}}\frac{d^Dk_2}{i\pi^{\frac{D}{2}}}\frac{1}{(-k_1^2+m^2)^2(-k_2^2+m^2)((-(p-k_1-k_2))^2+m^2)}.$$

$$I_{1002001}(D,p^2,m^2\mu^2) = (\mu^2)^{3-D}\int \frac{d^Dk_1}{i\pi^{\frac{D}{2}}}\frac{d^Dk_2}{i\pi^{\frac{D}{2}}}\frac{1}{(-k_1^2+m^2)(-k_2^2+m^2)^2((-(p-k_1-k_2))^2+m^2)}.$$

and

$$I_{1001002}(D,p^2,m^2\mu^2) = (\mu^2)^{3-D}\int \frac{d^Dk_1}{i\pi^{\frac{D}{2}}}\frac{d^Dk_2}{i\pi^{\frac{D}{2}}}\frac{1}{(-k_1^2+m^2)(-k_2^2+m^2)((-(p-k_1-k_2))^2+m^2)^2}.$$

Under the symmetry relations, we have

$$I_{2001001} = I_{1002001} = I_{1001002},$$

which is clear if we look at the graph shown in the figure 3.3.

These above relations can be used to bring down the integrals belonging to a family of Feynman integrals to a set of (independent) basis integrals, which we call the *master integrals*. The above identities are linear in the integrals, with the coefficients being rational functions of the kinematic invariants and the space-time dimension. As a result, **one can relate an integral with general integer powers to a finite set of master integrals (basis integrals)**.

In practice, the use of these identities generates, a large system of equations which needs to be solved in order to reduce to the set of master integrals. One possible elimination technique is the use of Laporta algorithm [34]: we can assign a “weight" to each integral which can be almost any increasing function of the indices denoting the power of the numerators and the denominators of the integral, such that integrals with higher indices have bigger weights. In other words, the system of equations is now ordered by their complexity. This system can be solved by Gauss' substitution rule, by considering the equations of the system one by one and using each equation for expressing the integral with the highest weight in terms of the integrals of lower weight and then substituting the result in the leftover equations. They are linear in the integrals, with the coefficients being rational functions of the kinematic invariants and the space-time dimension. As a result, one can relate an integral with general integer powers to a finite set of master (or basis) integrals. The algorithm is straightforward, but its execution requires a great amount of algebra, hence for practical purposes we use computer codes implementing the algorithm to get the set of master integrals [36].

The next step consists of the actual evaluation of the master integrals. The identities mentioned above can be further used to set up a linear system of first-order differential equations for the occurring master integrals and by construction we get a block triangular structure, which has a huge advantage that it makes the iterative solution for the differential equations manifest, beginning from simple to more complicated diagrams [31]. Then we do a Laurent-expansion around the dimensional regulation parameter ϵ, which gives a system of equation coupled in coefficients of the expansions (i.e order of ϵ).

Let us briefly go through the concept of irreducible scalar products (ISPs). For an l-loop integral depending on e linearly dependent external momenta $p_1, ..., p_e$, the number of ISPs depending on the loop momenta k_i are

$$n = l(l+1)/2 + le \tag{4.1.3}$$

and are given by:

$$s_{ik} = k_i \cdot q_k, \quad i = 1, ..., l, \quad k = 1, ..., l+e$$

where $q_{1,...,l} = k_{1,...,l}$, $q_{l+1,...,l+e} = p_{1,...,e}$. We define a topology (sector) as the set of propagators (with positive exponents), sufficient to express all the ISPs. Using this, we can, therefore, express any scalar product in the numerator in terms of denominators.

In this way, Feynman integrals can be classified according to their topology, starting with the integrals where the maximal number of propagators is present. Let the propagators, labelled by i, be raised to powers ν_i. Sub-topologies, where certain propagators are absent, are obtained by pinching the propagators, i.e. by setting the corresponding indices a_i to zero. The set of identities presented above also relate integrals with different values of the a_i within a topology.

Following are the examples of some famous programs which can be used for the reduction to master integrals:

1. Reduze [37]
2. Kira [38]
3. Fire [39]
4. LiteRed [40] [47].

All the above programs have their advantages and short-comings and it depends on the user the type of IBP reduction program he/she wants to use.

It is also useful to define the so-called sector-id which is a way to uniquely define a sector by associating a number against it:

$$\text{id} = \sum_{j=1}^{n} 2^{j-1} \Theta(\nu_j).$$

Sector-id is a common occurrence in computer implementations for IBP reductions.

4.1.1 Dimensional shift relations (DSR)

In our calculations, most often, we deal with integrals that are regulated using DR. By lowering the number of dimensions we can improve their UV behavior. In [41] and [45], Tarasov presented an algorithm for systematically obtaining recurrence relations for dimensionally regularized Feynman integrals with respect to the space-time dimension D. The relation between D and $D-2$ dimensional integrals is given in terms of a differential operator with which one can obtain an explicit formula for each Feynman diagrams. One may observe that while using IBP identities, we get relations connecting integrals with some exponents changed by ± 1. Without going into too much detail, let us straight-away discuss how we can use these shift relations in our calculations.

In order to explain it very clearly, we take the example of the Feynman integral $I_{\nu_1\nu_2\nu_3\nu_4\nu_5\nu_6\nu_7}$ having 7 propagators with power ν_i (explained more clearly in chapter 5) We first introduce an operator

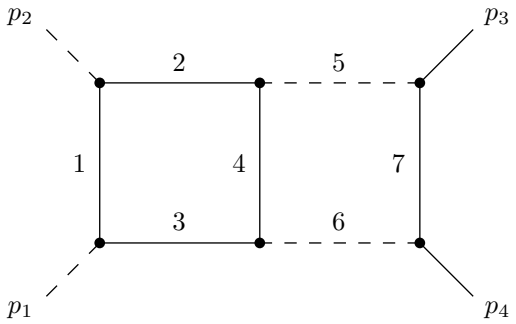

Figure 4.1. The planar double box with seven propagators.

$\mathbf{i}^+$, which raises the power of the propagator i by one, e.g.

$$\mathbf{1}^+ I_{\nu_1\nu_2\nu_3\nu_4\nu_5\nu_6\nu_7}(D) = I_{(\nu_1+1)\nu_2\nu_3\nu_4\nu_5\nu_6\nu_7}(D). \tag{4.1.4}$$

Along with this, we define two operators $\mathbf{D}^{\pm}$, which perform the task of shifting the dimension of space-time by two:

$$\mathbf{D}^{\pm} I_{\nu_1\nu_2\nu_3\nu_4\nu_5\nu_6\nu_7}(D) = I_{\nu_1\nu_2\nu_3\nu_4\nu_5\nu_6\nu_7}(D \pm 2). \tag{4.1.5}$$

We can calculate the Feynman graph polynomials $\mathcal{U}$ and $\mathcal{F}$ using the formula presented in section ⟨1.3.1⟩. Then we can obtain the DSR for $\nu_1, ..., \nu_7 \geq 0$ in terms of the differential operator as

$$\mathbf{D}^{-} I_{\nu_1\nu_2\nu_3\nu_4\nu_5\nu_6\nu_7}(D) = \mathcal{U}(\nu_1\mathbf{1}^+, \nu_2\mathbf{2}^+, \nu_3\mathbf{3}^+, \nu_4\mathbf{4}^+, \nu_5\mathbf{5}^+, \nu_6\mathbf{6}^+, \nu_7\mathbf{7}^+) I_{\nu_1\nu_2\nu_3\nu_4\nu_5\nu_6\nu_7}(D). \tag{4.1.6}$$

For integrals with irreducible numerators (i.e. $\nu_8 < 0$ or $\nu_9 < 0$), in order to get the DSR, we can proceed as follows: we can first convert to a basis of master integrals with $\nu_8 = \nu_9 = 0$ (and raised propagators), and then apply the DSR to the latter and converts back to the original basis.

It is also possible to obtain the differential equations for the master integrals using the DSR. For $\nu_1, ..., \nu_7 \geq 0$, we get

$$\begin{aligned} \mu^2 \frac{d}{ds} I_{\nu_1\nu_2\nu_3\nu_4\nu_5\nu_6\nu_7}(D) &= \mathbf{D}^+ \mathcal{F}'_s(\nu_1\mathbf{1}^+, ..., \nu_7\mathbf{7}^+) I_{\nu_1\nu_2\nu_3\nu_4\nu_5\nu_6\nu_7}(D), \\ \mu^2 \frac{d}{dt} I_{\nu_1\nu_2\nu_3\nu_4\nu_5\nu_6\nu_7}(D) &= \mathbf{D}^+ \mathcal{F}'_t(\nu_1\mathbf{1}^+, ..., \nu_7\mathbf{7}^+) I_{\nu_1\nu_2\nu_3\nu_4\nu_5\nu_6\nu_7}(D). \end{aligned} \tag{4.1.7}$$

The right-hand side is given by integrals in $(D+2)$ dimensions with three propagators (from the $\mathcal{F}$ polynomial for this graph) raised by an additional unit. We can obtain the differential equation by reducing these integrals on the right-hand side of the eq. (4.1.7) to the basis in D dimensions.

We see that these relations offer an easy and compact way to set up the differential equations for a particular Feynman integral in a compact way. However, from a computational point of view, it is not the most advantageous representation since it requires reduction of integrals with large ν, which requires a lot of computational memory.

4.2 Maximal cuts

Now, we discuss the maximal cuts, which often play a major role as a guiding principle for the choice of master integrals, as will be explained in section ⟨4.3⟩. In very simple terminology cutting a propagator means forcing the particle propagating through it to be on-shell. Mathematically, we achieve this easily if the propagator is raised to power one. We simply substitute the propagator with a Dirac δ-function which forces the momentum of the propagator to be on-shell to get the cut, as also mentioned in the previous chapters. The maximal cut is defined as the simultaneous cutting of all its propagators. In this case, it corresponds to taking the n-fold residue of the integrand in the complex plane, where n is the number of propagators. Such multiple cuts always exist for the non-reducible diagrams. *The maximal cuts are solutions of the homogeneous differential equations* [21]. Any such solution remains a solution upon multiplication with a non-zero constant. We can obtain an integral representation for the homogeneous solutions of the differential equation satisfied by the Feynman integral, in any number of dimensions D, by computing its maximal cut. The computation of the maximal cut can be simplified by the use of the so-called Baikov representation. In [44] it was shown that all independent homogeneous solutions for higher-order (third or more) differential equations can be obtained by evaluating the maximal cut along different independent contours, which do not cross any branch cut of the integrand.

Baikov representation. Recurrence relations are powerful tools for evaluating multi-loop Feynman integrals. In an approach using explicit formulae for the solutions of the recurrence relations for Feynman integrals, Baikov in [42], derived what we now know as the Baikov's representation for the Feynman integral. Let us consider a loop integral of the form

$$I_{\alpha_1....\alpha_n} = \int \frac{d^D k_1 ... d^D k_l}{i\pi^{\frac{Dl}{2}}} \prod_{j=1}^{n} \frac{1}{P_j^{\nu_j}}$$

where the scalar functions P_α are linear polynomials with respect to s_{ij} and n is the number of ISPs, defined in eq. (4.1.3). The symbol ν_i denotes the power of the propagator P_i. These propagators P are assumed to be linearly independent and to form a complete basis in the sense that any non-zero linear combination of them depends on the loop momenta, as shown in the equation:

$$P_a = \sum_{i=1}^{l}\sum_{j=1}^{l} A^{ij} k_i \cdot k_j + \sum_{i=1}^{l}\sum_{j=l+1}^{M} A_a^{ij} k_i \cdot p_{j-l} + f_a, \quad a = 1, ..., n \tag{4.2.1}$$

where f_a depends on external kinematics and internal masses and $M = l + e$ (recall that e is the number of independent external propagators). Here, we have separated out the denominators in terms of the external momenta and loop momenta. The aim is to replace the loop momenta by the set of propagators. In order to do so, we can project each of the loop momenta with respect to the space spanned by the external momenta involved plus a transverse component,

$$I_{\alpha_1....\alpha_n} = C_n^l (G(p_1, ..., p_e))^{(-D+e+1)/2} \int \frac{dx_1 ... dx_n}{x_1^{\alpha_1} ... x_n^{\alpha_n}} P_n^l (x_1 - f_1, ..., x_n - f_n)^{(D-M-1)/2} \tag{4.2.2}$$

with

$$C_l^n = \frac{\pi^{-l(l-1)/4 - le/2}}{\prod_{i=1}^{l} \Gamma(\frac{D-M+i}{2})} \det(A_{ij}^a)$$

and

$$P_n^l(x_1,x_2,...,x_n) = G(k_1,...,k_l,p_1,...p_e)|_{s_{ij}=\sum_{a=1}^n A_{ij}^a \,\&\, s_{ij}=s_{ji}}$$

with G representing the Gram determinant, which is the jacobian of this transformation and A_{ij}^a is the inverse of the topology matrix A_a^{ij}.

Loop by loop approach: At one loop the number of Baikov variables and the number of propagators of a generic Feynman integral can be the same. However, at higher loops, this might not be the case anymore. To consider an example, in the case of the planar double box, with E=3 independent external momenta and L=2, we get N=9 and $M = L + E$=5. In this case, we have to integrate over nine variables whereas the double graph has only seven denominators. Therefore we need to add 2 more denominators in order to complete the list of 9 denominators to express all the ISPs. Hence it is desirable to have a representation having the minimal number of integration variables. This can be achieved by considering the projection over the space spanned by the external momenta of *each loop* integration momentum separately. This method is known by the loop by loop method. [43].

Let us first assume that all propagators in our Feynman diagram occur to the power one. We first consider a one-loop sub-graph with a minimal number of propagators such that the dimension of the sub-space spanned by the external momenta or this sub-graph is minimal. Let the sub-graph contain $(e+1)$ propagators $P_1, ..., P_{e+1}$. Therefore the sub-space spanned by the external momenta for this sub-graph has the dimension e. Following eq. (4.2.2), we can calculate the Jacobian, which is equal to replacing the measure corresponding to the loop momentum for the sub-graphs by the following:

$$\frac{d^Dk}{i\pi^{\frac{D}{2}}} = \; u\,\frac{2^{-e}\pi^{-\frac{e}{2}}}{\Gamma\left(\frac{D-e}{2}\right)} G(p_1,...,p_e)^{\frac{1+e-D}{2}}\, G(k,p_1,...,p_e)^{\frac{D-e-2}{2}} \prod_{j=1}^{e+1} dP_j,$$

where the momenta $p_1, ..., p_e$ denote the linearly independent external momenta for this sub-graph, the Gram determinant (in Minkowski space) is defined by

$$G(p_1,...,p_e) = \det\left(-p_i\cdot p_j\right)_{1\le i,j\le e},$$

and u denotes an (irrelevant) phase ($|u| = 1$).

We then repeat this procedure for the second loop, replacing $p_1, ..., p_e$ by the set of independent external momenta for the full graph. The loop by loop approach hence is a very fast approach to calculate the maximal cuts.

For an integral of the form

$$I = e^{2\gamma_E\epsilon}\left(\mu^2\right)^{n-D}\int \frac{d^Dk_1}{i\pi^{\frac{D}{2}}}\frac{d^Dk_2}{i\pi^{\frac{D}{2}}}\, N(k_1,k_2)\prod_{j=1}^{n}\frac{1}{P_j},$$

where $N(k_1,k_2)$ is a polynomial in k_1 and k_2, a maximal cut is given by

$$\text{MaxCut}_C\, I = e^{2\gamma_E\epsilon}\left(\mu^2\right)^{n-D}\int_C \frac{d^Dk_1}{i\pi^{\frac{D}{2}}}\frac{d^Dk_2}{i\pi^{\frac{D}{2}}}\, N(k_1,k_2)\prod_{j=1}^{n}\delta\left(P_j\right),$$

where the integration measure is re-written according to eq. (4.2) and the integration is over a specified contour in the variables P_j which is not eliminated because of the delta distributions.

For the case of integrals with higher powers of the propagators, i.e. $\nu_j > 1$, a very easy way to compute the corresponding maximal cut is by first converting to a basis with $\nu_j = 1$, which often gives irreducible numerators, and then computing the maximal cut in this basis. We can also interpret the delta distribution $\delta(P_j)$ as a contour integration along a small circle around $P_j = 0$, and then compute the maximal cut from $n-$fold residues, as given in the eq.(3.4.2). To be noted that the phase u is not relevant as any solution of the homogeneous solution remains a solution upon multiplication with a constant.

The use of the maximal cut plays an important role in the identification of the elliptic curve present in it, as we already saw in the previous chapter. Using the loop by loop approach we can very quickly evaluate the integral representation for the maximal cut, from where we can identify the elliptic curve. The exact definition of the integration contour in the maximal cut is not relevant for the extraction of the elliptic curves as we are only interested in the integral form with the square root of a quartic or cubic polynomial in the denominator from which we can calculate the periods as explained before.

4.3 Canonical form for the differential equations

We are now familiar with the fact that the calculation of an arbitrary loop integral can always be reduced to the calculation of a finite set of master integrals [99]. Starting with a 'good' set of master integrals makes the task of evaluation of these master integrals very easy. Now it is obvious to ask what is a good basis to start with. Henn in [35] gave an idea of what can be a good starting point.

He used the concept of 'transcendentality' as a guiding principle since we work with differential operators. Let $\mathcal{T}(f)$ be the degree of transcendentality for a function f which is defined as the number of iterated integrals needed to define the function f, for eg., $\mathcal{T}(\epsilon) = -1$, $\mathcal{T}(log) = 1$, $\mathcal{T}(Li_n) = n$. Constants objects like ζ_n also have a degree of transcendentality equal to n. Algebraic functions have degree zero. The good master integrals are considered to be the ones having a uniform degree of transcendality, i.e. if f is a sum of terms, all summands have the same degree.

Consider the case of a set of M integrals, denoted by $\vec{I}$, depending on kinematic variables, s and t (put $m = 1$). In such case, the set of the differential equations looks like

$$d\vec{I}(s,t;\epsilon) = A(s,t;\epsilon)\,\vec{I}(s,t;\epsilon), \quad A = A_s\,ds + A_t\,dt, \tag{4.3.1}$$

where A_i denotes the differential equation with respect to the variable i. The matrix A has a dimension $M \times M$. These matrix-valued one-form satisfies the integrability condition:

$$dA - A \wedge A = 0.$$

or in other words,

$$\partial_s A_t - \partial_t A_s + [A_s, A_t] = 0, \tag{4.3.2}$$

where $[A,B] := AB - BA$. The matrix A depends on the variable s, t and ϵ in a rational way. In practice, we want to solve the eq. (4.3.1) as a Laurent expansion around $\epsilon = 0$. To do so, we can

change the basis

$$\vec{J}(s,t;\epsilon) \to U(s,t;\epsilon)\vec{I}(s,t;\epsilon), \tag{4.3.3}$$

to obtain

$$d\vec{J}(s,t;\epsilon) = A'(s,t;\epsilon)\vec{J}(s,t;\epsilon).$$

The matrix A transforms to A' as

$$A' \;=\; UAU^{-1} - U(dU^{-1}). \tag{4.3.4}$$

Using this technique one can transform to a basis of integrals where we obtain the form

$$d\vec{J'}(s,t;\epsilon) = \epsilon A''(s,t)\; \vec{J'}(s,t;\epsilon), \tag{4.3.5}$$

such that the dependence of the dimensional regulator ϵ completely factors out of the differential equations. This system of differential equations is 'fuchsian' in the sense that the singularities of this differential system are regular, i.e. the original Feynman integral grows only as a finite power at all the singularities of the system. This form for the differential equation for the master integrals is called the canonical form or the ϵ-$form$.

The differential equation is said to be in the $d$log-form if the matrix A'' can be written as,

$$dA(s,t) = A''(s,t), \tag{4.3.6}$$

with

$$A(s,t) = \sum_{l=1}^{N} A_l \log(L_l(s,t)), \tag{4.3.7}$$

where $L_l(s,t)$ denotes the polynomials in s and t and A_l are constant $M \times M$ matrices. The set of polynomials $\mathcal{A} = \{L_1(s,t),...,L_N(s,t)\}$ is referred to as the alphabet of the differential equation and the letters are given by the individual polynomials. We can immediately see that it solves the differential equation in terms of a path-ordered exponential

$$J' = Pe^{\epsilon \int_c dA''} J'(\epsilon = 0), \tag{4.3.8}$$

where the integration contour C connects the point representing the boundary condition to x_n. In other words, the perturbative solution in ϵ is given by iterated integrals where the entries of $d\,A''$ determine the integration kernels. In this way, we see that choosing an optimal choice of integral basis can make the integration of the system of differential equations trivial.

To give a very simple example in order to set up the basic idea, let us consider an integral I in one variable x with boundary condition $I(0) = 1$. Now, consider the differential equation

$$(d + A)\, I = 0,$$

with the one-dimensional matrix A given by -$\epsilon d\,\ln(x-1)$. We can quickly note that

$$d\,\ln(x-1) = \frac{dx}{x-1}$$

and which lets us write the solution immediately when we make an expansion $I = I_0 + \epsilon\, I_1 + \epsilon^2\, I_2 + ..$ and compare each of the terms in the series expansion.

$$I(x) = 1 + \epsilon\, G(1;x) + \epsilon^2\, G(1,1;x) + \epsilon^3\, G(1,1,1;x) + ...$$

Hence, we effectively bring the task of solving the integral to finding the correct master integrals or the correct transformation which brings the system of master integrals to the canonical form.

A big question to investigate is how to find these nice master integrals which satisfy this canonical form. One of the fundamental properties of a canonical form, which we can easily see from the eq. (4.3.5), is that the homogeneous part of the system of differential equations becomes trivial in the limit $\epsilon \to 0$. This implies that the homogeneous solution for $\epsilon = 0$ is constant. We are now familiar with the concept of maximal cuts and know that they give us the solution for the homogeneous differential equations. For the Feynman integrals which evaluate to MPLs, the maximal cut is an algebraic function, while in the case of integrals containing elliptic curves, they contain transcendental functions within them. For example, for the case of the sunrise integral, the maximal cut is given by a complete elliptic integral. One more clue is to obtained by evaluating the 'leading singularities' of the candidate integrals by inspecting their generalized cuts. The objects having constant leading singularities have the properties of uniform transcendentalities. Leading singularities are defined by analytically continuing the momenta to complex values and replacing the integration over space-time by contour integrals around poles of the integrand. A complete understanding of the concept of leading singularity is available only in the case of integrals that evaluate to MPLs (and their generalizations). The maximal cut is a natural starting point to extend these to more complicated cases. Another way to make these properties manifest is to get the 'd-log' representations, where the integrand is written as a logarithmic differential form.

Note: In the appendix, we take an example of a bubble graph and employ the above techniques to see how these methods are useful in solving a graph very easily.

4.4 Picard–Fuchs Equation

We already are a bit familiar with the differential equations corresponding to the case of elliptic curves. The Picard–Fuchs equation, named after Emile Picard and Lazarus Fuchs, is usually associated to be linear ordinary differential equation whose solutions describe the periods of elliptic curves. However, the same name is also used for generalizations, as will be clear in this section. Here, we wish to talk about the differential operator associated with this equation, with the motivation of being useful in the evaluation of Feynman integrals.

4.4.1 The formal definition

In [100], the authors showed that finding the ordinary differential equation for any Feynman integral is equivalent to solving a linear system of equations. Let us have a look at the method to get some general features of the Picard–Fuchs equation. Let us consider a Feynman Integral with l-loops and m external and n internal lines. We label the external momenta by $p_1, ..., p_m$ and the independent loop momenta by $k_1, ..., k_l$. We denote the Mandelstam variables by

$$s_{jk} = (p_j + p_k)^2, \quad 1 \leq j,k \leq m.$$

The set of kinematical invariants is given by $\{s_{ij}, m_i^2\}$ for the masses given by m_i with $1 \leq i \leq n$. The Feynman integral is given by

$$I = \frac{\prod_{j=1}^{n} \Gamma(\nu_j)}{\Gamma(\nu - lD/2)} (\mu^2)^{\nu - lD/2} \int \prod_{r=1}^{l} \frac{d^D k_r}{i\pi^{D/2}} \prod_{j=1}^{n} \frac{1}{(-q_j^2 + m_j^2)^{\nu_j}},$$

with $\nu = \nu_1 + ... + \nu_n$. Using Feynman parametrization, explained in section ⟨1.3.1⟩, gives us

$$I = \int_{\Delta} f\omega. \tag{4.4.1}$$

$$\Delta = \{[x_1 : x_2 : ... : x_n]\} \in \mathbb{P}^{n-1} | x_i \geq 0, 1 \leq i \leq n\}.$$

Here, ω is a differential $(n-1)$ form given by

$$\omega = \sum_{j=1}^{n} (-1)^{j-1} x_j \, dx_1 \wedge ... \wedge d\hat{x}_j \wedge ... \wedge dx_n, \tag{4.4.2}$$

where the corresponding term being omitted is displayed with a hat. The function f is given by

$$f(x_1, ..., x_n) = (\mu^2)^{\nu - lD/2} \Big(\prod_{j=1}^{n} x_j^{\nu_j - 1} \Big) \frac{\mathcal{U}^{\nu - (l+1)D/2}}{\mathcal{F}^{\nu - lD/2}}. \tag{4.4.3}$$

The graph polynomial $\mathcal{U}$ is independent of the kinematical invariants, while $\mathcal{F}$ depends linearly on the kinematical invariants, as we saw. Let t be an element from the set of kinematic invariants. We aim to get an ordinary differential equation with respect to the variable t for the Feynman integral. We look for a differential equation of the form

$$L^r \omega_t = d\beta \tag{4.4.4}$$

where ω_t is a $(n-1)$ form of homogeneous of degree $(1-n)$ in the variables x_i and is given by $\omega_t = f\omega$. $L^{(r)}$ is the Picard–Fuchs operator which is given by

$$L^{(r)} = \sum_{j=0}^{r} p_j \left(\mu^2 \frac{d}{dt} \right)^j. \tag{4.4.5}$$

The coefficients p_j may depend on the kinematical invariants from the set of invariants, the scale μ^2, the space-time dimension D and the exponents ν_i, but not on the Feynman parameters x_i. We can normalize the Picard–Fuchs operator such that $p_r = 1$. β is an $(n-2)$ form which depends on the Feynman parameters x_i. Assuming a form as shown in eq. (4.4.4) exists, we can integrate it to get

$$L^{(r)} I = \int_{\Delta} d\beta \tag{4.4.6}$$

We can apply Stokes'theorem to this equation (which is applicable within dimensional regularization), to obtain

$$L^{(r)} I = \int_{\partial\Delta} \beta. \tag{4.4.7}$$

This is the required ordinary differential equation for I. It is a differential operator of order r in the variable t. The right-hand side is given as a sum of integrals with (n-1) Feynman parameters and

hence are considered simpler. These integrals correspond to graphs which have one propagator less than the integral I and hence can be considered simpler. Knowing these simpler integrals along with the boundary conditions corresponds to obtaining the Feynman integral I, by solving the differential equations. The task of actually finding the differential equation is a bit cumbersone. It can be reduced to solving linear equations as follows: the unknown quantities in this equation are r, $p_j(0 \leq j \leq r)$ and the differential form β. One can start with $r = 1$ and an ansatz for the coefficients p_j and the differential form β. This ansatz gives us a system of linear equations. We can check for the solution for this sytem, and in case it does not exist we can repeat the same step for $r+1$. For finite integrals in even integer space time dimensions this method of solving the ansatz is guaranteed to work. Hence the problem of finding the differential equation gets effectively reduced to solving linear equations. Here we can explicitly see that the eq. (4.4.5) is of Fuchsian type if all coefficients p_j are meromorphic functions of t and if p_j has at most poles of order $(r-j)$.

4.4.2 Application of Picard–Fuchs operator

After a general overview of Picard–Fuchs operator, we now discuss an algorithm which explains the method of utilizing the factorization properties of this operator to decouple differential equations for multi-scale Feynman integrals. The algorithm reduces the differential equations to blocks of size of the order of the irreducible factors of the Picard–Fuchs operator. This also presents a way in which the differential equations for Feynman integrals evaluating to MPLs can be brought to an ϵ-form. Consider a Picard–Fuchs operator of the form

$$L = \sum_{j=0}^{r} p_j(\lambda) \frac{d^j}{d\lambda^j}. \tag{4.4.8}$$

Let us now consider the case in when this operator factorizes into linear factors:

$$L = \Big(a_r(\lambda)\frac{d}{d\lambda} + b_r(\lambda)\Big) \ldots \Big(a_2(\lambda)\frac{d}{d\lambda} + b_2(\lambda)\Big)\Big(a_1(\lambda)\frac{d}{d\lambda} + b_1(\lambda)\Big). \tag{4.4.9}$$

Such a differential equation can be easily solved and the answer can be written down easily in terms of iterated integrals. Let the j-th factor of the differential operator be given by (can be seen when expanded to first order),

$$\psi_j(\lambda) = exp\Big(-\int_0^\lambda d\kappa \frac{b_j(\kappa)}{a_j(\kappa)}\Big). \tag{4.4.10}$$

The full solution is written as

$$\begin{aligned} f(\lambda) =& C_1\psi_1(\lambda) + C_2\psi_1(\lambda)\int_0^\lambda d\lambda_1 \frac{\psi_2(\lambda_1)}{a_1(\lambda_1)\psi_1(\lambda_1)} \\ &+ C_3\psi_1(\lambda)\int_0^\lambda d\lambda_1 \frac{\psi_2(\lambda_1)}{a_1(\lambda_1)\psi_1(\lambda_1)}\int_0^{\lambda_1} d\lambda_2 \frac{\psi_3(\lambda_2)}{a_2(\lambda_2)\psi_2(\lambda_2)} + \ldots . \end{aligned} \tag{4.4.11}$$

Hence it is evident that it can be expressed in terms of MPLs, for rational a_i and b_i. There are cases when this differential operator cannot be factorized and contains irreducible differential operators like

$$a_j(\lambda)\frac{d^2}{d\lambda^2} + b_j(\lambda)\frac{d}{d\lambda} + c_j(\lambda). \tag{4.4.12}$$

Let us consider the example of the differential operator:

$$\left[\lambda(1-\lambda^2\frac{d^2}{d\lambda^2}+(1-3\lambda^2)\frac{d}{d\lambda}-\lambda)\right]f(\lambda)=0 \tag{4.4.13}$$

This second-order differential operator is irreducible (i.e. cannot be factorized any further). The solutions of this differential equations are $K(\lambda)$ and $K(\sqrt{1-\lambda^2})$, where $K(\lambda)$ is the complete elliptic integral of the first kind:

$$K(\lambda)=\int_0^1 \frac{dx}{\sqrt{(1-x^2)(1-\lambda^2x^2)}}. \tag{4.4.14}$$

This is a clear way of observing how an elliptic integral occurs naturally in Picard–Fuchs equations.

4.4.2.1 The physical motivation

In the calculation of scattering processes with massive particles, it is very common that within one topology we have several master integrals, coupled together at order ϵ^0 by differential equations. Denoting the number of master integrals by N, we see that, for example, for the $2\to 2$ processes at NNLO, it is not unsual that we have topologies with 5 master integrals. Solving a coupled system of N differential equations is a nasty task, but to some relieve, there are indications that topologies with three or more master integrals can be decoupled into blocks of size 2×2 at worse [24–28]. It is hence very obvious to ask if there exists a systematic method which transforms a system into an equivalent system, where at order ϵ^0 the differential equations split into small blocks. Now we discuss the algorithm which completes this task [49].

4.4.2.2 The framework for the differential equation

We consider the master integrals in $D=2m-2\epsilon$ space-time dimensions, with $m\in\mathbb{Z}$ and ϵ being the dimensional regularization parameter. As usual, we use IBPs to derive a set of differential equations of Fuchsian type

$$d\vec{I}=A\vec{I},$$

with A being a matrix values one-form

$$A=\sum_{i=1}^{N}A_i\,dx_i.$$

The other properties follow from section ⟨4.3⟩. We assume that A has an ϵ-expansion

$$A=\sum_{j\geq 0}\epsilon^j A^{(j)}=\sum_{i=1}^{n}\sum_{j\geq 0}\epsilon^j A_i^{(j)}dx_i. \tag{4.4.15}$$

Our aim is to solve the differential equations order by order in ϵ. Here, the term $A^{(0)}$ which is constant in ϵ plays a crucial role. With the higher terms $A^{(j)}$ with $(j\geq 1)$, we only get additional integration over lower-order expressions. Therefore we specifically are interested in a transformation which simplifies $A^{(0)}$. We can change the basis for the master integrals

$$\vec{J}=U\vec{I},$$

to obtain

$$d\vec{J} = \tilde{A}\vec{J},$$

where, as explained before, $\tilde{A}$ is related to A by

$$\tilde{A} = UAU^{-1} - UdU^{-1}. \tag{4.4.16}$$

Here we have dropped the explicit dependence on the parameters. The master integrals are expressible in terms of MPLs if there is a transformation U such that $\tilde{A}^{(0)} = 0$ and $\tilde{A} = d\log(L)$, where L denotes the polynomial in the invariants. Also, as discussed before, the matrix A has a natural lower block triangular structure, which derives from the top topology and its sub-topologies. The inclusion of sub-topologies only leads to integration over already determined terms, therefore **we work modulo sub-topologies**.

Let us assume that a particular top topology has N master integrals. If we consider the case where no transformation U exists, such that $\tilde{A}^{((0)} = 0$, we might think that at order ϵ^0, we have a coupled system of N differential equations (and therefore a mess!), but often it the case that the system decouples into blocks of smaller size. This can be done by exploiting the factorization properties of the Picard–Fuchs operator for the integral [49]. Let us now look at how we achieve this.

4.4.2.3 The technique to decouple the coupled differential system

The algorithm for using the Picard–Fuchs operator to decouple the system coupled at ϵ^0 can be divided into five steps:

- We reduce a multi-scale problem to a single-scale problem with scale λ.
- We pick a master integral I and determine at order ϵ^0 and modulo sub-topologies the maximal number of independent derivatives I, $\left(\frac{d}{d\lambda}\right) I$,..., $\left(\frac{d}{d\lambda}\right)^{r-1} I$. This defines the Picard–Fuchs operator of order r for us. For $r < N$, the system decouples into a system of r master integrals and $(N-r)$ master integrals.
- Let us look at the sector with r master integral. Now we factorize the Picard–Fuchs operator for this sector.
- We then construct the transformation using this factorized Picard–Fuchs operator. This decouples the system into blocks of the size of the order of the irreducible factors of the Picard–Fuchs operator.
- In the last step, we reconstruct the multi-variable transformation matrix from the single-variable one.

Let us go through each of the points above separately and elaborate on them.

1. From a multi-scale to a single-scale problem: Let us consider a set of master integrals $I_1, I_2, ..., I_N$ depending on kinematic variables $x_1, x_2, ..., x_n$. The ordered set of master integrals is denoted by the vector $\vec{I} = (I_1, I_2, ..., I_N)$. If we have only one kinematic variable x_1, it is called a single-scale problem, whereas for two or more kinematic variables ($n \geq 2$), we have a multi-scale problem. Let $\alpha = [\alpha_1 : ...\alpha_n] \in \mathbb{C}\,\mathbb{P}^{n-1}$ be a point in projective space.

Without loss of generality we can set $\alpha_n = 1$. We then consider a path $\gamma_\alpha : [0,1] \to \mathbb{C}^n$ which is parametrized by a variable λ and indexed by α. We have,

$$x_i(\lambda) = \alpha_i \lambda, \quad 1 \leq i \leq n. \tag{4.4.17}$$

The master integrals are viewed as functions of λ, in other words, we look at the variation of the master integrals in the direction specified by α. The derivative with respect to λ is given by

$$\frac{d}{d\lambda}\vec{I} = B\vec{I}, \quad B = \sum_{i=1}^{n} \alpha_i A_i. \tag{4.4.18}$$

The transformed matrix is also given by a Taylor expansion in ϵ:

$$B = B^{(0)} + \sum_{j>0} \epsilon^j B^{(j)}. \tag{4.4.19}$$

2. Consider one of the master integrals I from $\vec{I}$. Using eq. (4.4.18) we can express the k-th derivative of I with respect to λ as a linear combination of the original master integrals. We now determine the largest number r, such that the matrix which expresses I, $(d/d\lambda)$ I,..., $(d/d\lambda)^{r-1}$ I in terms of the original set $\{I_1, ..., I_N\}$ has full rank, where $r \leq N$. For the case $r < N$, we complement the set $I, (d/d\lambda)I, ..., (d/d\lambda)^{r-1}$ by $(N-r)$ elements $I_{\sigma_{r+1}}, ..., I_{\sigma_N} \in \{I_1, ..., I_N\}$ such that the transformation matrix has rank N. This already decouples the system into a block of size r, which is closed under differentiation at order ϵ^0 module sub-topologies and a remaining sector of size $(N-r)$.

3. Now we investigate the conditions under which the block of size r can be decomposed further. We see that $(d/d\lambda)^r I$ can be written as a linear combination of $I, (d/d\lambda)$ $I, ..., (d/d\lambda)^{r-1}$ I. This gives us the Picard–Fuchs operator L_r for the master integral I with respect to λ:

$$L_r I = 0, \quad L_r = \sum_{k=0}^{r} R_k \frac{d^k}{d\lambda^k}, \tag{4.4.20}$$

where R_k are rational functions in λ and we have normalized $R_r = 1$. The Picard–Fuchs operator L_r often factorizes

$$L_r = L_{1,r_1} L_{2,r_2} ... L_{s,r_s}, \tag{4.4.21}$$

where L_{i,r_i} denotes a differential operator of order r_i. Obviously $r_1 + ... + r_s = r$. For the case of linear factors, i.e. when the Picard–Fuchs operator L_r factorizes completely into linear factors, we get

$$L_r = L_{1,1} L_{2,1} ... L_{r,1} \tag{4.4.22}$$

with

$$L_{i,1} = \frac{d}{d\lambda} + R_{i,0}.$$

4. The factorization can be used to convert the system of differential equations into a block triangular form, at order ϵ^0, with the sizes of the blocks given by $r_1, r_2, ..., r_s$. A basis for block i is given by

$$J_{i,j} = \frac{d^{j-1}}{d\lambda^{j-1}} L_{i+1,r_{i+1}} ... L_{s,r_s} I, \quad 1 \leq j \leq r_i. \tag{4.4.23}$$

For the case of linear factors, we use the transformation,

$$J_{i,1} = exp\left(\int^{\lambda} d\tilde{\lambda} R_{i,0}\right) L_{i+1,1}...L_{r,1} I$$

to bring the system to an equivalent system with $\tilde{A}^{(0)} = 0$. The elements of the transformed matrix is related to the original integrals $\vec{I}$ is given by

$$\vec{J} = V\vec{I},$$

where $\vec{J} = (J_{1,1},...,J_{1,r_1}J_{2,1},...,J_{s,r_S})$. V is a function of parameters α and λ.

5. If we set

$$U = V\left(\frac{x_1}{x_n},...,\frac{x_{n-1}}{x_n},x_n\right), \tag{4.4.24}$$

we get the transformation in terms of the original variables $x_1,...,x_n$.

Note: There might be some terms in the original A, which map to zero in B for the class of paths we consider in eq. (4.4.17). These terms are the ones that have derivatives constant on lines through the origin. For example, $d \ln Z(x_1,...,x_n)$, where $Z(x_1,...,x_n)$ is a rational function in $(x_,...,x_n)$ and homogeneous of degree zero in $(x_1,...,x_n)$. These terms do not contribute while integrating the system of differential equations along the path of eq. (4.4.17) and they can also be easily removed by a subsequent transformation.

4.4.2.4 Examples

Now we look at some topologies which contain hints for being elliptic and apply the above formalism to find the tricks to decouple the coupled system at order ϵ^0 in sizes of 2×2 at worst.

Example 1: No new elliptic integration introduced Consider the example of a two-loop four-point integral with six propagators, $I_{\nu_1,\nu_2,\nu_3,\nu_4,\nu_5,\nu_6,\nu_7}$, where ν_i denotes the power to the propagator i, as shown in the figure

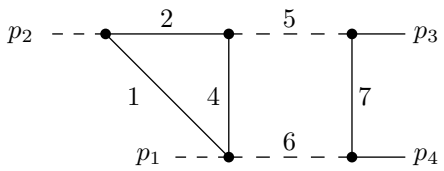

Figure 4.2. A two-loop four-point integral with six propagators.

Internal solid lines in this figure correspond to mass m, dashed lines to mass zero. The external momenta are on-shell, $p_1^2 = p_2^2 = 0$ and $p_3^2 = p_4^2 = m^2$. The Mandelstam variables are given by $s = (p_1 + p_2)^2$ and $t = (p_2 + p_3)^2$. We may choose two dimensionless variables as

$$s = -m^2\frac{(1-x_1)^2}{x_1}, \quad t = -m^2 x_2. \tag{4.4.25}$$

This integral has an elliptic sub-topology which is obtained by pinching propagators 2,5 and 6. The topology shown here has two master integrals, which we choose as

$$\vec{I} = \Big((1+2\epsilon)\, I_{1101111}, I_{1101211} \Big), \tag{4.4.26}$$

where we chose the pre-factor in front of the first master integral to ensure that only $A^{(0)}$ and $A^{(1)}$ occur in the ϵ-expansion of A. The Picard–Fuchs operator for the first master integral is of order 2 and factorizes into linear factors:

$$L_2 = \left(\frac{d}{d\lambda} + \frac{1}{\lambda+1} + \frac{2\alpha_1}{\alpha_1\lambda-1} + \frac{2\alpha_1\lambda}{\alpha_1\lambda^2+1} - \frac{2\alpha_1\lambda}{\alpha_1\lambda^2-1}\right)\left(\frac{d}{d\lambda} - \frac{1}{\lambda} + \frac{1}{\lambda+1} + \frac{2\alpha}{\alpha_1\lambda-1}\right). \tag{4.4.27}$$

This factorization can, for example, be obtained with the help of the command "DFactor" in Maple. Therefore, we may now transform to a basis where $\tilde{B}^{(0)}$ is lower triangular with zeroes on the diagonal. The entry on the lower-left corner of $\tilde{B}^{(0)}$ has only single poles and is removed by re-scaling the first master integral with $(1+2\epsilon)$ and the second master integral by ϵ, which brings the system (in the variable λ) to $\epsilon-$form. Going back to the original variables, we get

$$\tilde{A} = \begin{pmatrix} 1 & 0 \\ 0 & 1 \end{pmatrix} d\ln\left(\frac{x_1}{x_2}\right) + \epsilon\tilde{A}^{(1)}.$$

The ϵ^0-term is easily removed by multiplying both master integrals by x_2/x_1. Overall, we find that

$$U = \begin{pmatrix} U_{11} & -\frac{(1+2\epsilon)(x_1-1)^3(x_2+1)^2}{2x_1(x_1+1)} \\ \frac{\epsilon(x_2+1)(x_1-1)^2}{x_1} & 0 \end{pmatrix},$$
$$U_{11} = \frac{(1+2\epsilon)(x_1-1)\left(x_2^2x_1+x_2x_1^2+x_2-x_1^2+3x_1-1\right)}{2x_1(x_1+1)}$$

and the transformed system is given by

$$\begin{aligned}\tilde{A} = \epsilon\Bigg[&\begin{pmatrix} 2 & 0 \\ 0 & 0 \end{pmatrix} d\ln(x_1+1) - \begin{pmatrix} 2 & 0 \\ 0 & 2 \end{pmatrix} d\ln(x_1-1) \\ &- \begin{pmatrix} 0 & 0 \\ 0 & 2 \end{pmatrix} d\ln(x_2+1) + \begin{pmatrix} 0 & 0 \\ -1 & 1 \end{pmatrix} d\ln(x_1+x_2) \\ &+ \begin{pmatrix} 0 & 0 \\ 1 & 1 \end{pmatrix} d\ln(x_1x_2+1)\Bigg].\end{aligned}$$

So, we see that this topology can be transformed to $\epsilon-$ form and does not introduce new elliptic integrations.

Example 2: Elliptic integration within the sector needed We now look at a more involved topology as shown in the figure 4.3. This is an example of a two-loop four-point integral with five propagators. The kinematics is the same as in our first example. This topology has five master integrals. As our initial basis, we take

$$\vec{I} = (\epsilon I_{1011101}, I_{2011101}, I_{1021101}, I_{1012101}, I_{1011201}).$$

Again we choose the pre-factors to ensure that only $A^{(0)}$ and $A^{(1)}$ appear in the ϵ-expansion of A. For this system, this also happens to decouple the first master integral $I_1 = \epsilon I_{1011101}$ at order ϵ^0 from the remaining ones. Therefore, we have to consider only a 4×4-system. Let us pick $I_2 = I_{2011101}$. Working modulo ϵ-terms, we find that already the third derivative of I_2 can be

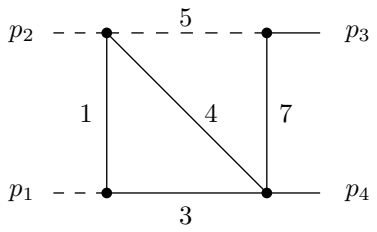

Figure 4.3. A two-loop four-point integral with five propagators.

expressed as a linear combination of the lower ones. Adding $I_5 = I_{1011201}$ to $I_2, (d/d\lambda)I_2, (d/d\lambda)^2 I_2$ will give a transformation matrix of full rank. This decouples I_5 from the 3×3-system formed by $I_2, (d/d\lambda)I_2, (d/d\lambda)^2 I_2$. The Picard–Fuchs operator for I_2 is therefore of order 3. It factorizes into a second-order operator and a first-order operator:

$$L_3 = \quad L_2 L_1.$$

As a result, we see that the 3×3-system gets decoupled into a 2×2-system and a 1×1-system. The 2×2-system is irreducible. When lifting the result from the single-scale case to the multi-scale case with the variables $\{x_1, x_2\}$ we again perform an additional transformation, which removes $d\ln(x_1/x_2)$-terms. In summary, we are able to decompose the five master integrals for this topology at order ϵ^0 in blocks of size

$$1, 2, 1, 1.$$

The explicit expressions are longer, however, we may display the structure of $\tilde{A}$. We have

$$\tilde{A} = \begin{pmatrix} 0 & 0 & 0 & 0 & 0 \\ 0 & * & * & 0 & 0 \\ 0 & * & * & 0 & 0 \\ 0 & * & * & 0 & 0 \\ 0 & * & * & 0 & 0 \end{pmatrix} + \epsilon \tilde{A}^{(1)},$$

where $*$ indicates a non-zero entry. In this example, we see that $A^{(0)}$ cannot be transformed to zero by rational transformations and we find an irreducible 2×2-system at order ϵ^0. Nevertheless, we still achieved to simplify the original 5×5-system to smaller blocks.

4.5 Algorithms for obtaining the canonical form

In this section, we wish to briefly mention the various algorithms we may use in order to obtain the canonical form for the differential equation for the master integrals.

1. Choice of coordinate system: Choosing a good coordinate system to get the differential equation, is one of the key tricks in order to efficiently solve the differential equations. Often the most naive choice turns out to be a bad one as we are stuck we a lot of square roots in our differential system. We then need to change our differential equations to the ones with respect to a smarter choice. For the case of multiple polylogarithms, this smart choice would be the coordinate system which rationalizes all the occurring square roots simultaneously. There exists an algorithm which we can use to rationalize our square roots simultaneously.

The authors in [101] present an algorithm to be applicable in the physics community, that rationalized a given square root by first associating an algebraic hypersurface to the root and then parametrizing this hypersurface by and n-parameter family of lines, n denoting the number of variables in the root.

However, rationalizing square roots increases the degree of the polynomials in intermediate stages of the calculation. In order to handle this, we can choose to work bottom-up and treat each sub-topology in a coordinate system that is best suited to this sub-topology, this is the method we have followed in order to solve the two topologies mentioned in the next chapters. We now briefly explain the various algorithms available in literature which we can use to bring our system of differential equation to a canonical form (or linear form).

2. Roman Lee's algorithm: The Lee algorithm is based on the Moser reduction algorithm [102] in order to find a Fuchsian form for the differential system. In order to find the canonical form one then needs to normalize the eigenvalues of the Fuchsian system in all singular points. Few public implementations of this algorithm are present in [103, 104]. However, this algorithm can only be used for single scale applications.

3. Christoph Meyer's algorithm: Christoph Meyer in [105] presented an algorithm which is applicable to problems involving multiple scales. Both of these algorithms need the existence of a rational transformation, in order to obtain the canonical form for the differential equation for the master integrals.

4. The Magnus expansion method: For a differential equation of the form

$$\partial_x J(\epsilon, x) = A(\epsilon, x) J(\epsilon, x),$$

for a vector J of the master integrals, and x depends on the kinematic variable and the masses. We can change this basis via the Magnus series obtained using A_0 as the kernel where A_0 is the ϵ^0 part of the differential matrix A,

$$J(\epsilon, x) = B_0(x) I(\epsilon, x),\ B_0(x) = exp[\Omega[A_0](x, x_0)].$$

Here $\Omega(x)$ is the Magnus expansion and x_0 is the boundary point. Using this we can obtain the canonical form in the vector $I(\epsilon, x)$ [106].

5. In [22], it was shown that the canonical form can even be achieved for the cases where rational transformation does not exist, in particular for the sunrise/kite system. This can be down if one allows algebraic functions in the kinematic variables, periods of the elliptic curves and their derivatives to occur in the transformation equation. It is easier a smart idea to relax the condition of a canonical form (i.e. proportional in the dimensional regulator) and allow constants in the ϵ to appear in the differential equation, on the condition that the matrix corresponding to this part is strictly lower triangular. This does not break the property that we are able to write down the master integral as an iterated integral. On the other hand, it saves us from introducing additional transcendental functions. This form is called the **linear form** for the differential equation. Since the matrix constant in ϵ is strictly lower triangular we can easily transform to a canonical form by introducing primitives for the terms in this matrix. In the case of elliptic multi-scale integrals, this method terms out to be quite convenient to write down the results.

4.6 Boundary Conditions

The last but equally important step in solving a differential equation is to acquire knowledge about the boundary conditions. This section is devoted to that task. In order to solve the differential equations, we also require the boundary value, for which we take carry out the following steps.

1. We can in principle evaluate the boundary conditions independently of the differential equations, by calculating the integral at a preferred kinematic point. It is useful to express these boundary constants in a basis of transcendental constants suitable for our representation. A good basis of transcendental constants up to weight four is also shown in the next chapter. We can obtain the coefficients of these constants using the PSLQ algorithm.

2. Often a master integral vanishes or reduces to simpler integrals at a specific point. Choosing these points as the boundary points provide us the boundary constants for those integrals. Also, the master integrals often have boundary constants which are products of one-loop integrals and can be easily computed. One such example which the master integral is often a product of is the tadpole integral.

$$T_\nu\left(D,m^2,\mu^2\right) = e^{\gamma_E\epsilon}\left(\mu^2\right)^{\nu-\frac{D}{2}} \int \frac{d^Dk}{i\pi^{\frac{D}{2}}} \frac{1}{\left(-k^2+m^2\right)^\nu} \;=\; e^{\gamma_E\epsilon}\frac{\Gamma\left(\nu-\frac{D}{2}\right)}{\Gamma(\nu)}\left(\frac{m^2}{\mu^2}\right)^{\frac{D}{2}-\nu}. \tag{4.6.1}$$

   For $D = 2-2\epsilon$, $\mu = m$ and $\nu = 1$ we have

$$T_1(2-2\epsilon) = e^{\gamma_E\epsilon}\Gamma(\epsilon) \;=\; \frac{1}{\epsilon}\left[1+\frac{1}{2}\zeta_2\epsilon^2-\frac{1}{3}\zeta_3\epsilon^3+\frac{9}{16}\zeta_4\epsilon^4+O\left(\epsilon^5\right)\right].$$

   This is also shown in the next chapter.

3. The differential equations themselves also give insights regarding the choice of a boundary condition. One can study the singularity structure explicit in the differential equation which in many cases allows us to determine the boundary conditions without explicit calculation.

5 Planar double box with a closed top loop

Contents

5.1 Physical importance

The top quark has been in or near the center of attention in high-energy physics since its discovery in 1995. It couples strongly to the agents of electroweak symmetry breaking because of the large mass, $m_t = 173 \pm 1.3 GeV$, making it both an object of interest itself, as well as a tool to investigate the Higgs mechanism in detail. Top quark pair production at hadron colliders is amongst the

most challenging processes to the theory. The large production rate of the top quark at the CERN LHC and the decay gives rise to several jets or leptons which is required for testing the Standard Model of particle physics at an unprecedented level, and also for uncovering indirect evidence for new physics. Top-quark production can also be used to determine the top-quark mass, the strong coupling constant α_s, and the gluon parton distribution functions. Therefore, it is highly important to have a precise understanding of this process. Higher-order perturbation theory for top-quark observables requires precise multi-loop and multi-scale computations. At a fixed loop Feynman integrals depending on multiple scales often turn out to be a bottleneck. A prominent example for this is given by the planar double box integral to $t\bar{t}$ production with a closed top loop 5.1, which we discuss in this chapter.

5.1.1 State of the art

The total cross sections and differential distributions of the top-quark pair production have been in focus for quite some time now. Some of the results in this area are as follows: The numerical results for the NNLO calculation for the process $pp \to t\bar{t}$ were presented in [50–53, 55]. The analytic results are valuable in the sense that they provide a faster and stable evaluation of the virtual corrections and to understand the structure of the loop integral. In [56], the authors presented the master integrals of a planar double-box family for top-quark pair production and in [54], they calculated all the non-planar two-loop functions required for the quark initiated channel $q\bar{q} \to t\bar{t}$ at NNLO in QCD, both of these gave rise to multiple polylogarithms. The technique for solving the diagram 5.1 which consisted of elliptic curve(s) was shown in [22] and the full analytic results for the diagram were published for the first time in [48].

5.2 Set-up for solving the master integrals

The integral shown below enter the next-to-next-to-leading order (NNLO) contribution for the process $pp \to t\bar{t}$.

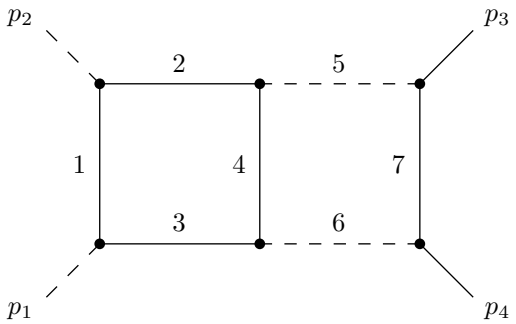

Figure 5.1. The planar double box with a massive top quark loop.

5.2.1 Kinematical set-up

The solid lines denote massive propagators of mass m, dashed lines correspond to massless propagators. All external momenta are taken to be out-going and on-shell.

$$p_1^2 = p_2^2 = 0 \quad \text{and} \quad p_3^2 = p_4^2 = m^2$$

From momentum conservation we have,

$$p_1 + p_2 + p_3 + p_4 = 0.$$

The Mandelstam variables in our system are

$$s = (p_1 + p_2)^2, \quad t = (p_2 + p_3)^2 \quad u = (p_2 + p_4)^2,$$

with $s + t + u = 2m^2$. We can see from the topology that it contains the sunrise graph as a sub-topology (by pinching propagators 2,3,5 and 6), which makes us expect the presence of functions beyond multiple polylogarithms. Also, the presence of two scales, s and t, along with massive internal propagators makes it a comparatively difficult diagram to tackle, in the field of Feynman integral computations. In order to solve this topology, i.e. to write it as a Laurent expansion in the dimensional regulator, we chose the method of differential eq. 4. As mentioned in 4.5, we relax the form of the differential equation slightly and consider

$$d\vec{J} = (A^{(0)} + \epsilon A^{(1)})\vec{J}, \tag{5.2.1}$$

where A^0 is strictly lower-triangular and $A^{(0)}$ and $A^{(1)}$ are independent of ϵ. We stress again the following two points:

- this linear form does not spoil the property that the system of differential equations is solved in terms of iterated integrals,
- the choice of $\vec{J}$ is not unique. This chapter discusses **one particular choice** in order to solve the system of differential equations for the master integrals in this system.

For differential one-forms in our system, we introduce the notation

$$\omega_j = \sum_{r=1}^{r_j} c_{j,r} \frac{dy}{y - z_{j,r}} \tag{5.2.2}$$

where $G(\omega_1, ..., \omega_k; y)$ is the integral representation of MPLs defined recursively through

$$G(\omega_1, \omega_2, ..., \omega_k; y) = \sum_{r=1}^{r_1} c_{1,r} \int_0^y dy_1 \, g(z_{1,r}, y_1) \, G(\omega_2, ..., \omega_k; y_1). \tag{5.2.3}$$

In our topology, 5.1, we have two independent loop momenta and three independent external momenta. Therefore we have nine independent scalar products involving the loop momenta. So, we need to consider an auxiliary topology, with nine propagators, which are sufficient to express all the independent scalar products. One possible choice for such a topology, which we consider in this calculation is shown in figure 5.2.

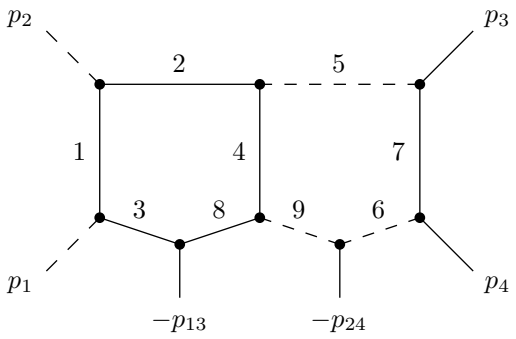

Figure 5.2. The auxiliary topology with nine propagators.

The integral family for this auxiliary topology is given in D-dimensional Minkowski space by

$$I_{\nu_1\nu_2\nu_3\nu_4\nu_5\nu_6\nu_7\nu_8\nu_9}\left(D,s,t,m^2,\mu^2\right) = e^{2\gamma_E\epsilon}\left(\mu^2\right)^{\nu-D}\int\frac{d^Dk_1}{i\pi^{\frac{D}{2}}}\frac{d^Dk_2}{i\pi^{\frac{D}{2}}}\prod_{j=1}^{9}\frac{1}{P_j^{\nu_j}}, \tag{5.2.4}$$

where γ_E denotes the Euler-Mascheroni constant, μ is an arbitrary scale introduced to keep the Feynman integral dimensionless, the quantity ν is given by

$$\nu = \sum_{j=1}^{9}\nu_j$$

and the set of propagators for the auxiliary topology are

$$\begin{aligned}
&P_1 = -(k_1+p_2)^2+m^2, \quad && P_2 = -k_1^2+m^2, && P_3 = -(k_1+p_1+p_2)^2+m^2,\\
&P_4 = -(k_1+k_2)^2+m^2, && P_5 = -k_2^2, && P_6 = -(k_2+p_3+p_4)^2,\\
&P_7 = -(k_2+p_3)^2+m^2, && P_8 = -(k_1+p_2-p_3)^2+m^2, && P_9 = -(k_2-p_2+p_3)^2,
\end{aligned} \tag{5.2.5}$$

with $p_{ij} = p_i + p_j$. We obtain the original double box integral by putting $\nu_8 = \nu_9 = 0$. For the Laurent expansion, we write,

$$I_{\nu_1\nu_2\nu_3\nu_4\nu_5\nu_6\nu_7}(4-2\epsilon) = \sum_{j=j_{\min}}^{\infty}\epsilon^j\, I^{(j)}_{\nu_1\nu_2\nu_3\nu_4\nu_5\nu_6\nu_7},$$

where we suppress ν_8 and ν_9 and the explicit dependence on mandelstam variables, masses and μ is assumed.

Graph Polynomial: The graph polynomial for our topology 5.1 is given by

$$\begin{aligned}
\mathcal{U} &= (x_1+x_2+x_3)(x_5+x_6+x_7)+x_4(x_1+x_2+x_3+x_5+x_6+x_7),\\
\mathcal{F} &= [x_2x_3(x_4+x_5+x_6+x_7)+x_5x_6(x_1+x_2+x_3+x_4)+x_2x_4x_6+x_3x_4x_5]\left(\frac{-s}{\mu^2}\right)\\
&\quad + x_1x_4x_7\left(\frac{-t}{\mu^2}\right)+x_7[(x_2+x_3)x_4+(x_5+x_6)(x_1+x_2+x_3+x_4)]\left(\frac{-m^2}{\mu^2}\right)\\
&\quad +(x_1+x_2+x_3+x_4+x_7)\mathcal{U}\frac{m^2}{\mu^2},
\end{aligned}$$

where, in the expanded form, the graph polynomial $\mathcal{U}$ looks like

$$\begin{aligned}\mathcal{U} =& x_1x_5 + x_1x_6 + x_1x_7 + x_2x_5 + x_2x_6 + x_2x_7 + x_3x_5 + x_3x_6 + x_3x_7 \\ &+ x_1x_4 + x_2x_4 + x_3x_4 + x_4x_5 + x_4x_6 + x_4x_7.\end{aligned}$$

In the appendix, we also have a look at all the contributing master topologies for this graph.

5.2.2 Modular weight

The topology 5.1 contains not one but three different elliptic curves, which we show explicitly in section ⟨5.3.2⟩. However, at this stage, we would like to discuss the concept of modular weight and the usage in our calculation. We can infer the concept of modular weight from the scaling behaviour under a re-scaling of the periods. Let our graph contain three elliptic curves, with periods, $\psi_1^{(a)}, \psi_1^{(b)}$, and $\psi_1^{(c)}$. Then we have

$$\text{modular weight} = \quad \text{scaling power} + 2,$$

where the additional 2 is due to the Jacobian we obtain after replacing dy by $d\tau_6^r$, where $r \in \{(a),(b),(c)\}$.

We may view the entries of the differential equation in eq. (5.2.1),

$$A = \quad A^{(0)} + \epsilon A^{(1)}$$

as differential one-forms rational in

$$\epsilon, \tilde{x}, y, \psi_1^{(a)}, \psi_1^{(b)}, \psi_1^{(c)}, \partial_y\psi_1^{(a)}, \partial_y\psi_1^{(b)}, \partial_y\psi_1^{(c)},$$

where $\tilde{x}$ and y are the good choice of coordinates to represent the differential equations for our system. We also observe that each entry of A is homogeneous under a simultaneous re-scaling of all periods and their derivatives

$$\psi_1^{(r)} \to \lambda\, \psi_1^{(r)},\ \partial_y\psi_1^{(r)} \to \lambda\, \partial_y\psi_1^{(r)}, \qquad r \in \{a,b,c\}.$$

This allows us to group the entries of A according to the scaling behavior under a simultaneous re-scaling of all periods and their derivatives.

5.2.3 Master integrals

For our differential system, we need to evaluate 44 master integrals. The set of integrals having the linear form in ϵ is denoted by $\vec{J}$. We construct this basis J as follows: The master integrals, which only depend on s do not pose any problems and are constructed with the algorithms mentioned in section ⟨4.5⟩. The master integrals which only depend on t are similar to the kite/sunrise system and are constructed along the lines of [27, 28, 57–59, 73]. The master integrals which depend on both s and t are the most complicated ones. In such cases, we follow the following steps: for the diagonal blocks, we use the method of Picard-Fuchs operators, mentioned in section ⟨4.4⟩, where we also explicitly showed the algorithm and applied to few sub-topologies related to our case, and combine it with the information from the maximal cuts (discussed in 4.2). For the non-diagonal blocks, we follow the algorithm of Meyer [105], which is a method to construct the canonical form for the differential equation for our set of integrals, however we modify the algorithm a little in

order to obtain the linear form for differential equation, for the non-diagonal blocks and this fixes the sub-topologies for our differential system.

In the basis $\vec{J}$, the system of differential equations is linear in ϵ, i.e. of the form

$$d\vec{J} = (A^{(0)} + \epsilon A^{(1)})\vec{J}. \tag{5.2.6}$$

The matrices $A^{(0)}$ and $A^{(1)}$ are independent of ϵ. Furthermore, $A^{(0)}$ is strictly lower-triangular, i.e.

$$A^{(0)}_{ij} = \quad 0 \quad \text{for} \quad j \geq i.$$

and follows from the set up of the differential equation, $A^{(1)}$ is block-triangular.

5.3 Coordinate system and differential forms

We may view the integrals $I^{(j)}_{\nu_1\nu_2\nu_3\nu_4\nu_5\nu_6\nu_7}$ as functions on $M = \mathbb{P}^2(\mathbb{C})$, where $\left[s : t : m^2\right]$ denote the homogeneous coordinates. For this, we can choose the two dimensionless ratios to be

$$\frac{s}{m^2}, \frac{t}{m^2}. \tag{5.3.1}$$

We express $I^{(j)}_{\nu_1\nu_2\nu_3\nu_4\nu_5\nu_6\nu_7}$ as iterated integrals on $\mathbb{P}^2(\mathbb{C})$.

Let us now have a look at the coordinate systems most suitable for the various (sub-) topologies. We are free to choose any convenient coordinates on M.

5.3.1 Non-elliptic sectors

We start with discussing the appropriate coordinate system suitable for the non-elliptic topologies, i.e. the ones which are expressible in terms of MPLs. One possibility, which is the closest to physics, is given by the eq. (5.3.1), which we refer to as (s,t)-coordinates. However, in this coordinate system we encounter many square roots, some of them even in very simple sub-topologies. There may be many coordinate systems which rationalize a particular square root, we may choose to work with any of them. We can make this choice depending on the degree of polynomials we need to handle in a particular topology. In table 6.1, we mention the occurring square roots in all the topologies, the coordinate system we choose in our case to remove the corresponding square roots and the relationship between various choice of coordinates. Along with this, we also mention the Jacobian we obtain due to the change of variables which gives us the occurring differential form.

Square root	New choice of coordinates	Differential forms
$\sqrt{-s(4m^2-s)}$	$\frac{s}{m^2} = -\frac{(1-x)^2}{x}, \quad \frac{t}{m^2} = y$	$\frac{ds}{s} = \frac{2dx}{x-1} - \frac{dx}{x},$ $\frac{ds}{s-4m^2} = \frac{2dx}{x+1} - \frac{dx}{x},$ $\frac{ds}{\sqrt{-s(4m^2-s)}} = \frac{dx}{x}.$
$\sqrt{-s(-4m^2-s)}$	$\frac{s}{m^2} = -\frac{(1+x')^2}{x'},$ $x' = \frac{1}{2}\left(\frac{-s}{m^2} - 2 - \sqrt{-\frac{s}{m^2}}\sqrt{-4-\frac{s}{m^2}}\right)$ $x' = -1 + \frac{(1-x)^2}{2x} - \frac{1-x}{2x}\sqrt{x^2-6x+1},$ $x = 1 + \frac{(1+x')^2}{2x'} - \frac{1+x'}{2x'}\sqrt{x'^2+6x'+1}$	$\frac{ds}{s} = \frac{2dx'}{x'+1} - \frac{dx'}{x'},$ $\frac{ds}{s+4m^2} = \frac{2dx'}{x'-1} - \frac{dx'}{x'},$ $\frac{ds}{\sqrt{-s(-4m^2-s)}} = \frac{dx'}{x'}$
$\sqrt{-s(4m^2-s)}$ & $\sqrt{-s(-4m^2-s)}$	$x = \tilde{x}\frac{(1-\tilde{x})}{(1+\tilde{x})},$ $\tilde{x} = \frac{1}{2}\left(1 - x - \sqrt{x^2-6x+1}\right)$ $x' = \tilde{x}\frac{(1+\tilde{x})}{(1-\tilde{x})}$	$\omega_0 = \frac{ds}{s} = \frac{2(2\tilde{x})d\tilde{x}}{\tilde{x}^2+1} - \frac{d\tilde{x}}{\tilde{x}-1} - \frac{d\tilde{x}}{\tilde{x}+1} - \frac{d\tilde{x}}{\tilde{x}},$ $\omega_4 = \frac{ds}{s-4m^2} = \frac{2(2\tilde{x}-2)d\tilde{x}}{\tilde{x}^2-2\tilde{x}-1} - \frac{d\tilde{x}}{\tilde{x}-1} - \frac{d\tilde{x}}{\tilde{x}+1} - \frac{d\tilde{x}}{\tilde{x}},$ $\omega_{-4} = \frac{ds}{s+4m^2} = \frac{2(2\tilde{x}+2)d\tilde{x}}{\tilde{x}^2+2\tilde{x}-1} - \frac{d\tilde{x}}{\tilde{x}-1} - \frac{d\tilde{x}}{\tilde{x}+1} - \frac{d\tilde{x}}{\tilde{x}},$ $\omega_{0,4} = \frac{ds}{\sqrt{-s(4m^2-s)}} = \frac{d\tilde{x}}{\tilde{x}-1} - \frac{d\tilde{x}}{\tilde{x}+1} + \frac{d\tilde{x}}{\tilde{x}},$ $\omega_{-4,0} = \frac{ds}{\sqrt{-s(-4m^2-s)}} = -\frac{d\tilde{x}}{\tilde{x}-1} + \frac{d\tilde{x}}{\tilde{x}+1} + \frac{d\tilde{x}}{\tilde{x}}$

Table 5.1. The various square roots occurring in the differential system and the corresponding coordinate choices. For the first case, the interval $s \in]-\infty, 0]$ is mapped to $x \in [0,1]$, with the point $s = -\infty$ being mapped to $x = 0$ and the point $s = 0$ being mapped to $x = 1$. For the second case, the interval $s \in]-\infty, -4m^2]$ is mapped to $x' \in [0,1]$. The point $s = -\infty$ is mapped to $x' = 0$, the point $s = 0$ is mapped to $x' = -1$.

As explained before, we adapt the coordinate system most suitable for a particular sub-topology. In our case, the results for the more complicated integrals are most compactly expressed by introducing the notation of eq. (5.2.3). All sub-topologies, which depend only on s, can be expressed as iterated integrals with integration kernels given by the five differential one-forms

$$\{\omega_0, \omega_4, \omega_{-4}, \omega_{0,4}, \omega_{-4,0}\}.$$

In addition, for $t = m^2$, or equivalently $y = 1$ (see table 6.1 for the definition of y), all master integrals can be expressed as iterated integrals with these integration kernels. It is clear that all the iterated integrals in these integration kernels are expressible in terms of MPLs.

5.3.2 Elliptic Curves

In this section, we talk about all the 'complicated' topologies, i.e. those which depend on both s and t, and extract the elliptic curves for the corresponding topologies by studying their maximal cuts. For the maximal cut, we use the loop by loop approach mentioned in section ⟨4.2⟩. Now we discuss each of the elliptic sectors present in our topology. It is to be kept in mind that here it is not possible to choose any coordinate system which rationalizes the occurring (elliptic) square roots.

Let us recall the definition of the elliptic curve and the periods here,

$$E : w^2 - (z-z_1)(z-z_2)(z-z_3)(z-z_4) \;=\; 0, \tag{5.3.2}$$

where the roots z_j may depend on variables $x = (x_1, ..., x_n)$:

$$z_j = z_j(x), \qquad j \in \{1,2,3,4\}. \tag{5.3.3}$$

We use the notation

$$df(x) = \sum_{i=1}^{n} \left(\frac{\partial f}{\partial x_i} \right) dx_i. \tag{5.3.4}$$

We set

$$Z_1 \;=\; (z_2 - z_1)(z_4 - z_3), \quad Z_2 \;=\; (z_3 - z_2)(z_4 - z_1), \quad Z_3 \;=\; (z_3 - z_1)(z_4 - z_2). \tag{5.3.5}$$

Note that we have

$$Z_1 + Z_2 = Z_3. \tag{5.3.6}$$

We define the modulus and the complementary modulus of the elliptic curve E by

$$k^2 \;=\; \frac{Z_1}{Z_3}, \; \bar{k}^2 \;=\; 1 - k^2 \;=\; \frac{Z_2}{Z_3}. \tag{5.3.7}$$

There are six possibilities of defining k^2. Our standard choice for the periods and quasi-periods is

$$\begin{aligned} \psi_1 \;&=\; \frac{4K(k)}{Z_3^{\frac{1}{2}}}, \; \psi_2 \;=\; \frac{4iK\left(\bar{k}\right)}{Z_3^{\frac{1}{2}}}, \\ \phi_1 \;&=\; \frac{4\left[K(k) - E(k)\right]}{Z_3^{\frac{1}{2}}}, \; \phi_2 \;=\; \frac{4iE\left(\bar{k}\right)}{Z_3^{\frac{1}{2}}}. \end{aligned} \tag{5.3.8}$$

Also the Dedekind's eta function is defined by

$$\eta(\tau) \;=\; e^{\frac{i\pi\tau}{12}} \prod_{n=1}^{\infty} (1 - e^{2\pi i n \tau}) \;=\; q^{\frac{1}{24}} \prod_{n=1}^{\infty} (1 - q^n), \qquad q = e^{2\pi i \tau}.$$

Extraction of (all) the elliptic curve(s) For extracting the elliptic curves, we use the loop by loop method in the Baikov representation. Using this approach, we aim for a one-dimensional integral representation for the maximal cut with a constant in the numerator and square root of a quartic polynomial in the denominator which defines the elliptic curve. The possible choices for the integration contour are then given by integration between any pair of roots of the quartic polynomial. This integration gives a period of the elliptic curve. The result for any choice of integration contour may be expressed as a linear combination of two independent periods. In practice we label/order the roots and define the periods by eq. (5.3.8).

1. **Sector 73:** Let us start with the equal mass sunrise integral in two space-time dimensions. It is convenient to deal with the sunrise in dimension 2 as only depends on the graph

polynomial $\mathcal{F}$ apart from being free from UV divergence. Starting first with the sub-loop containing P_1 and P_4, we obtain

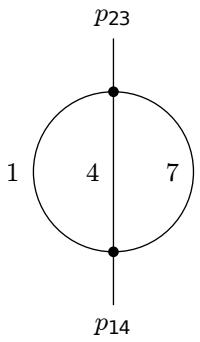

Figure 5.3. Sector 73

Here $p_{23} = p_2 + p_3$ and $p_{14} = p_1 + p_4$.

$$\begin{aligned}&\text{MaxCut}_C\, I_{1001001}\,(2-2\epsilon) = \\ &\frac{u\mu^2}{\pi^2}\int_C \frac{dP'}{(P'-t+2m^2)^{\frac{1}{2}}\,(P'-t+6m^2)^{\frac{1}{2}}\,(P'^2+6m^2P'-4m^2t+9m^4)^{\frac{1}{2}}} + O(\epsilon)\,.\end{aligned} \tag{5.3.9}$$

It is to be noted that for this topology we could have equally well start with the sub-loop containing the propagators P_7 and P_4. Doing so, we find

$$\begin{aligned}&\text{MaxCut}_C\, I_{1001001}\,(2-2\epsilon) = \\ &\frac{u\mu^2}{\pi^2}\int_C \frac{dP}{(P-t)^{\frac{1}{2}}\,(P-t+4m^2)^{\frac{1}{2}}\,(P^2+2m^2P-4m^2t+m^4)^{\frac{1}{2}}} + O(\epsilon)\,.\end{aligned} \tag{5.3.10}$$

We can see that these two representations are related to each other by by $P' = P - 2m^2$.

2. **Sector 127:** Let us now look at the maximal cut of the double box integral, this time in four space-time dimensions.

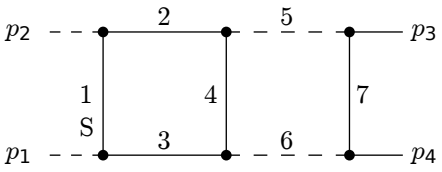

Figure 5.4. Sector 127

We have

$$\begin{aligned}&\text{MaxCut}_C\, I_{1111111}\,(4-2\epsilon) = \\ &\frac{u\mu^6}{4\pi^4 s^2}\int_C \frac{dP}{(P-t)^{\frac{1}{2}}\,(P-t+4m^2)^{\frac{1}{2}}\left(P^2+2m^2P-4m^2t+m^4-\frac{4m^2(m^2-t)^2}{s}\right)^{\frac{1}{2}}} + O(\epsilon)\,.\end{aligned} \tag{5.3.11}$$

One recognizes in eq. (5.3.9), eq. (5.3.10) and eq. (5.3.11) the typical period integrals of an elliptic curve. We note that the integrand of eq. (5.3.11) differs from the one of eq. (5.3.10). The difference is given by the additional term

$$-\frac{4m^2\left(m^2-t\right)^2}{s}.$$

This term vanishes in the limit $s \to \infty$.

3. **Sector 79:** Let us now look at the maximal cut in sector 79.

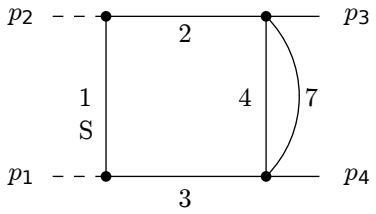

Figure 5.5. Sector 79

We find with $P = P_8$

$$\text{MaxCut}_C\, I_{1112001}\,(4-2\epsilon) = \tag{5.3.12}$$
$$\frac{u\mu^4}{4\pi^3 s}\int_C \frac{dP}{(P-t)^{\frac{1}{2}}\,(P-t+4m^2)^{\frac{1}{2}}\left(P^2+2m^2P-4m^2t+m^4-\frac{4m^2\left(m^2-t\right)^2}{s}\right)^{\frac{1}{2}}} + O(\epsilon).$$

Up to the prefactor, this is the same maximal cut integral as in eq. (5.3.11). Therefore the sectors 79 and 127 are associated to the same elliptic curve.

4. **Sector 93:** The most complicated example is the maximal cut in sector 93.

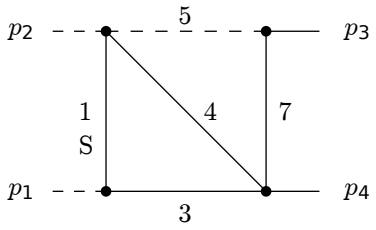

Figure 5.6. Sector 93

For this sector, we find first within the loop-by-loop approach a two-fold integral representation in P_2 and P_8 for the maximal cut. The integrand has a single pole at $P_2 = 0$. Choosing as a contour for the P_2-integration a small circle around this pole leads (with $P = P_8$) to

$$\frac{1}{\epsilon}\,\text{MaxCut}_C\, I_{1012101}\,(4-2\epsilon) =$$
$$\frac{u\mu^4}{\pi^2 s}\int_C \frac{dP}{(P-t)^{\frac{1}{2}}\,(P-t+4m^2)^{\frac{1}{2}}\left(P^2+2m^2P-4m^2t+m^4-\frac{4m^2\left(m^2-t\right)^2}{s}\right)^{\frac{1}{2}}} + O(\epsilon).$$

We recognize again the elliptic curve of sector 79 and 127.

5. **Sector 121:** Our next example is the maximal cut in sector 121.

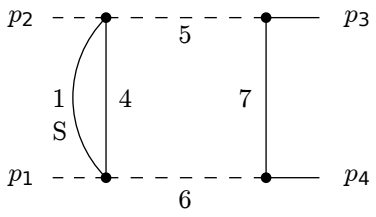

Figure 5.7. Sector 121

Here we find with $P = P_9 + 2m^2$

$$\text{MaxCut}_C\, I_{2001111}(4-2\epsilon) = \frac{u\mu^4}{4\pi^3(-s)^{\frac{1}{2}}(4m^2-s)^{\frac{1}{2}}} \tag{5.3.13}$$
$$\times \int_C \frac{dP}{(P-t)^{\frac{1}{2}}(P-t+4m^2)^{\frac{1}{2}}\left(P^2+2m^2\frac{(s+4t)}{(s-4m^2)}P+m^2(m^2-4t)\frac{s}{s-4m^2}-\frac{4m^2t^2}{s-4m^2}\right)^{\frac{1}{2}}} + O(\epsilon).$$

This corresponds to an elliptic curve different from the one found in sectors 79 and 127. In the limit $s \to \infty$ the maximal cut integral reduces again up to a prefactor to the one of eq. (5.3.10).

6. **Sector 123:** Our last example is the maximal cut in sector 123.

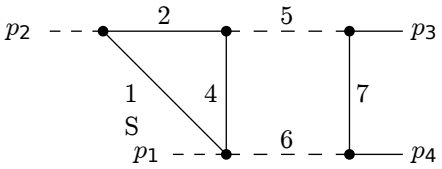

Figure 5.8. Sector 123

Here we find with $P = P_9 + 2m^2$

$$\text{MaxCut}_C\, I_{1101111}(4-2\epsilon) = \frac{u\mu^4}{4\pi^3(-s)^{\frac{1}{2}}(4m^2-s)^{\frac{1}{2}}} \tag{5.3.14}$$
$$\times \int_C \frac{dP}{(P-t)\left(P^2+2m^2\frac{(s+4t)}{(s-4m^2)}P+m^2(m^2-4t)\frac{s}{s-4m^2}-\frac{4m^2t^2}{s-4m^2}\right)^{\frac{1}{2}}} + O(\epsilon).$$

The denominator may be viewed as a square root of a quartic polynomial, where two roots coincide. This does not involve an elliptic curve and corresponds to genus zero.

5.3.3 Definition of all the elliptic curves

Now we define all the three elliptic curves according to the definition given in section ⟨3.4⟩. The coordinate system of interest here are denoted by (x, y). We can also express the Wronskian and

the Picard-Fuchs operator from the roots z_1, z_2, z_3 and z_4 in terms of the variables (x, y) for the variation of the elliptic curve along the paths

$$\gamma_\alpha : [0,1] \to \mathbb{C}^2, \quad x(\lambda) = x + \alpha_1 \lambda, \quad y(\lambda) = y + \alpha_2 \lambda. \tag{5.3.15}$$

We denote the derivatives of the Wronskian in the direction of x and y by W_x and W_y, which are expressed as

$$W_x = \psi_1 \frac{d}{dx}\psi_2 - \psi_2 \frac{d}{dx}\psi_1, \quad W_y = \psi_1 \frac{d}{dy}\psi_2 - \psi_2 \frac{d}{dy}\psi_1. \tag{5.3.16}$$

The derivatives of Wronskian in the directions x and y are given by

$$W_x = \psi_1 \frac{d}{dx}\psi_2 - \psi_2 \frac{d}{dx}\psi_1, \; W_y = \psi_1 \frac{d}{dy}\psi_2 - \psi_2 \frac{d}{dy}\psi_1. \tag{5.3.17}$$

We have

$$\begin{aligned} W_{\gamma_\alpha} &= \alpha_1 W_x + \alpha_2 W_y, \\ 2\pi i d\tau = \frac{2\pi i W_{\gamma_\alpha}}{\psi_1^2} d\lambda &= \frac{2\pi i}{\psi_1^2}\Big(W_x dx + W_y dy\Big). \end{aligned} \tag{5.3.18}$$

We may use the Picard-Fuchs operator to eliminate second derivatives:

$$\begin{aligned} \frac{d^2}{dx^2}\psi_1 &= -p_{1,x}\frac{d}{dx}\psi_1 - p_{0,x}\psi_1, \\ \frac{d^2}{dy^2}\psi_1 &= -p_{1,y}\frac{d}{dy}\psi_1 - p_{0,y}\psi_1, \\ 2\frac{d^2}{dxdy}\psi_1 &= -\Big(p_{1,x+y} - p_{1,x}\Big)\frac{d}{dx}\psi_1 - \Big(p_{1,x+y} - p_{1,y}\Big)\frac{d}{dy}\psi_1 - \Big(p_{0,x+y} - p_{0,x} - p_{0,y}\Big)\psi_1, \end{aligned}$$

where the subscript $x+y$ refers to the path with $(\alpha_1, \alpha_2) = (1,1)$. This leaves us with

$$\psi_1, \qquad \frac{d}{dx}\psi_1, \qquad \frac{d}{dy}\psi_1.$$

There is a further relation, since we may exchange any derivative of ψ_1 in favour of ϕ_1:

$$\frac{\frac{1}{2}\left(\frac{d}{dx}\ln Z_2\right)\psi_1 + \frac{d}{dx}\psi_1}{\frac{1}{2}\frac{d}{dx}\ln\frac{Z_2}{Z_1}} = \phi_1 = \frac{\frac{1}{2}\left(\frac{d}{dy}\ln Z_2\right)\psi_1 + \frac{d}{dy}\psi_1}{\frac{1}{2}\frac{d}{dy}\ln\frac{Z_2}{Z_1}}.$$

This yields

$$\begin{aligned} &\frac{1}{2}\left(\frac{d}{dy}\ln\frac{Z_2}{Z_1}\right)\frac{d}{dx}\psi_1 - \frac{1}{2}\left(\frac{d}{dx}\ln\frac{Z_2}{Z_1}\right)\frac{d}{dy}\psi_1 = \\ &\frac{1}{4}\left[\left(\frac{d}{dx}\ln Z_2\right)\left(\frac{d}{dy}\ln Z_1\right) - \left(\frac{d}{dy}\ln Z_2\right)\left(\frac{d}{dx}\ln Z_1\right)\right]\psi_1. \end{aligned} \tag{5.3.19}$$

Using eq. (5.3.19) we may eliminate one derivative, say $\frac{d}{dx}\psi_1$. This leaves us with

$$\psi_1, \qquad \frac{d}{dy}\psi_1,$$

as expected, since the first cohomology group of an elliptic curve is two dimensional.

Elliptic curve (a). From eq. (5.3.10) we may read off the elliptic curve for the sunrise integral:

$$E^{(a)} : w^2 - \left(z - \frac{t}{\mu^2}\right)\left(z - \frac{t-4m^2}{\mu^2}\right)\left(z^2 + \frac{2m^2}{\mu^2}z + \frac{m^4 - 4m^2 t}{\mu^4}\right) = 0.$$

The roots of the quartic polynomial are

$$z_1^{(a)} = \frac{t-4m^2}{\mu^2}, \quad z_2^{(a)} = \frac{-m^2 - 2m\sqrt{t}}{\mu^2}, \quad z_3^{(a)} = \frac{-m^2 + 2m\sqrt{t}}{\mu^2}, \quad z_4^{(a)} = \frac{t}{\mu^2}.$$

This curve has the j-invariant

$$j\left(E^{(a)}\right) = \frac{\left(3m^2+t\right)^3\left(3m^6 + 75m^4 t - 15m^2 t^2 + t^3\right)^3}{m^6 t\left(m^2-t\right)^6\left(9m^2-t\right)^2}.$$

Two elliptic curves over $\mathbb{C}$ are isomorphic, if and only if they have the same j-invariant. Let us now consider a path γ_β in (s,t)-space parametrized by

$$s = s_0 + \beta_1 \lambda \mu^2, \quad t = t_0 + \beta_2 \lambda \mu^2.$$

For the Wronskian and the Picard-Fuchs operator $\frac{d}{d\lambda^2} + p^{(a)}_{1,\gamma_\beta}\frac{d}{d\lambda} + p^{(a)}_{0,\gamma_\beta}$ we find

$$\begin{aligned}
W^{(a)}_{\gamma_\beta} &= 2\pi i \mu^6 \frac{3\beta_2}{t\left(t-m^2\right)\left(t-9m^2\right)}, \\
p^{(a)}_{1,\gamma_\beta} &= -\mu^2\left(\beta_1\frac{d}{ds} + \beta_2\frac{d}{dt}\right)\ln W^{(a)}_{\gamma_\beta}, \\
p^{(a)}_{0,\gamma_\beta} &= \mu^{10}\frac{2\pi i}{W^{(a)}_{\gamma_\beta}}\frac{3\beta_2^3\left(t-3m^2\right)}{t^2\left(t-m^2\right)^2\left(t-9m^2\right)^2}.
\end{aligned}$$

Eq. (5.3.19) reduces to the trivial equation

$$0 = 0.$$

We have

$$16\frac{\eta\left(\frac{\tau^{(a)}}{2}\right)^{24}\eta\left(2\tau^{(a)}\right)^{24}}{\eta\left(\tau^{(a)}\right)^{48}} = \left(k^{(a)}\bar{k}^{(a)}\right)^2 = 16\frac{m^3\sqrt{t}\left(m-\sqrt{t}\right)^3\left(3m+\sqrt{t}\right)}{\left(m+\sqrt{t}\right)^6\left(3m-\sqrt{t}\right)^2}.$$

For a path γ_α in (x,y)-space

$$x = \alpha_1\lambda, \quad y = 1 + \alpha_2\lambda$$

we may use eq. (5.3.3) to express λ as a power series in $q^{(a)}$ and vice versa. The point $(x,y) = (0,1)$ corresponds to $\tau^{(a)} = i\infty$.

For $y = 1$ we have

$$\psi_1^{(a)}\Big|_{y=1} = \frac{\pi}{2}, \quad \frac{d}{dy}\psi_1^{(a)}\Big|_{y=1} = -\frac{\pi}{8}.$$

Elliptic curve (b). From eq. (5.3.11) we obtain the elliptic curve associated to the double box integral:

$$E^{(b)}: w^2 - \left(z - \frac{t}{\mu^2}\right)\left(z - \frac{t-4m^2}{\mu^2}\right)\left(z^2 + \frac{2m^2}{\mu^2}z + \frac{m^4-4m^2t}{\mu^4} - \frac{4m^2\left(m^2-t\right)^2}{\mu^4 s}\right) = 0.$$

The roots of the quartic polynomial are now

$$z_1^{(b)} = \frac{t-4m^2}{\mu^2}, \quad z_2^{(b)} = \frac{-m^2 - 2m\sqrt{t + \frac{\left(m^2-t\right)^2}{s}}}{\mu^2}, \quad z_3^{(b)} = \frac{-m^2 + 2m\sqrt{t + \frac{\left(m^2-t\right)^2}{s}}}{\mu^2},$$
$$z_4^{(b)} = \frac{t}{\mu^2}.$$

The j-invariant is given by

$$j\left(E^{(b)}\right) = \frac{\left\{s\left(3m^2+t\right)\left[s\left(3m^6+75m^4t-15m^2t+t^3\right)+8m^2\left(m^2-t\right)^2\left(9m^2-t\right)\right]+16m^4\left(m^2-t\right)^4\right\}^3}{sm^6\left(s-4m^2\right)^2\left[st+\left(m^2-t\right)^2\right]\left(m^2-t\right)^6\left[s\left(9m^2-t\right)-4m^2\left(m^2-t\right)\right]^2}.$$

For the Wronskian and the Picard-Fuchs operator $\frac{d}{d\lambda^2} + p_{1,\gamma_\beta}^{(b)}\frac{d}{d\lambda} + p_{0,\gamma_\beta}^{(b)}$ we find for the path γ_β defined in eq. (5.3.3)

$$W_{\gamma_\beta}^{(b)} = 2\pi i\mu^6 \frac{\beta_1\left(m^2-t\right)\left[s\left(t+3m^2\right)-4m^2\left(m^2-t\right)\right]+\beta_2 s\left(s-4m^2\right)\left(2m^2-3s-2t\right)}{\left(s-4m^2\right)\left(t-m^2\right)\left[st+\left(m^2-t\right)^2\right]\left[s\left(9m^2-t\right)-4m^2\left(m^2-t\right)\right]},$$
$$p_{1,\gamma_\beta}^{(b)} = -\mu^2\left(\beta_1\frac{d}{ds}+\beta_2\frac{d}{dt}\right)\ln W_{\gamma_\beta}^{(b)},$$
$$p_{0,\gamma_\beta}^{(b)} = \mu^{10}\frac{2\pi i}{W_{\gamma_\beta}^{(b)}}\frac{N^{(b)}}{s^2\left(s-4m^2\right)^2\left(t-m^2\right)^2\left[st+\left(m^2-t\right)^2\right]^2\left[s\left(9m^2-t\right)-4m^2\left(m^2-t\right)\right]^2},$$

with

$$\begin{aligned}
N^{(b)} = {} & 2\beta_1^3\left(m^2-t\right)^4 m^2\left(8m^8-10m^6s-16m^6t+9m^4s^2+4m^4st+8m^4t^2+8m^2s^2t\right.\\
& \left.+6m^2st^2-s^2t^2\right)\\
& +\beta_1^2\beta_2 s\left(m^2-t\right)^2\left(96m^{12}-248m^{10}s-288m^{10}t+276m^8s^2+504m^8st+288m^8t^2\right.\\
& -63m^6s^3-360m^6s^2t-264m^6st^2-96m^6t^3+119m^4s^3t+84m^4s^2t^2+8m^4st^3\\
& \left.-18m^2s^4t-25m^2s^3t^2+2s^4t^2+s^3t^3\right)\\
& +2\beta_1\beta_2^2 s^2\left(4m^2-s\right)\left(m^2-t\right)^2\left(24m^8-78m^6s-48m^6t+88m^4s^2+84m^4st\right.\\
& \left.+24m^4t^2-18m^2s^3-24m^2s^2t-6m^2st^2+s^3t\right)\\
& +\beta_2^3 s^3\left(4m^2-s\right)^2\left(8m^8-30m^6s-24m^6t+36m^4s^2+62m^4st+24m^4t^2-9m^2s^3\right.\\
& \left.-42m^2s^2t-34m^2st^2-8m^2t^3+3s^3t+6s^2t^2+2st^3\right).
\end{aligned}$$

The relation between the period and its two derivatives, using eq. (5.3.19), is given by

$$\psi_1^{(b)} = \frac{\left(s-4m^2\right)\left(3s+2t-2m^2\right)}{t-m^2}\frac{d}{ds}\psi_1^{(b)} - \frac{s\left(t+3m^2\right)-4m^2\left(m^2-t\right)}{s}\frac{d}{dt}\psi_1^{(b)}.$$

In (x,y)-space this translates to

$$\psi_1^{(b)} = -\frac{(x+1)\left(3x^2-2xy-4x+3\right)}{(x-1)(y-1)}\frac{d}{dx}\psi_1^{(b)} - \frac{x^2y+3x^2-6xy-2x+y+3}{(x-1)^2}\frac{d}{dy}\psi_1^{(b)}.$$

We have with

$$\chi^{(b)} = \sqrt{t+\frac{(m^2-t)^2}{s}}$$

the relation

$$\begin{aligned}16\frac{\eta\left(\frac{\tau^{(b)}}{2}\right)^{24}\eta\left(2\tau^{(b)}\right)^{24}}{\eta\left(\tau^{(b)}\right)^{48}} &= \left(k^{(b)}\bar{k}^{(b)}\right)^2 \\ &= 16\frac{m^3\chi^{(b)}\left(m^2+t-2m\chi^{(b)}\right)\left(3m^2-t-2m\chi^{(b)}\right)}{\left(m^2+t+2m\chi^{(b)}\right)^2\left(3m^2-t+2m\chi^{(b)}\right)^2}.\end{aligned}$$

For a path γ_α in (x,y)-space

$$x = \alpha_1\lambda,\ y = 1+\alpha_2\lambda$$

we may use eq. (5.3.3) to express λ as a power series in $q^{(b)}$ and vice versa. The point $(x,y)=(0,1)$ corresponds to $\tau^{(b)} = i\infty$.

For $y=1$, we have

$$\psi_1^{(b)}\Big|_{y=1} = \frac{\pi}{2},\ \frac{d}{dy}\psi_1^{(b)}\Big|_{y=1} = -\frac{\pi}{8}.$$

Elliptic curve (c). From eq. (5.3.13) we obtain the elliptic curve associated to sector 121:

$$E^{(c)}: w^2 - \left(z-\frac{t}{\mu^2}\right)\left(z-\frac{t-4m^2}{\mu^2}\right)\left(z^2+\frac{2m^2(s+4t)}{\mu^2(s-4m^2)}z+\frac{sm^2\left(m^2-4t\right)-4m^2t^2}{\mu^4(s-4m^2)}\right) = 0.$$

The roots of the quartic polynomial are now

$$\begin{aligned}z_1^{(c)} &= \frac{t-4m^2}{\mu^2},\ z_2^{(c)} = \frac{1}{\mu^2}\left(-m^2\frac{(s+4t)}{(s-4m^2)} - \frac{2}{4m^2-s}\sqrt{sm^2\left(st+(m^2-t)^2\right)}\right), \\ z_3^{(c)} &= \frac{1}{\mu^2}\left(-m^2\frac{(s+4t)}{(s-4m^2)} + \frac{2}{4m^2-s}\sqrt{sm^2\left(st+(m^2-t)^2\right)}\right),\ z_4^{(c)} = \frac{t}{\mu^2}.\end{aligned}$$

The j-invariant is given by

$$j\left(E^{(c)}\right) = \frac{\left\{s\left(3m^2+t\right)\left(3m^6+75m^4t-15m^2t+t^3\right)+192m^6\left(m^2-t\right)^2\right\}^3}{m^6\left[st+(m^2-t)^2\right](m^2-t)^4\left[s(m^2-t)(9m^2-t)-64m^6\right]^2}.$$

For the Wronskian and the Picard-Fuchs operator $\frac{d}{d\lambda^2} + p^{(c)}_{1,\gamma_\beta}\frac{d}{d\lambda} + p^{(c)}_{0,\gamma_\beta}$ we find for the path γ_β defined in eq. (5.3.3)

$$W^{(c)}_{\gamma_\beta} = 2\pi i\mu^6 \frac{\left(s-4m^2\right)\left\{\beta_1\left(t-m^2\right)\left(t^2-6m^2t-3m^4\right)+\beta_2 s\left(3s\left(t-m^2\right)+2\left(t-m^2\right)^2+16m^4\right)\right\}}{s\left(t-m^2\right)\left[st+\left(m^2-t\right)^2\right]\left[s\left(m^2-t\right)\left(9m^2-t\right)-64m^6\right]},$$

$$p^{(c)}_{1,\gamma_\beta} = -\mu^2\left(\beta_1\frac{d}{ds}+\beta_2\frac{d}{dt}\right)\ln W^{(c)}_{\gamma_\beta},$$

$$p^{(c)}_{0,\gamma_\beta} = \mu^{10}\frac{2\pi i}{W^{(c)}_{\gamma_\beta}}\frac{N^{(c)}}{s^3\left(s-4m^2\right)\left(t-m^2\right)^2\left[st+\left(m^2-t\right)^2\right]^2\left[s\left(m^2-t\right)\left(9m^2-t\right)-64m^6\right]^2},$$

with

$$\begin{aligned}
N^{(c)} = {} & -2\beta_1^3m^2\left(m^2-t\right)^2\left(3m^4+6m^2t-t^2\right)\left(32m^{12}-62m^{10}s-64m^{10}t+3m^8s^2-24m^8st\right.\\
& \left.+32m^8t^2-26m^6s^2t-20m^6st^2-36m^4s^2t^2-24m^4st^3-6m^2s^2t^3+2m^2st^4+s^2t^4\right)\\
& -\beta_1^2\beta_2 s\left(m^2-t\right)\left(9600m^{18}-8232m^{16}s-17920m^{16}t+1656m^{14}s^2+18736m^{14}st\right.\\
& +7424m^{14}t^2-81m^{12}s^3-8724m^{12}s^2t-7512m^{12}st^2+512m^{12}t^3+1356m^{10}s^3t\\
& +2972m^{10}s^2t^2-416m^{10}st^3+384m^{10}t^4-54m^8s^4t-1045m^8s^3t^2+632m^8s^2t^3+1896m^8st^4\\
& +96m^6s^4t^2-256m^6s^3t^3-720m^6s^2t^4-400m^6st^5-28m^4s^4t^3+37m^4s^3t^4+92m^4s^2t^5\\
& \left.+24m^4st^6-16m^2s^4t^4-12m^2s^3t^5-4m^2s^2t^6+2s^4t^5+s^3t^6\right)\\
& -2\beta_1\beta_2^2s^2\left(4m^2-s\right)\left(544m^{16}-518m^{14}s-768m^{14}t+84m^{12}s^2+1252m^{12}st-192m^{12}t^2\right.\\
& -420m^{10}s^2t-58m^{10}st^2+512m^{10}t^3+39m^8s^3t+416m^8s^2t^2+536m^8st^3-96m^8t^4\\
& -76m^6s^3t^2-176m^6s^2t^3-250m^6st^4+34m^4s^3t^3+108m^4s^2t^4+68m^4st^5+4m^2s^3t^4\\
& \left.-12m^2s^2t^5-6m^2st^6-s^3t^5\right)\\
& +\beta_2^3s^3\left(4m^2-s\right)^2\left(736m^{12}-542m^{10}s-672m^{10}t+120m^8s^2+562m^8st-96m^8t^2-9m^6s^3\right.\\
& -206m^6s^2t-340m^6st^2+32m^6t^3+21m^4s^3t+122m^4s^2t^2+76m^4st^3-15m^2s^3t^2\\
& \left.-42m^2s^2t^3-14m^2st^4+3s^3t^3+6s^2t^4+2st^5\right).
\end{aligned}$$

Eq. (5.3.19) yields

$$\begin{aligned}
\psi^{(c)}_1 = {} & \frac{s\left(s-4m^2\right)\left[3s\left(t-m^2\right)+2\left(t-m^2\right)^2+16m^4\right]}{\left(t+3m^2\right)\left[s\left(t-m^2\right)+8m^4\right]}\frac{d}{ds}\psi^{(c)}_1\\
& -\frac{\left(s-4m^2\right)\left(t-m^2\right)\left(t^2-6m^2t-3m^4\right)}{\left(t+3m^2\right)\left[s\left(t-m^2\right)+8m^4\right]}\frac{d}{dt}\psi^{(c)}_1.
\end{aligned}$$

In (x,y)-space this translates to

$$\begin{aligned}
\psi^{(c)}_1 = {} & -\frac{(x+1)(x-1)\left(3x^2y-2xy^2-3x^2-2xy-12x+3y-3\right)}{(y+3)\left(x^2y-x^2-2xy-6x+y-1\right)}\frac{d}{dx}\psi^{(c)}_1\\
& -\frac{(x+1)^2(y-1)\left(y^2-6y-3\right)}{(y+3)\left(x^2y-x^2-2xy-6x+y-1\right)}\frac{d}{dy}\psi^{(c)}_1.
\end{aligned}$$

We have with

$$\chi^{(c)} = \sqrt{sm^2\left(st+(m^2-t)^2\right)}$$

the relation

$$\begin{aligned}16\frac{\eta\left(\frac{\tau^{(c)}}{2}\right)^{24}\eta\left(2\tau^{(c)}\right)^{24}}{\eta\left(\tau^{(c)}\right)^{48}} &= \left(k^{(c)}\bar{k}^{(c)}\right)^2\\ =16\frac{m^2\left(4m^2-s\right)\chi^{(c)}\left(sm^2+st+2\chi^{(c)}\right)\left(3sm^2-st-16m^4+2\chi^{(c)}\right)}{\left(sm^2+st-2\chi^{(c)}\right)^2\left(3sm^2-st-16m^4-2\chi^{(c)}\right)^2}&.\end{aligned}$$

For a path γ_α in (x,y)-space

$$x = \alpha_1\lambda,\ y = 1+\alpha_2\lambda$$

we may use eq. (5.3.3) to express λ as a power series in $q^{(c)}$ and vice versa. The point $(x,y)=(0,1)$ corresponds to $\tau^{(c)} = i\infty$.

For $y=1$ we have

$$\psi_1^{(c)}\Big|_{y=1} = \frac{\pi}{2}\frac{(1+x)}{(1-x)},\ \frac{d}{dy}\psi_1^{(c)}\Big|_{y=1} = -\frac{\pi}{8}\frac{(1+x)}{(1-x)}.$$

5.4 The transformation for the master integrals

One choice for the transformation which brings the integrals from the Laporta basis I (the one obtained using IBPs) to the linear form J is given as,

$$\begin{aligned}
\text{Sector 9:}\quad J_1 &= \epsilon^2\,\mathbf{D}^-I_{1001000},\\
\text{Sector 14:}\quad J_2 &= \epsilon^2\frac{(1-x)(1+x)}{2x}\,\mathbf{D}^-I_{0111000},\\
\text{Sector 28:}\quad J_3 &= \epsilon^2\frac{\left(1-x^2\right)}{x}\left[I_{0021200}+\frac{1}{2}I_{0022100}\right],\\
J_4 &= \epsilon^2\frac{(1-x)^2}{x}I_{0022100},\\
\text{Sector 49:}\quad J_5 &= -\frac{(1-x)^2}{2x}\epsilon^2\,\mathbf{D}^-I_{1000110},\\
\text{Sector 73:}\quad J_6 &= \epsilon^2\frac{\pi}{\psi_1^{(a)}}\,\mathbf{D}^-I_{1001001},\\
J_7 &= \frac{6}{\epsilon}\frac{\left(\psi_1^{(a)}\right)^2}{2\pi i W_y^{(a)}}\frac{d}{dy}J_6-\frac{1}{4}\left(3y^2-10y-9\right)\left(\frac{\psi_1^{(a)}}{\pi}\right)^2J_6,\\
\text{Sector 74:}\quad J_8 &= 4\epsilon^2\,\mathbf{D}^-I_{0101001},\\
\text{Sector 15:}\quad J_9 &= -\epsilon^3(1-\epsilon)\frac{(1-x)^2}{x}I_{1111000},\\
\text{Sector 29:}\quad J_{10} &= -\epsilon^3\frac{(1-x)^2}{x}I_{1012100},\\
\text{Sector 54:}\quad J_{11} &= -\epsilon^2\frac{(1+x)(1-x)^3}{4x^2}\,\mathbf{D}^-I_{0110110},\\
\text{Sector 57:}\quad J_{12} &= \epsilon^2\frac{\left(1-x'^2\right)}{x'}\left[-\frac{(1+x')^2}{x'}I_{2001210}-\frac{\epsilon}{2(1+2\epsilon)}I_{2002000}\right],
\end{aligned}$$

$$J_{13} = -\epsilon^3 \frac{(1+x')^2}{x'} I_{2001110},$$

Sector 75: $$J_{14} = \epsilon^3 (1-y) I_{1102001},$$

Sector 78: $$J_{15} = \epsilon^2 \frac{\left(1-x^2\right)^2}{x^2} I_{0212001} - \frac{3\epsilon^2 (1-x)^2}{2x} I_{0202001},$$

$$J_{16} = \epsilon^3 \frac{\left(1-x^2\right)}{x} I_{0112001},$$

Sector 89: $$J_{17} = \epsilon^3 (1-y) I_{2001101},$$

Sector 92: $$J_{18} = \epsilon^2 \frac{(1+x)^2}{x} I_{0021102} - \epsilon^2 \frac{(1+x)}{x} \left(I_{0021200} + \frac{1}{2} I_{0022100} \right),$$

$$J_{19} = \epsilon^3 \frac{\left(1-x^2\right)}{x} I_{0021101},$$

Sector 113: $$J_{20} = \epsilon^3 (1-\epsilon) \frac{\left(1-x^2\right)}{x} I_{1000111},$$

Sector 55: $$J_{21} = \epsilon^3 (1-2\epsilon) \frac{(1-x)^2}{x} I_{1110110},$$

Sector 59: $$J_{22} = \epsilon^4 \frac{(1-x)^2}{x} I_{1101110},$$

Sector 62: $$J_{23} = \epsilon^3 (1-2\epsilon) \frac{(1-x)^2}{x} I_{0111110},$$

Sector 79: $$J_{24} = \epsilon^3 \frac{(1-x)^2}{x} \frac{\pi}{\psi_1^{(b)}} I_{1112001},$$

$$J_{25} = \epsilon^3 (1-2\epsilon) \frac{(1-x)^2}{x} I_{1111001} - \frac{1}{3} (y-9) \frac{\psi_1^{(b)}}{\pi} J_{24},$$

$$J_{26} = \frac{6}{\epsilon} \frac{\left(\psi_1^{(b)}\right)^2}{2\pi i W_y^{(b)}} \frac{d}{dy} J_{24} - \frac{1}{4} \left(3y^2 - 10y - 9\right) \left(\frac{\psi_1^{(b)}}{\pi} \right)^2 J_{24} - \frac{1}{24} \left(y^2 - 30y - 27\right) \frac{\psi_1^{(b)}}{\pi} \frac{\psi_1^{(a)}}{\pi} J_6,$$

Sector 93: $$J_{27} = \epsilon^3 \frac{(1-x)^2}{x} \frac{\pi}{\psi_1^{(b)}} I_{1012101},$$

$$J_{28} = \epsilon^3 \left[1 - y + \frac{(1-x)^2}{x} \right] (I_{1021101} + I_{2011101}) - \frac{1}{6} (y-3) \frac{\psi_1^{(b)}}{\pi} J_{27},$$

$$J_{29} = \epsilon^4 \left[1 - y + \frac{(1-x)^2}{x} \right] I_{1011101},$$

$$J_{30} = \frac{6}{\epsilon} \frac{\left(\psi_1^{(b)}\right)^2}{2\pi i W_y^{(b)}} \frac{d}{dy} J_{27} - \frac{1}{4} \left(3y^2 - 10y - 9\right) \left(\frac{\psi_1^{(b)}}{\pi} \right)^2 J_{27} - \frac{1}{12} \left(y^2 - 30y - 27\right) \frac{\psi_1^{(b)}}{\pi} \frac{\psi_1^{(a)}}{\pi} J_6,$$

Sector 118: $$J_{32} = \epsilon^3 (1-2\epsilon) \frac{(1-x)^2}{x} I_{0110111} + 2\epsilon^3 (1-\epsilon) \frac{(1-x)}{x} I_{1000111},$$

Sector 121:
$$J_{33} = \epsilon^3 \frac{\left(1-x^2\right)}{x} \frac{\pi}{\psi_1^{(c)}} I_{2001111},$$
$$J_{34} = \epsilon^3 (1-2\epsilon) \frac{\left(1-x^2\right)}{x} I_{1001111} - \frac{1}{3}(y-9) \frac{(1+2x)}{(1+x)} \frac{\psi_1^{(c)}}{\pi} J_{33},$$
$$J_{35} = \frac{6}{\epsilon} \frac{\left(\psi_1^{(c)}\right)^2}{2\pi i W_y^{(c)}} \frac{d}{dy} J_{33} - \frac{1}{4}\left(3y^2-10y-9\right) \frac{(1-x)^2}{(1+x)^2} \left(\frac{\psi_1^{(c)}}{\pi}\right)^2 J_{33}$$
$$+ \frac{1}{8}\left(y^2-2y+9\right) \frac{(1-x)}{(1+x)} \frac{\psi_1^{(c)}}{\pi} \frac{\psi_1^{(a)}}{\pi} J_6,$$

Sector 63:
$$J_{36} = \epsilon^4 \frac{(x+1)(x-1)^3}{x^2} I_{1111110},$$

Sector 119:
$$J_{37} = \epsilon^4 \frac{(x+1)(x-1)^3}{x^2} I_{1110111},$$

Sector 123:
$$J_{38} = 2\epsilon^4 \frac{\left(x^2-1\right)}{x} \left[I_{11011110(-1)} - (y-2) I_{1101111}\right] - \frac{4}{x-1} J_{22},$$
$$J_{39} = \epsilon^4 (1-y) \frac{(1-x)^2}{x} I_{1101111},$$

Sector 126:
$$J_{40} = \epsilon^4 \frac{(x+1)(x-1)^3}{x^2} I_{0111111},$$

Sector 127:
$$J_{41} = \epsilon^4 \frac{(1-x)^4}{x^2} \frac{\pi}{\psi_1^{(b)}} I_{1111111},$$
$$J_{42} = 8\epsilon^4 \frac{(1-x)^2}{x} I_{1111111(-1)(-1)} - 8\epsilon^4 \frac{(y-2)(1-x)^2}{x} I_{1111111(-1)0}$$
$$- 8\epsilon^4 \frac{y(1-x)^2}{x} I_{11111110(-1)} - \frac{8x}{(1-x)^2} \frac{\psi_1^{(b)}}{\pi} J_{41}$$
$$- 4 \frac{(x-1)\left(x^2-2xy+1\right)}{(x+1)^3} J_{40} - 4 \frac{x^2-2xy+1}{(x-1)(x+1)} J_{37}$$
$$- 4 \frac{x^2-2xy-4x+1}{(x-1)(x+1)} J_{36} - \frac{4}{3}(y+3) \frac{\psi_1^{(b)}}{\pi} J_{27} + \frac{8}{3}(y+3) \frac{\psi_1^{(b)}}{\pi} J_{24}$$
$$- \left(4 + \frac{32\epsilon}{(1-2\epsilon)} \frac{\left(x^4-yx^3-xy+1\right)}{(x-1)^2(x+1)^2}\right) J_{23} - 16 \frac{(y-1)x}{(x-1)^2} J_{22}$$
$$- 8 \frac{(x-1)\left(x^2-xy+x+1\right)}{(x+1)^3} J_{19} + 4 \frac{(x-1)^2}{(y-1)x} J_{17}$$
$$+ 16 \frac{(x-1)\left(x^2-xy+x+1\right)}{(x+1)^3} J_{16} - \frac{4}{3} \frac{\left(6x^2-5xy-7x+6\right)}{(y-1)x} J_{14},$$
$$J_{43} = \frac{6}{\epsilon} \frac{\left(\psi_1^{(b)}\right)^2}{2\pi i W_y^{(b)}} \frac{d}{dy} J_{41} - \frac{1}{4}\left(3y^2-10y-9\right) \left(\frac{\psi_1^{(b)}}{\pi}\right)^2 J_{41} + 4y \frac{(1-x)}{(1+x)} \frac{\psi_1^{(b)}}{\pi} \frac{\psi_1^{(c)}}{\pi} J_{33}$$
$$+ \frac{2}{3} y(y-9) \left(\frac{\psi_1^{(b)}}{\pi}\right)^2 J_{27} + \frac{2}{3} y(y-3) \left(\frac{\psi_1^{(b)}}{\pi}\right)^2 J_{24},$$
$$J_{44} = \epsilon^4 \frac{(1-x)^4}{x^2} I_{1111111(-1)0} - \frac{1}{3}(2y-3) \frac{\psi_1^{(b)}}{\pi} J_{41} - \epsilon^4 \frac{(1-x)^4}{x^2} I_{0111111}$$

$$
\begin{aligned}
&+\epsilon^4 \frac{(1-x)^2\left(x^2-2xy+1\right)}{x^2} I_{1101111}, \\
J_{45} = \; &\epsilon^4 \frac{(x-1)^2(x+1)^2}{x^2} I_{11111110(-1)} - \frac{\left(2x^2y-9x^2+8xy-6x+2y-9\right)}{3(x-1)^2} \frac{\psi_1^{(b)}}{\pi} J_{41} \\
&- \frac{2}{x-1} J_{36} + \frac{1}{2}\left(\frac{1}{x}+x-\frac{2}{3}y\right)\frac{\psi_1^{(b)}}{\pi} J_{27} - \left(\frac{1}{x}+x-\frac{2}{3}y\right)\frac{\psi_1^{(b)}}{\pi} J_{24}.
\end{aligned} \tag{5.4.1}
$$

5.5 Integration kernels

For the linear form for the differential equation we required the following conditions for matrix A:

- A linear in ϵ,
- $A^{(0)}$ strictly lower-triangular,
- $A^{(0)}$ vanish for $x = 0$ or $y = 1$,
- $A^{(1)}$ reduce to integration kernels for multiple polylogarithms for $y = 1$,
- $A^{(1)}$ reduce to modular forms for $x = 0$,

It is to be noted that these conditions still do not uniquely fix the set of master integrals $\vec{J}$ and the matrix A. There is a "gauge freedom" of transformations which leaves these conditions intact. In other words, we could in principle have another system of equations with all these conditions satisfied. In this section we discuss the integration kernels appearing in the matrix A.

The system of differential equations simplifies for $t = m^2$ (corresponding to $y = 1$) as well as for $s = \infty$ (corresponding to $x = 0$). In both limits the matrix $A^{(0)}$ in our differential eq. (5.2.6) vanishes. In the former case ($t = m^2$), the integration kernels are linear combinations of the one-forms given in eq. (5.3.1) and the solution for the master integrals can be expressed in terms of MPLs. In the latter case ($s = \infty$), the integration kernels are of the form

$$
f \; (2\pi i)\, d\tau_6^{(a)},
$$

where f is a modular form of the congruence subgroup $\Gamma_1(6)$ from the set given in eq. (5.5.3). In this case the solution for the master integrals can be expressed in terms of iterated integrals of modular forms [73]. We discuss this case in detail in the following sections.

5.5.1 Polylogarithmic one-forms

From the table 6.1, we can read off the differential forms ω_0, ω_4, ω_{-4}, $\omega_{0,4}$ and $\omega_{-4,0}$. To get the set of alphabet for the differential equation system evaluating to MPLs we see that,

$$
\begin{aligned}
\frac{2\tilde{x}d\tilde{x}}{\tilde{x}^2+1} &= \frac{d\tilde{x}}{\tilde{x}-i} + \frac{d\tilde{x}}{\tilde{x}+i}, \\
\frac{(2\tilde{x}-2)d\tilde{x}}{\tilde{x}^2-2\tilde{x}-1} &= \frac{d\tilde{x}}{\tilde{x}-\left(1+\sqrt{2}\right)} + \frac{d\tilde{x}}{\tilde{x}-\left(1-\sqrt{2}\right)}, \\
\frac{(2\tilde{x}+2)d\tilde{x}}{\tilde{x}^2+2\tilde{x}-1} &= \frac{d\tilde{x}}{\tilde{x}-\left(-1+\sqrt{2}\right)} + \frac{d\tilde{x}}{\tilde{x}-\left(-1-\sqrt{2}\right)}.
\end{aligned}
$$

Thus, the set of alphabets $\mathcal{A}$, $\mathcal{A}'$ and $\tilde{\mathcal{A}}$ for the variables x, x' and $\tilde{x}$, respectively is given by

$$\begin{aligned}\mathcal{A} &= \{-1,0,1\},\\ \mathcal{A}' &= \{-1,0,1\},\\ \tilde{\mathcal{A}} &= \left\{-1,0,1,i,-i,1+\sqrt{2},1-\sqrt{2},-1+\sqrt{2},-1-\sqrt{2}\right\}.\end{aligned}$$

Therefore, for the three cases above we have

- iterated integrals in the variable x involving the differential forms of the first row of table 6.1 may be expressed in terms of the smaller class of harmonic polylogarithms.
- The same holds for iterated integrals in the variable x' involving the differential forms of the second row of table 6.1.
- On the other hand, iterated integrals in the variable $\tilde{x}$ involving the differential forms of the third row of table 6.1 have a larger alphabet and are expressed in terms of MPLs.

The entries of the matrix A can be written as linear combinations (with rational coefficients) of fewer $\mathbb{Q}$-independent basic building blocks, such that no further linear relations with rational coefficients exist among these building blocks. In order to understand this concept let us restrict to the subset of Feynman integrals which only depend on s. For this subset of Feynman integrals, all entries of A are linear combinations of

$$\frac{d\tilde{x}}{\tilde{x}-c},$$

with

$$c \in \quad \tilde{\mathcal{A}} \;=\; \left\{-1,0,1,i,-i,1+\sqrt{2},1-\sqrt{2},-1+\sqrt{2},-1-\sqrt{2}\right\}.$$

The alphabet $\tilde{\mathcal{A}}$ has nine letters. However, in the matrix A only specific linear combinations of these one-forms appear. All entries of A can be expressed as $\mathbb{Q}$-linear combinations of

$$\{\omega_0,\omega_4,\omega_{-4},\omega_{0,4},\omega_{-4,0}\}, \tag{5.5.1}$$

where the ω's have been defined in table 6.1. Thus the set of $\mathbb{Q}$-independent integration kernels contains for this example only five elements, given by eq. (5.5.1). Hence, the results in terms of iterated integrals are shorter, if we work with a $\mathbb{Q}$-independent set of integration kernels.

5.5.2 Modular forms

We may consider the topologies evaluating to MPLs to be 'simple' to work within this case. However, we also have several elliptic topologies present. Here the obvious variable to work with is the modular parameter τ of the associated elliptic curve.

There are integrals which only depend on t, but not on s and are all related to the elliptic curve $E^{(a)}$. The curve $E^{(a)}$ is associated with the modular forms of $\Gamma_1(6)$. Therefore, we can write the differential one-forms which are relevant to the integrals dependent on t but not on s in the form

$$f\ (2\pi i)\, d\tau_6^{(a)},$$

where

$$\tau_6^{(a)} = \frac{1}{6}\frac{\psi_2^{(a)}}{\psi_1^{(a)}},$$

which we substitute for y (or t). Furthermore, f is a modular form of $\Gamma_1(6)$ from the set

$$\{1, f_2, f_3, f_4, g_{2,1}\}.$$

The modular weights (explained in the section ⟨5.2.2⟩) are given by 0, 2, 3, 4 and 2, respectively. The non-trivial modular forms are given by

$$f_2 = -\frac{1}{4}\left(3y^2-10y-9\right)\left(\frac{\psi_1^{(a)}}{\pi}\right)^2,\ f_3 = -\frac{3}{2}y(y-1)(y-9)\left(\frac{\psi_1^{(a)}}{\pi}\right)^3,$$
$$f_4 = \frac{1}{16}(y+3)^4\left(\frac{\psi_1^{(a)}}{\pi}\right)^4,\ g_{2,1} = -\frac{1}{2}y(y-9)\left(\frac{\psi_1^{(a)}}{\pi}\right)^2.$$

5.5.3 The high-energy limit

A very interesting thing to note about these integral kernels is their behaviour in the high-energy limit $s \to \infty$ (or equivalently $x = 0$). In this limit, the elliptic curves $E^{(b)}$ and $E^{(c)}$ degenerate to the elliptic curve $E^{(a)}$. Therefore, in this limit, we have only one elliptic curve $E^{(a)}$ and we are able to express all master integrals in terms of iterated integrals of modular forms. The resulting set of modular forms is slightly larger than eq. (5.5.2). In order to present this set compactly, we first set

$$g_{n,r} = -\frac{1}{2}\frac{y(y-1)(y-9)}{y-r}\left(\frac{\psi_1^{(a)}}{\pi}\right)^n,$$
$$h_{n,s} = -\frac{1}{2}y(y-1)^{1+s}(y-9)\left(\frac{\psi_1^{(a)}}{\pi}\right)^n.$$

The set relevant to the high-energy limit is

$$\{1, g_{2,0}, g_{2,1}, g_{2,9}, g_{3,1}, h_{3,0}, g_{4,0}, g_{4,1}, g_{4,9}, h_{4,0}, h_{4,1}\}.$$

These are again modular forms of $\Gamma_1(6)$ in the variable $\tau_6^{(a)}$. All integration kernels reduce to $\mathbb{Q}$-linear combinations of elements of this set (times $(2\pi i)\,d\tau_6^{(a)}$) in the high-energy limit. Also, the m-weight agrees with the modular weight in this limit.

5.5.4 The general case

We now discuss the general case. For our choice of basis $\vec{J}$ we find **107** $\mathbb{Q}$-independent integration kernels. In order to present some features of the differential system we group the integration kernels according to their m-weight. In our system, we have integration kernels with m-weight 0, 1, 2, 3 and 4, with the complexity increasing with the increase in the m-weight. The ϵ^0-part $A^{(0)}$ contains only integration kernels of m-weight 3 and 4.

The naming system for the integral kernels is as follows:

- For the special cases $t = m^2$ or $s = \infty$ the naming remains the same as before.

$$\{\omega_0, \omega_4, \omega_{-4}, \omega_{0,4}, \omega_{-4,0}, f_2, f_3, f_4, g_{2,1}\}.$$

- Integration kernels appearing in the ϵ^0-part $A^{(0)}$ are denoted by

$$a^{(r)}_{n,j},$$

  where n gives the m-weight, (r) indicates the periods appearing in the integration kernel and j indexes different integration kernels with the same n and (r).

- The integration kernels appearing in the ϵ^1-part $A^{(1)}$ is generically denoted by

$$\eta^{(r)}_{n,j},$$

  where the superscript (r) and the second subscript j are optional.

- For the dlog-forms, we use the notation

$$d_{2,j}.$$

  These are necessarily of m-weight 2.

Let us now discuss for all m-weights typical examples, the cases of m-weight 0 and 1 are discussed completely. The full list of integration kernels is given in the supplementary electronic file attached to the arXiv [48], which consists of the integration kernels

$$\begin{aligned}&\Big\{\omega_0,\omega_4,\omega_{-4},\omega_{0,4},\omega_{-4,0},f_2,f_3,f_4,g_{2,1},\eta^{(r)}_0,\eta^{(b)}_{1,1-4},\eta^{(c)}_{1,1-3},d_{2,1-5},\eta_{2,1-12},\eta^{(\frac{r}{s})}_2,\\&a^{(b)}_{3,1-4},a^{(c)}_{3,1-3},\eta^{(a)}_{3,1-3},\eta^{(b)}_{3,1-24},\eta^{(c)}_{3,1-11},a^{(a,b)}_{4,1},a^{(a,c)}_{4,1},a^{(b,b)}_{4,1-5},a^{(c,c)}_{4,1},a^{(b,c)}_{4,1},\\&\eta^{(a,b)}_{4,1-3},\eta^{(a,c)}_{4,1},\eta^{(b,b)}_{4,1-5},\eta^{(c,c)}_{4,1},\eta^{(b,c)}_{4,1}\Big\}.\end{aligned}$$

with $r,s\in\{a,b,c\}$ and $r\neq s$.

We can categorize the different integration kernels present in our system belonging to each modular weights.

5.5.4.1 m-weight 0

At m-weight 0 we have three integration kernels. They are given by

$$\begin{aligned}\eta^{(a)}_0 &= 2\pi i\, d\tau^{(a)}_6,\\ \eta^{(b)}_0 &= 2\pi i\, d\tau^{(b)}_6,\\ \eta^{(c)}_0 &= 2\pi i\, d\tau^{(c)}_6.\end{aligned}$$

These are exactly the integration kernels we expect at m-weight 0. We expressed them (compactly) in terms of the variables $\tau^{(a)}_6$, $\tau^{(b)}_6$ or $\tau^{(c)}_6$, respectively. Of course we may re-write them in terms of the variables x and y. For example, for $\eta^{(b)}_0$ one has

$$\begin{aligned}\eta^{(b)}_0 =&\frac{2}{3}\frac{(x-1)\left(x^2y+3x^2-6xy-2x+y+3\right)}{(x^2y-9x^2+2xy+14x+y-9)(xy-1)(x-y)(x+1)}\left(\frac{\pi}{\psi^{(b)}_1}\right)^2dx\\&-\frac{2}{3}\frac{(x-1)^2\left(3x^2-2xy-4x+3\right)}{(y-1)(x^2y-9x^2+2xy+14x+y-9)(xy-1)(x-y)}\left(\frac{\pi}{\psi^{(b)}_1}\right)^2dy.\end{aligned}$$

5.5.4.2 *m*-weight 1

We find 7 integration kernels of *m*-weight 1, four of them are associated to the elliptic curve $E^{(b)}$, three of them to the elliptic curve $E^{(c)}$. There are no integration kernels of *m*-weight 1 for the elliptic curve $E^{(a)}$. The integration kernels of *m*-weight associated to the elliptic curve $E^{(b)}$ are

$$\begin{aligned}
\eta^{(b)}_{1,1} =& \frac{(x-1)}{(3x^2-2xy-4x+3)(x+1)}\frac{\pi}{\psi^{(b)}_1}dx,\\
\eta^{(b)}_{1,2} =& \frac{(x-1)\left(x^2y^2-9x^2y+6xy^2-2xy+y^2+12x-9y\right)}{(x+1)(x^2y-9x^2+2xy+14x+y-9)(xy-1)(x-y)}\frac{\pi}{\psi^{(b)}_1}dx\\
&-\frac{x(x-1)^2(y-3)}{(x^2y-9x^2+2xy+14x+y-9)(xy-1)(x-y)}\frac{\pi}{\psi^{(b)}_1}dy,\\
\eta^{(b)}_{1,3} =& \frac{\left(x^2y-9x^2-6xy+22x+y-9\right)}{(x+1)(x^2y-9x^2+2xy+14x+y-9)(x-1)}\frac{\pi}{\psi^{(b)}_1}dx\\
&+2\frac{x}{(x^2y-9x^2+2xy+14x+y-9)}\frac{\pi}{\psi^{(b)}_1}dy,\\
\eta^{(b)}_{1,4} =& \frac{x(y-1)\left(-6xy+y+x^2y-2x+3+3x^2\right)}{(x+1)(x-1)(xy-1)(x-y)(x^2y-9x^2+2xy+14x+y-9)}\frac{\pi}{\psi^{(b)}_1}dx\\
&-\frac{x\left(3x^2-2xy-4x+3\right)}{(x^2y-9x^2+2xy+14x+y-9)(xy-1)(x-y)}\frac{\pi}{\psi^{(b)}_1}dy.
\end{aligned}$$

Associated to the elliptic curve $E^{(c)}$ are

$$\begin{aligned}
\eta^{(c)}_{1,1} =& \frac{(x+1)(y+3)}{(x-1)(3x^2y-2xy^2-3x^2-2xy-12x+3y-3)}\frac{\pi}{\psi^{(c)}_1}dx,\\
\eta^{(c)}_{1,2} =& (x+1)\frac{\pi}{\psi^{(c)}_1}\\
&\left[\frac{\left(x^2y^3+3x^2y^2-9xy^3-105x^2y+99xy^2+2y^3-27x^2+45xy-12y^2+57x-54y\right)}{(x-1)(x^2y^2-10x^2y-2xy^2+9x^2+20xy+y^2+46x-10y+9)(xy-1)(x-y)}dx\right.\\
&\left.+\frac{x\left(3x^2y^2-4xy^3-30x^2y+38xy^2-2y^3+27x^2-48xy+25y^2+78x-84y-3\right)}{(y-1)(x^2y^2-10x^2y-2xy^2+9x^2+20xy+y^2+46x-10y+9)(x-y)(xy-1)}dy\right],\\
\eta^{(c)}_{1,3} =& \frac{(x+1)^2(y-3)}{(x-1)(3x^2y-2xy^2-3x^2-2xy-12x+3y-3)\sqrt{x^2-6x+1}}\frac{\pi}{\psi^{(c)}_1}dx.
\end{aligned}$$

5.5.4.3 *m*-weight 2

The integration kernels of *m*-weight 2 are numerous and we only list a few typical cases. The integration kernels for the multiple polylogarithms

$$\omega_0,\ \omega_4,\ \omega_{-4},\ \omega_{0,4},\ \omega_{-4,0},$$

defined in eq. (**??**) belong to this class. Furthermore, the modular forms of modular weight 2 clearly belong to this class:

$$f_2\ (2\pi i)\, d\tau_6^{(a)} = \frac{dy}{y-1} + \frac{dy}{y-9} - \frac{dy}{2y},$$
$$g_{2,1}\ (2\pi i)\, d\tau_6^{(a)} = \frac{dy}{y-1}.$$

The differential one-forms in eq. (5.5.4.3) and eq. (5.5.4.3) are all dlog-forms, depending either on x (or alternatively on $\tilde{x}$) or y, but not both. There are further dlog-forms, depending on both variables x and y. These are

$$\begin{aligned}
d_{2,1} &= d\ln(x-y) + d\ln(xy-1),\\
d_{2,2} &= d\ln(xy-1),\\
d_{2,3} &= d\ln\left(x^2 - xy - x + 1\right),\\
d_{2,4} &= d\ln\left(3x^2 - 2xy - 4x + 3\right),\\
d_{2,5} &= d\ln\left(x^2 y - 9x^2 + 2xy + 14x + y - 9\right).
\end{aligned}$$

There are six differential one-forms involving ratios of periods, one for each ratio. For example

$$\begin{aligned}
\eta_2^{(\frac{b}{a})} &= \frac{1}{2}\frac{(x+1)}{x(x-1)}\frac{\psi_1^{(b)}}{\psi_1^{(a)}}dx\\
&- \frac{1}{12}\frac{\left(3x^2y^2 + 2xy^3 - 90x^2y + 52xy^2 - 81x^2 + 138xy + 3y^2 + 144x - 90y - 81\right)}{y(y-1)(y-9)(3x^2 - 2xy - 4x + 3)}\frac{\psi_1^{(b)}}{\psi_1^{(a)}}dy.
\end{aligned}$$

In addition there are 12 differential one-forms of m-weight 2, which do not belong to any class discussed up to now. An example is given by

$$\eta_{2,1} = \frac{(x-1)}{(x+1)(3x^2 - 2xy - 4x + 3)}dx.$$

For our choice of master integrals $\vec{J}$ we observe that in the integration kernels of m-weight 2 polynomials in denominator occur only as a single power, i.e. there are no higher poles in m-weight 2.

5.5.4.4 m-weight 3

At m-weight 3, we have first of all the modular form of weight 3 from the sunrise sector

$$f_3\ (2\pi i)\, d\tau_6^{(a)} = 3\frac{\psi_1^{(a)}}{\pi}dy.$$

At m-weight 3 we have integration kernels appearing in the ϵ^0-part $A^{(0)}$, an example is given by

$$\begin{aligned}
a_{3,1}^{(b)} &= \frac{\left(x^2y - 3x^2 + 4xy + y - 3\right)(y-1)}{(x-1)(3x^2 - 2xy - 4x + 3)(x+1)}\frac{\psi_1^{(b)}}{\pi}dx\\
&+ \frac{\left(x^2y^2 - 9x^2y + 6xy^2 - 2xy + y^2 + 12x - 9y\right)(y-1)}{(x-1)(3x^2 - 2xy - 4x + 3)(x+1)}\left(\frac{\partial_y\psi_1^{(b)}}{\pi}\right)dx\\
&- \frac{x(y-1)}{(3x^2 - 2xy - 4x + 3)}\frac{\psi_1^{(b)}}{\pi}dy - \frac{(y-3)x(y-1)}{(3x^2 - 2xy - 4x + 3)}\left(\frac{\partial_y\psi_1^{(b)}}{\pi}\right)dy.
\end{aligned}$$

In addition, there are integration kernels of m-weight 3 in the ϵ^1-part $A^{(1)}$, an example is given by

$$\eta^{(b)}_{3,1} = 4\,\frac{(y-1)}{(3x^2-2xy-4x+3)}\,\frac{\psi^{(b)}_1}{\pi}dx - \frac{(x-1)(x+1)}{(3x^2-2xy-4x+3)}\,\frac{\psi^{(b)}_1}{\pi}dy.$$

5.5.4.5 m-weight 4

At m-weight 4, we have one modular form of weight 4 from the sunrise sector

$$f_4\ (2\pi i)\,d\tau^{(a)}_6 = -\frac{(y+3)^4}{8y(y-1)(y-9)}\left(\frac{\psi^{(a)}_1}{\pi}\right)^2 dy.$$

In addition, we encounter integration kernels appearing in the ϵ^0-part $A^{(0)}$. An example is given by

$$\begin{aligned}
a^{(b,b)}_{4,3} = &-\frac{2}{3}\,\frac{(y-3)(y-1)N^{(b,b)}_{4,3,1}}{(x-1)(x+1)(3x^2-2xy-4x+3)^2}\left(\frac{\psi^{(b)}_1}{\pi}\right)^2 dx\\
&+\frac{4}{3}\,\frac{x(y-3)(y-1)^2 N^{(b,b)}_{4,3,2}}{(x-1)(x+1)(3x^2-2xy-4x+3)^2}\left(\frac{\psi^{(b)}_1}{\pi}\right)\left(\frac{\partial_y\psi^{(b)}_1}{\pi}\right)dx\\
&+\frac{2}{3}\,\frac{x N^{(b,b)}_{4,3,3}}{(3x^2-2xy-4x+3)^2}\left(\frac{\psi^{(b)}_1}{\pi}\right)^2 dy\\
&+\frac{4}{3}\,\frac{x(y-3)(y-1)N^{(b,b)}_{4,3,4}}{(3x^2-2xy-4x+3)^2}\left(\frac{\psi^{(b)}_1}{\pi}\right)\left(\frac{\partial_y\psi^{(b)}_1}{\pi}\right)dy,
\end{aligned}$$

with

$$\begin{aligned}
N^{(b,b)}_{4,3,1} =&\, 3x^4y - 2x^3y^2 + 9x^4 + 20x^3y - 20x^2y^2 - 18x^3 + 2x^2y - 2xy^2 - 6x^2 + 20xy - 18x\\
&+ 3y + 9,\\
N^{(b,b)}_{4,3,2} =&\, x^2y^2 - 24x^2y + 18xy^2 - 9x^2 + 16xy + y^2 + 30x - 24y - 9,\\
N^{(b,b)}_{4,3,3} =&\, 9x^2y^2 - 8xy^3 - 6x^2y + 10xy^2 - 27x^2 - 20xy + 9y^2 + 66x - 6y - 27,\\
N^{(b,b)}_{4,3,4} =&\, 3x^2y - 4xy^2 + 9x^2 - 2xy - 18x + 3y + 9.
\end{aligned}$$

Finally, there are integration kernels of m-weight 4 appearing in the ϵ^1-part $A^{(1)}$. An example is given by

$$\begin{aligned}
\eta^{(b,b)}_{4,3} = &\,\frac{1}{9}\,\frac{1}{(xy-1)(x-y)(3x^2-2xy-4x+3)^2(x^2y-9x^2+2xy+14x+y-9)}\\
&\left[\frac{(y-1)P^{(b,b)}_{4,3,1}}{(x-1)(x+1)}dx - \frac{(x-1)^2 P^{(b,b)}_{4,3,2}}{(y-1)}dy\right]\left(\frac{\psi^{(b)}_1}{\pi}\right)^2,
\end{aligned}$$

with

$$
\begin{aligned}
P^{(b,b)}_{4,3,1} =& 27x^8y^4 - 75x^7y^5 + 48x^6y^6 - 243x^8y^3 + 909x^7y^4 - 946x^6y^5 + 288x^5y^6 + 2673x^8y^2 \\
&- 7182x^7y^3 + 5914x^6y^4 - 1237x^5y^5 - 288x^4y^6 - 729x^8y - 6966x^7y^2 + 17592x^6y^3 \\
&- 11277x^5y^4 + 1828x^4y^5 + 288x^3y^6 - 3159x^7y + 22392x^6y^2 - 36146x^5y^3 \\
&+ 15766x^4y^4 - 1237x^3y^5 + 48x^2y^6 + 729x^7 + 13770x^6y - 41898x^5y^2 + 43510x^4y^3 \\
&- 11277x^3y^4 - 946x^2y^5 + 1134x^6 - 25929x^5y + 52590x^4y^2 - 36146x^3y^3 \\
&+ 5914x^2y^4 - 75xy^5 - 9369x^5 + 30942x^4y - 41898x^3y^2 + 17592x^2y^3 + 909xy^4 \\
&+ 15012x^4 - 25929x^3y + 22392x^2y^2 - 7182xy^3 + 27y^4 - 9369x^3 + 13770x^2y \\
&- 6966xy^2 - 243y^3 + 1134x^2 - 3159xy + 2673y^2 + 729x - 729y, \\
P^{(b,b)}_{4,3,2} =& 27x^6y^4 - 45x^5y^5 - 30x^4y^6 + 48x^3y^7 + 243x^6y^3 - 603x^5y^4 + 828x^4y^5 - 460x^3y^6 \\
&+ 729x^6y^2 - 2592x^5y^3 + 1899x^4y^4 - 126x^3y^5 - 30x^2y^6 + 729x^6y - 4212x^5y^2 \\
&+ 8085x^4y^3 - 4686x^3y^4 + 828x^2y^5 - 2187x^5y + 6741x^4y^2 - 8864x^3y^3 + 1899x^2y^4 \\
&- 45xy^5 - 729x^5 + 7587x^4y - 9708x^3y^2 + 8085x^2y^3 - 603xy^4 + 810x^4 - 9954x^3y \\
&+ 6741x^2y^2 - 2592xy^3 + 27y^4 - 810x^3 + 7587x^2y - 4212xy^2 + 243y^3 + 810x^2 \\
&- 2187xy + 729y^2 - 729x + 729y.
\end{aligned}
$$

5.5.5 Singularities

As already mentioned, the integration kernels are rational in

$$\epsilon, \tilde{x}, y, \psi_1^{(a)}, \psi_1^{(b)}, \psi_1^{(c)}, \partial_y\psi_1^{(a)}, \partial_y\psi_1^{(b)}, \partial_y\psi_1^{(c)}.$$

In the next section, we will choose as boundary point the point $(x,y) = (0,1)$ (or equivalently $(s,t) = (\infty, m^2)$). This motivates the introduction of the variable

$$\tilde{y} = 1 - y.$$

Therefore our boundary point is $(\tilde{x},\tilde{y}) = (0,0)$. The polynomials in our system are as follows.

- Polynomials which only depend on $\tilde{x}$ are

$$
\begin{aligned}
Q_1 =& \tilde{x}, \;\; Q_2 = \tilde{x} - 1, \;\; Q_3 = \tilde{x} + 1, \\
Q_4 =& \tilde{x}^2 + 1, \;\; Q_5 = \tilde{x}^2 - 2\tilde{x} - 1, \;\; Q_6 = \tilde{x}^2 + 2\tilde{x} - 1.
\end{aligned}
$$

- Polynomials which only depend on $\tilde{y}$ are

$$Q_7 = \tilde{y}, \;\; Q_8 = \tilde{y} - 1, \;\; Q_9 = \tilde{y} + 8.$$

- Polynomials which depend on $\tilde{x}$ and $\tilde{y}$ are

$$
\begin{aligned}
Q_{10} =& \tilde{x}^2 - \tilde{x}\tilde{y} - \tilde{y} + 1, \quad Q_{11} = -\tilde{x}^2\tilde{y} + \tilde{x}^2 + \tilde{x}\tilde{y} + 1, \quad Q_{12} = \tilde{x}^4 - \tilde{x}^3\tilde{y} + 2\tilde{x}^2 + \tilde{x}\tilde{y} + 1, \\
Q_{13} =& 3\tilde{x}^4 - 2\tilde{x}^3\tilde{y} + 6\tilde{x}^2 + 2\tilde{x}\tilde{y} + 3, \quad Q_{14} = \tilde{x}^4\tilde{y} + 8\tilde{x}^4 - 4\tilde{x}^3\tilde{y} + 2\tilde{x}^2\tilde{y} + 16\tilde{x}^2 + 4\tilde{x}\tilde{y} + \tilde{y} + 8, \\
Q_{15} =& 3\tilde{x}^4\tilde{y} - 2\tilde{x}^3\tilde{y}^2 - 16\tilde{x}^3 + 6\tilde{x}^2\tilde{y} + 2\tilde{x}\tilde{y}^2 + 16\tilde{x} + 3\tilde{y}, \quad Q_{16} = \tilde{x}^2\tilde{y} - 8\tilde{x} + \tilde{y} + 8, \\
Q_{17} =& \tilde{x}^2\tilde{y} + 8\tilde{x}^2 + 8\tilde{x} + \tilde{y}.
\end{aligned}
$$

Let us also have a look at the corresponding expressions in (s,t)-space: The polynomials Q_{10} and Q_{11} appear when the expression $st + (m^2 - t)^2$ is expressed in the variables $\tilde{x}$ and $\tilde{y}$:

$$
st + \left(m^2 - t\right)^2 = \frac{Q_{10}Q_{11}}{\tilde{x}(\tilde{x}-1)(\tilde{x}+1)}.
$$

The polynomial Q_{12} is related to

$$
m^2 - t - s = -\frac{Q_{12}}{\tilde{x}(\tilde{x}-1)(\tilde{x}+1)}.
$$

The polynomials Q_{13} and Q_{14} are related to the elliptic curve $E^{(b)}$. We have

$$
\begin{aligned}
3s + 2t - 2m^2 =& \frac{Q_{13}}{\tilde{x}(\tilde{x}-1)(\tilde{x}+1)}, \\
s\left(t - 9m^2\right) + 4m^2\left(m^2 - t\right) =& -\frac{Q_{14}}{\tilde{x}(\tilde{x}-1)(\tilde{x}+1)},
\end{aligned}
$$

The polynomial Q_{13} enters through eq. (5.3.3) or eq. (5.3.3), the polynomial Q_{14} appears in the Picard-Fuchs operator for $\psi_1^{(b)}$ in eq. (5.3.3).

The polynomials Q_{15}, Q_{16} and Q_{17} are related to the elliptic curve $E^{(c)}$. We have

$$
\begin{aligned}
3s\left(t - m^2\right) + 2\left(t - m^2\right)^2 + 16m^4 =& -\frac{Q_{15}}{\tilde{x}(\tilde{x}-1)(\tilde{x}+1)}, \\
s\left(t - 9m^2\right)\left(t - m^2\right) - 64m^6 =& \frac{Q_{16}Q_{17}}{\tilde{x}(\tilde{x}-1)(\tilde{x}+1)}.
\end{aligned}
$$

The polynomial Q_{15} enters through eq. (5.3.3) or eq. (5.3.3), the polynomials Q_{16} and Q_{17} appears in the Picard-Fuchs operator for $\psi_1^{(c)}$ in eq. (5.3.3).

It is to be noted that the polynomials Q_1, Q_7, Q_{15} and Q_{17} vanish for $(\tilde{x},\tilde{y}) = (0,0)$. We integrate the system of differential equations starting from the point $(x,y) = (0,1)$ (corresponding to $s = \infty$ and $t = m^2$). In order to do so, we need the boundary constants at this point. In the next section we discuss the evaluation of the boundary constants at these points.

5.6 Boundary conditions and boundary constants

In this section, we intend to discuss the last part in solving any differential equation, that is evaluating the boundary conditions. We wish to integrate the system of differential equations starting from the point $(x,y) = (0,1)$, which correspond to $s = \infty$ and $t = m^2$. Therefore, we require the boundary constants at this point. In order to express these boundary constants in a

basis of transcendental constants up to weight four [109], using PSLQ algorithm, we can use the following basis:

$$\begin{aligned}
w = 1 :& \ln(2),\\
w = 2 :& \zeta_2, \quad \ln^2(2),\\
w = 3 :& \zeta_3, \quad \zeta_2 \ln(2), \quad \ln^3(2),\\
w = 4 :& \zeta_4, \quad \mathrm{Li}_4\left(\frac{1}{2}\right), \quad \zeta_3 \ln(2), \quad \zeta_2 \ln^2(2), \quad \ln^4(2).
\end{aligned}$$

We need to calculate explicitly the boundary constants for the integrals, which neither depend on s nor on t. There are two such integrals: J_1 (which is also a product of tadpoles) and J_8 (the sunrise integral at the pseudo-threshold). For the result for J_1, we simply take the results from eq. (4.6.1). For J_8 we proceed as follows: We start from the Feynman parameter integral and we get

$$\begin{aligned}
J_8 =& 6\epsilon^2 e^{2\gamma_E \epsilon} \Gamma(1+2\epsilon) \int_0^1 dx_2 \int_0^1 dx_4 \left[\frac{1}{x_2-1} - \frac{1}{x_2+1}\right]\left[\frac{1}{x_4+1} - \frac{1}{x_4+x_2}\right]\\
& \times (x_2+1)^{\epsilon} (x_4+1)^{-2\epsilon} (x_4+x_2)^{-2\epsilon} \left(x_4 + \frac{x_2}{x_2+1}\right)^{\epsilon}.
\end{aligned}$$

We see that we can perform the x_4 integration at each order in ϵ and get the results in MPLs $G(z_1,...,z_k;x_2)$, where the remaining variable x_2 appears in the argument list z_1, ..., z_k. With the methods of [67] we can convert all polylogarithms to a form, where the parameters z_1, ..., z_k do not depend on x_2, the simplest example is given by

$$G(-x_2;1) = G(-1;x_2) - G(0;x_2).$$

We may then perform the integration over the variable x_2. The resulting expressions may also be simplified with the help of the PSLQ-algorithm. Apart from these two integrals there are other integrals which are products of simpler integrals and are calculated similarly.

For all other master integrals we obtain the boundary constants from the behavior at a specific point, where the master integral vanishes or reduces to simpler integrals. This specific points for our system are $(x,y) = (0,1)$, $(x,y) = (1,1)$ and $(x,y) = (-1,1)$. For the points $(x,y) = (1,1)$ or $(x,y) = (-1,1)$ we integrate the system along $y = 1$ from $x = 0$ to $x = \pm 1$. For $y = 1$ we only obtain MPLs. We evaluate the MPLs to high precision and use the PSLQ-algorithm to extract the transcendental constants.

The complete list of boundary constants is given in the appendix of the arXiv [48].

5.6.1 A peek at the results

For all the basis integrals, we write

$$J_k = \sum_{j=0}^{\infty} \epsilon^j J_k^{(j)}.$$

We now show examples for the result of a few of the master integrals. The integrals J_1 and J_8 are independent of s and t (or equivalently independent of x and y) and are given by

$$J_1 = 1 + \zeta_2 \epsilon^2 - \frac{2}{3}\zeta_3 \epsilon^3 + \frac{7}{4}\zeta_4 \epsilon^4 + O\left(\epsilon^5\right),$$

$$J_8 = 6\zeta_2\epsilon^2 + \epsilon^3(21\zeta_3 - 36\zeta_2\ln 2) + \epsilon^4\left(144\,\mathrm{Li}_4\left(\frac{1}{2}\right) - 78\zeta_4 + 72\zeta_2\ln^2(2) + 6\ln^4(2)\right) + O\left(\epsilon^5\right).$$

We also look at an example of one of the master integral which depends only on s.

$$\begin{aligned}
J_2^{(0)} &= 0,\\
J_2^{(1)} &= -G(0;x),\\
J_2^{(2)} &= 2G(-1,0;x) - G(0,0;x) + \zeta_2,\\
J_2^{(3)} &= -4G(-1,-1,0;x) + 2G(-1,0,0;x) + 2G(0,-1,0;x) - G(0,0,0;x) - 2\zeta_2 G(-1;x)\\
&\quad + 2\zeta_3,\\
J_2^{(4)} &= 8G(-1,-1,-1,0;x) - 4G(-1,-1,0,0;x) - 4G(-1,0,-1,0;x) - 4G(0,-1,-1,0;x)\\
&\quad + 2G(-1,0,0,0;x) + 2G(0,-1,0,0;x) + 2G(0,0,-1,0;x) - G(0,0,0,0;x)\\
&\quad + 4\zeta_2 G(-1,-1;x) - 2\zeta_2 G(0,-1;x) - 4\zeta_3 G(-1;x) + \frac{8}{3}\zeta_3 G(0;x) + \frac{19}{4}\zeta_4,
\end{aligned} \tag{5.6.1}$$

In the appendix, we present an example each of the cases when the integral depends only on t and when they depend both on s and t. In order to keep it very clear and simple, we avoid presenting the full result in the thesis, however, one is referred to [48] for the same.

5.6.2 Analytic continuation

Let us also discuss the regions where our results are valid. For most parts of our calculations, there are no restrictions on s and t for our calculations. The results are written in terms of iterated integrals which are valid for all values of s and t, if a proper analytic continuation around branch cuts according to Feynman's $i\epsilon$-prescription is understood [58]. In a neighbourhood of our boundary point, $s = \infty$ and $t = m^2$, we do not need analytic continuation. For the analytic continuation, we need to choose the integration path such that it avoids the singularities of the integration kernels according to Feynman's $i\epsilon$-prescription. We also need to take care that the integration kernels are continuous along the integration path at the same time. These integration kernels also involve the periods of the elliptic curves. Therefore we need to ensure that the periods vary continuously along the integration path. The periods are expressed in terms of complete elliptic integrals in a neighbourhood of the boundary point. The complete elliptic integral $K(k)$, when viewed as a function of k^2 has a branch cut along $[1,\infty[$. If the image of the integration path in k^2-space crosses this cut we have to compensate for the discontinuity of $K(k)$ by taking the monodromy around $k^2 = 1$ into account. The numerical checks, on the other hand, are limited to the region of convergence of the power series expansions.

5.7 Numerical Checks

All results have been verified numerically with the help of the program `sector_decomposition` [63]. The program `sector_decomposition` allows (as SecDec [69] or FIESTA [64] the numerical evaluation of multi-loop integrals. In order to check the numerical

results, we undertake the following methodoly. We evaluate all master integrals of the Laporta basis $\vec{I}$ at a few kinematic points numerically with the program `sector_decom- position`. We also evaluate our results in the basis $\vec{J}$ at the same kinematic points, converted to the basis $\vec{I}$ and compared the two results. We find a good agreement.

The evaluation of the iterated integrals appearing in our results is done as follows: We split the integration path into two pieces: First we integrate in $(\tilde{x},\tilde{y})$-space from $(0,0)$ to $(\tilde{x},0)$, then from $(\tilde{x},0)$ to $(\tilde{x},\tilde{y})$. The integration along the first part gives only multiple polylogarithms, which can be evaluated to high precision [67]. We use these results as new boundary constants for the integration along the second part. Assuming that $\tilde{y}$ is small, we may expand for the integration along the second part all integration kernels in $\tilde{y}$. As a reference we give numerical results for the master integrals in the basis $\vec{J}$ at the kinematic point

$$s = -\frac{12769}{840}m^2, \quad t = \frac{10}{11}m^2.$$

This point corresponds to

$$x = \frac{7}{120}, \quad y = \frac{10}{11},$$

or equivalently

$$\tilde{x} = \frac{1}{15}, \quad \tilde{y} = \frac{1}{11}.$$

We can see the numerical results for the first five terms of ϵ-expansion displayed in tables.

All results have been verified numerically with the help of the program `sector_decomposition` [63].

	ϵ^0	ϵ^1	ϵ^2	ϵ^3	ϵ^4
J_1	1	0	1.6449341	−0.80137127	1.8940657
J_2	0	2.8415816	−2.8295758	6.4116869	−7.7009279
J_3	0	−2.8415816	15.355894	−39.817554	97.903278
J_4	0	0	8.074586	−20.479468	55.140667
J_5	1	−2.7213737	3.7029375	−6.5645107	7.7616443
J_6	0	0	4.7951687	−7.7339091	23.583241
J_7	0	−0.13797489	5.0760627	−8.5195954	25.27333
J_8	0	0	9.8696044	−15.803336	48.383357
J_9	0	0	4.037293	−2.1975902	7.5750011
J_{10}	0	0	0	−10.577768	19.861743
J_{11}	0	2.8415816	−10.562581	19.960005	−34.628948
J_{12}	0	0	4.8094349	−23.163298	56.79741
J_{13}	0	0	0	−9.6340372	18.255071
J_{14}	0	0	0	0.074587202	−0.1198646
J_{15}	0	0	−4.037293	23.437914	−62.690651
J_{16}	0	0	0	8.4983135	−20.922966
J_{17}	0	0	0	0.1491744	0.058984085
J_{18}	0	1.4207908	−12.163995	44.930917	−88.809767
J_{19}	0	0	0	16.996627	−15.625817
J_{20}	0	0	−10.735443	−9.8004674	−37.795989
J_{21}	0	0	4.037293	−13.184573	21.864228
J_{22}	0	0	0	0	8.4599162
J_{23}	0	0	0	4.8796692	−25.793413
J_{24}	0	0	0	2.6138189	−0.23796592
J_{25}	0	0	4.037293	−9.2635254	25.950914
J_{26}	0	0	2.7276656	−1.848663	13.397014
J_{27}	0	0	0	5.2276379	8.7055971
J_{28}	0	0	0	8.9388561	12.795847
J_{29}	0	0	0	0	18.80581
J_{30}	0	0	5.4553312	−3.9355497	35.856907
J_{32}	0	0	−10.735443	−40.306104	−35.268067
J_{33}	0	0	0	7.3822471	10.116064
J_{34}	0	0	10.735443	−3.4643927	53.616756
J_{35}	0	0	0.97741243	5.1104476	15.424638
J_{36}	0	0	0	0	−13.214347
J_{37}	0	0	0	0	−43.342128
J_{38}	0	0	0	0	44.194787
J_{39}	0	0	0	0	0.28609557
J_{40}	0	0	0	0	−26.330837
J_{41}	0	0	0	0	11.147258
J_{42}	0	0	0	−19.021429	−320.23817
J_{43}	0	0	0	0.89070327	9.183764
J_{44}	0	0	0	0	21.040337
J_{45}	0	0	0	0	−1.4008206

Table 5.2. Numerical results for the first five terms of the ϵ-expansion of the master integrals at the kinematic point $s = -\frac{12769}{840}m^2$, $t = \frac{10}{11}m^2$.

5.8 Conclusion

In this chapter, we discussed the analytic calculation of the master integrals for the planar double box integral relevant to top-pair production with a closed top loop, given for the first time in [48]. This integral depends on two scales and involves several elliptic sub-sectors. The integral contains elliptic curves which can be extracted from the maximal cuts. The system involves three in-equivalent elliptic curves. This integral involves a special case of having more than one elliptic curve and was believed to be a roadblock for a long time. It is helpful to write down the results of these integrals in terms of well defined mathematical objects. However, since elliptic polylogarithms are by definition iterated integrals on a single elliptic curve we can not naturally express the result of this integral in terms of elliptic polylogarithms. We showed that the system of differential equations can be transformed to a form linear in ϵ, where the ϵ^0-term is strictly lower-triangular. This system of differential equations is easily solved to any desired order in ϵ. One may express the results in terms of iterated integrals of the occurring integration kernels and in this chapter we discussed the integration kernels particular to our choice of transformation for the master integrals. The techniques applied in this case and the (unexpected) results obtains open the door to a wider class of Feynman integrals and more detailed study of algebraic structure.

6 Higgs decay to two bottom quarks.

Contents

6.1 Physical importance

We know that the SM employs the Higgs mechanism, which can be tested by measuring the strength of the Higgs boson interactions with other fundamental particles. The strength of the Higgs boson interactions is proportional to the fermion mass and is, therefore, greatest for the top quark. Moreover, the stronger the interaction the larger the decay rate of the Higgs boson into a pair of fermions, and hence more probable the decay. Since the top quark is heavier than the Higgs boson, the most likely decay is into a pair of bottom quarks, the heaviest decay products allowed by energy conservation. The physics of bottom quark, in particular, sheds light on CP violation. Some important high-mass particles decay into bottom quarks. Top quarks nearly always do so and the Higgs boson is expected to decay into bottom quarks more than any other particle given

its mass. Since the discovery of a new boson with a mass near 124 GeV by the ATLAS and CMS collaborations, huge progress in the understanding of the properties and coupling of this particle has been made which is compatible with the Standard Model Higgs boson. The decay $H \to b\bar{b}$, is predicted to have a branching fraction of about 58%. the subleading fermionic decays $H \to \tau^+\tau^-$ and $H \to c\bar{c}$ reach branching ratios of about 6% and 3% respectively. A precise measurement of the rate for this process directly probes the Yukawa coupling of the Higgs boson to a down-type quark and provides a necessary test of the hypothesis that the Higgs field is the source of mass generation in the charged fermion sector of the SM. We can use perturbative calculations to compute QCD corrections for this process to the full $O(\alpha)$ result and obtain all contributions of order $\alpha\alpha_S$ to the partial decay rate. In this chapter, we are mainly interested in the mixed $O(\alpha\alpha_s)$-corrections to the decay $H \to b\bar{b}$ through a $Ht\bar{t}$-coupling. In the beginning, we show the extensive calculation of the master integrals for the Higgs decay to $b\bar{b}$ [108]. Examples of Feynman diagrams are shown in fig. 6.3. We exclude the diagrams whose master integrals are related to the master integrals of the diagrams of fig. 6.3 by symmetry. We also neglect the b-quark mass. However, the dependence on the top quark mass m_t, the W-boson mass m_W and the momentum p of the Higgs boson is treated exactly. These diagrams are useful in order to obtain the partial decay width of Higgs boson into a bottom quark pair. At the end of this chapter, we also briefly sketch how we can obtain the full decay width for this process using the optical theorem.

Observing Higgs decay experimentally

Because of the overwhelmingly large background contribution from several other SM processes that can mimic the experimental signature characterized by the appearance of a bottom quark, it is a challenge to observe it experimentally. The ATLAS and CMS Collaboration overcame this challenge by deploying modern sophisticated analysis tools and by focusing on particular signatures where a Higgs boson is produced in association with a vector boson V (a W or Z particle), a weak interaction process known as VH(bb), shown in the figure below, which leads to a significant reduction in the background. The experiment results for Higgs decay to two bottom quarks can be obtained from [96, 97].

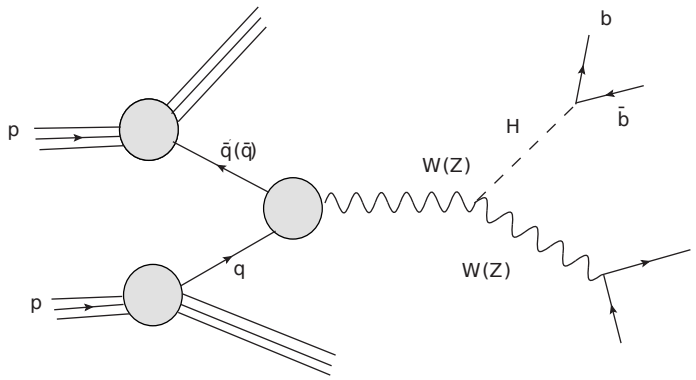

Figure 6.1. Associated production of Higgs

6.1.1 State of the art

The determination of the branching ratios of Higgs-boson decays necessitates the inclusion of the available higher-order corrections and a sophisticated estimate of the theoretical and parametric uncertainties. The present status of the partial decay widths can be summarized in terms of the expression

$$\Gamma(H \to f\bar{f}) = \frac{N_c G_F M_H}{4\sqrt{2}\pi} m_f^2 (1 + \delta_{QCD} + \delta_t + \delta_{mixed})(1 + \delta_{EW}),$$

where $N_c = 3(1)$ for quarks (leptons), G_F denotes the Fermi constant, M_H the Higgs mass and m_f the fermion mass. In general, the pure QCD corrections δ_{QCD} to the Higgs boson decays into quarks are known up to NLO including the full quark mass dependence, and up to N^4LO for the leading corrections with the leading mass effects. The dominant part of the QCD corrections can be absorbed in the running quark mass evaluated at the scale of the Higgs mass. The top-induced QCD corrections, which are related to interference effects between $H \to gg$ and $H \to q\bar{q}$, are known at NNLO in the limit of heavy top quarks and light bottom quarks. In the case of leptons, there are no QCD corrections ($\delta_{QCD} = \delta_t = \delta_{mixed} = 0$). The electroweak corrections δ are known at NLO exactly. In addition, the mixed QCD-EW corrections range at the one-per-mille level of the factorized expression with respect to QCD and EW corrections is used. The partial decay width of $H \to b\bar{b}$ is also known fully differential at N^{3}LO QCD [107].

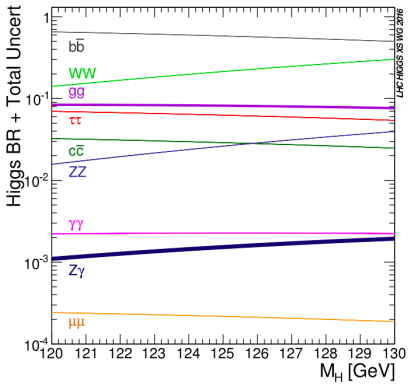

Figure 6.2. Higgs boson branching ratios and their uncertainties for Higgs masses around 125 GeV. From [60]

6.2 The setup for the master integrals

For an on-shell Higgs boson we have $p^2 = m_H^2$. In figure 6.3, we show all the diagrams contributing to the mixed QCD-EW corrections with an $Ht\bar{t}$ coupling. Not shown here are the diagrams related to these by symmetry.

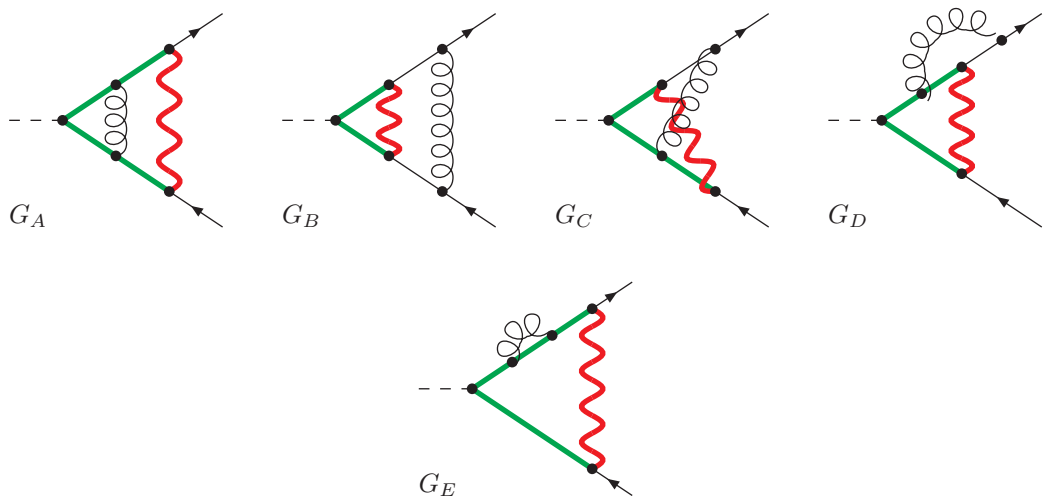

Figure 6.3. Examples of Feynman diagrams contributing to the mixed $O(\alpha\alpha_s)$-corrections to the decay $H \to b\bar{b}$ through a $Ht\bar{t}$-coupling. The Higgs boson is denoted by a dashed line, a top quark by a green line, a bottom quark with a black line and a gluon by a curly line. Particles with mass m_W are drawn with a wavy line.

For the two-loop contributions to the Higgs decay, we have two independent external momenta p_1 and p_2, which label the momenta of b-quark and $\bar{b}$-quark, respectively. With two independent loop momenta, we have seven ISPs, therefore we need to consider an auxiliary topology which contains all the seven propagators needed to express the ISPs. Therefore we introduce an auxiliary topology G_A-G_D with seven propagators for each of the four Feynman diagrams, as shown in figure 6.4. The master integrals related to diagram G_E are a subset of the master integrals related to diagram G_A and similarly also a subset of the master integrals related to diagram G_D. We consider the integrals

$$I^X_{\nu_1\nu_2\nu_3\nu_4\nu_5\nu_6\nu_7} = e^{2\gamma_E\epsilon}\left(\mu^2\right)^{\nu-D} \int \frac{d^Dk_1}{i\pi^{\frac{D}{2}}} \frac{d^Dk_2}{i\pi^{\frac{D}{2}}} \prod_{j=1}^{7} \frac{1}{\left(P^X_j\right)^{\nu_j}}, \qquad X \in \{A,B,C,D\},$$

where $D = 4-2\epsilon$ denotes the number of space-time dimensions, γ_E denotes the Euler-Mascheroni constant, μ is an arbitrary scale introduced to render the Feynman integral dimensionless, and the quantity ν is defined by

$$\nu = \sum_{j=1}^{7} \nu_j.$$

The inverse propagators P^X_j are defined as follows:

Topology A:

$$\begin{aligned}
&P^A_1 = -k_1^2 + m_t^2, && P^A_2 = -(k_1 - p_1 - p_2)^2 + m_t^2, && P^A_3 = -(k_1 + k_2)^2, \\
&P^A_4 = -k_2^2 + m_t^2, && P^A_5 = -(k_2 + p_1)^2 + m_W^2, && P^A_6 = -(k_2 + p_1 + p_2)^2 + m_t^2, \\
&P^A_7 = -(k_1 - p_1)^2 + m_t^2. &&
\end{aligned} \tag{6.2.1}$$

Topology B:

$$P^B_1 = -k_1^2 + m_t^2, \qquad P^B_2 = -(k_1 - p_1 - p_2)^2 + m_t^2, \qquad P^B_3 = -(k_1 + k_2)^2 + m_W^2,$$

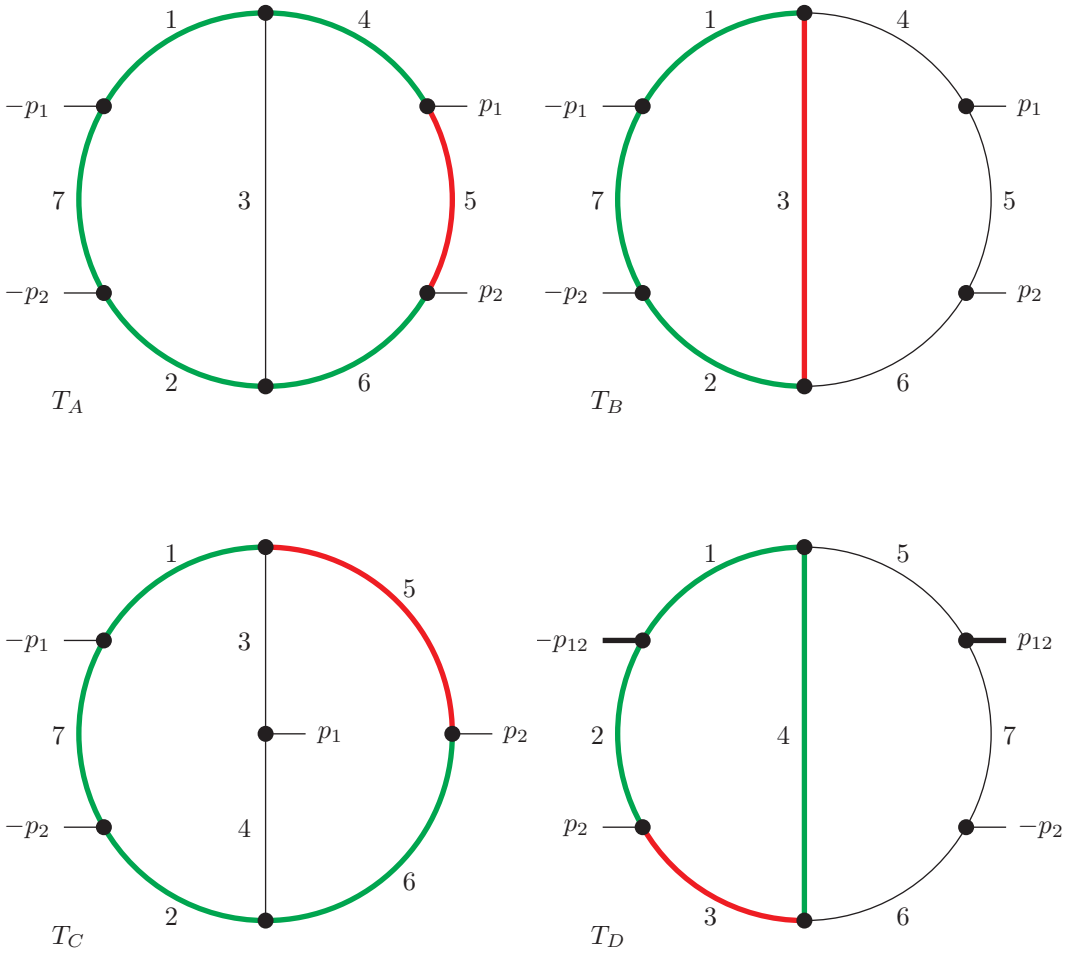

Figure 6.4. Auxiliary diagrams for the two planar vertex corrections, the non-planar vertex correction and topology D. The internal masses of the propagators are encoded by the colour of the propagators: massless (black), m_t (green), m_W (red).

$$P_4^B = -k_2^2, \qquad P_5^B = -(k_2+p_1)^2, \qquad P_6^B = -(k_2+p_1+p_2)^2,$$
$$P_7^B = -(k_1-p_1)^2 + m_t^2. \tag{6.2.2}$$

Topology C:

$$P_1^C = -k_1^2 + m_t^2, \qquad P_2^C = -(k_1-p_1-p_2)^2 + m_t^2, \qquad P_3^C = -(k_1+k_2)^2,$$
$$P_4^C = -(k_1+k_2-p_1)^2, \qquad P_5^C = -k_2^2 + m_W^2, \qquad P_6^C = -(k_2+p_2)^2 + m_t^2,$$
$$P_7^C = -(k_1-p_1)^2 + m_t^2. \tag{6.2.3}$$

Topology D:

$$P_1^D = -k_1^2 + m_t^2, \qquad P_2^D = -(k_1-p_1-p_2)^2 + m_t^2, \qquad P_3^D = -(k_1-p_1)^2 + m_W^2,$$
$$P_4^D = -(k_1+k_2)^2 + m_t^2, \qquad P_5^D = -k_2^2, \qquad P_6^D = -(k_2+p_1)^2,$$
$$P_7^D = -(k_2+p_1+p_2)^2. \tag{6.2.4}$$

We get our original three point diagrams when we substitute $\nu_7 = 0$. In our conventions, we are interested in the integrals with $\nu_7 \leq 0$.

Feynman parametrization: The Feynman parameter representations for the four topologies are given by

$$I^X_{\nu_1\nu_2\nu_3\nu_4\nu_5\nu_6\nu_7} = e^{2\gamma_E\epsilon}\frac{\Gamma(\nu-D)}{\prod_{j=1}^{7}\Gamma(\nu_j)}\int_{x_i\geq 0} d^7x\,\delta\left(1-\sum_{j=1}^{7}x_j\right)\left(\prod_{j=1}^{7}x_j^{\nu_j-1}\right)\frac{\mathcal{U}_X^{\nu-\frac{3}{2}D}}{\mathcal{F}_X^{\nu-D}},$$

The graph polynomials are given by

$$\begin{aligned}
\mathcal{U}_A &= (x_1+x_2+x_7)(x_4+x_5+x_6) + x_3(x_1+x_2+x_4+x_5+x_6+x_7),\\
\mathcal{F}_A &= [x_1x_2(x_3+x_4+x_5+x_6) + x_4x_6(x_1+x_2+x_3+x_7) + x_3(x_1x_6+x_2x_4)]\left(\frac{-p^2}{\mu^2}\right)\\
&\quad + \mathcal{U}_A\left[(x_1+x_2+x_4+x_6+x_7)\frac{m_t^2}{\mu^2} + x_5\frac{m_W^2}{\mu^2}\right],\\
\mathcal{U}_B &= (x_1+x_2+x_7)(x_4+x_5+x_6) + x_3(x_1+x_2+x_4+x_5+x_6+x_7),\\
\mathcal{F}_B &= [x_1x_2(x_3+x_4+x_5+x_6) + x_4x_6(x_1+x_2+x_3+x_7) + x_3(x_1x_6+x_2x_4)]\left(\frac{-p^2}{\mu^2}\right)\\
&\quad + \mathcal{U}_B\left[(x_1+x_2+x_7)\frac{m_t^2}{\mu^2} + x_3\frac{m_W^2}{\mu^2}\right],\\
\mathcal{U}_C &= (x_1+x_2+x_7)(x_5+x_6) + (x_3+x_4)(x_1+x_2+x_5+x_6+x_7),\\
\mathcal{F}_C &= [x_1x_2(x_3+x_4+x_5+x_6) + x_1x_4x_6 + x_2x_3x_5 - x_3x_6x_7]\left(\frac{-p^2}{\mu^2}\right)\\
&\quad + \mathcal{U}_C\left[(x_1+x_2+x_6+x_7)\frac{m_t^2}{\mu^2} + x_5\frac{m_W^2}{\mu^2}\right],\\
\mathcal{U}_D &= (x_1+x_2+x_3)(x_5+x_6+x_7) + x_4(x_1+x_2+x_3+x_5+x_6+x_7),\\
\mathcal{F}_D &= [x_1x_2(x_4+x_5+x_6+x_7) + x_5x_7(x_1+x_2+x_3+x_4) + x_4(x_1x_7+x_2x_5)]\left(\frac{-p^2}{\mu^2}\right)\\
&\quad + \mathcal{U}_D\left[(x_1+x_2+x_4)\frac{m_t^2}{\mu^2} + x_3\frac{m_W^2}{\mu^2}\right].
\end{aligned}$$

Using these graph polynomials, we can set up the differential equation system for our master integrals. We can have a look at all the (sub-) topologies of these graphs in the appendix.

6.2.1 Hint of ellipticity

In [26], the authors present an example of a non-planar two-loop three-point function which contributes to two-loop amplitudes for $t\bar{t}$ production and $\gamma\gamma$ production in gluon fusion.

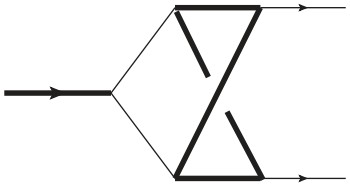

Figure 6.5. A non-planar three-point function belonging to the class functions that goes beyond MPLs.

In figure 6.5, we can see a graph which differs from topology C only in external momenta if we put $m_W = m_t$. This topology is associated to an elliptic curve and is not expressible entirely in terms of MPLs. This gives us a hint that the class of function the topology shown in figure 6.3 goes beyond the class of MPLs. However, this is not the case and we are able to express the result of the master integrals in this case in terms of MPLs. The only difficulty we face is the simultaneous rationalization of all the occurring (particularly two) square roots.

6.2.2 Technique to solve the system of differential equations

The technique we follow to solve the master integrals, i.e. to write down the master integrals as a Laurent series expansion in the dimensional regularization parameter, is to use the method of differential equations. In order to find the master integrals, we find the minimal set of integrals sufficient to express all the diagrams of the family of diagrams from the topologies shown in figure 6.3. We aim to bring the set of master integrals to the canonical form explained in section ⟨4.3⟩. In this process, as we already know that we encounter square roots, our aim is to find the coordinate system in which we can rationalize all the square roots simultaneously. At the end we write down the results as a Laurent series in the parameter ϵ.

6.2.3 A common set of master integrals

For the reduction to master integrals, we use the programs `Reduze` [37], `Kira` [38] or `Fire` [39] combined with `LiteRed` [40, 47]. Each topology involves a certain number of master integrals.

Topology	Number of master integrals
A	18
B	15
C	31
D	14

Table 6.1. The number of master integrals for a given topology.

This number of master integrals for each topology separately is shown in table 6.1. However, not all of these master integrals are independent and are related to each other, which brings the number of master integrals we need to solve in order to express all of these down to 39. We now show the relations between these master integrals:

$$
\begin{aligned}
I^A_{\mu 00\nu 000} &= I^C_{\mu 0000\nu 0} = I^D_{\mu 00\nu 000},\\
I^A_{\mu 000\nu 00} &= I^B_{\mu 0\nu 0000} = I^C_{\mu 000\nu 00} = I^D_{00\nu\mu 000},\\
I^A_{\mu\nu 0\rho 000} &= I^C_{\mu\nu 000\rho 0} = I^D_{\mu\nu 0\rho 000},\\
I^A_{\mu\nu 00\rho 00} &= I^B_{\mu\nu\rho 0000} = I^C_{\mu\nu 00\rho 00},\\
I^A_{0\mu\nu\rho 000} &= I^C_{\mu 00\nu 0\rho 0} = I^D_{0\mu 0\rho\nu 00},\\
I^B_{0\mu\nu\rho 000} &= I^C_{0\mu\rho 0\nu 00},\\
I^A_{\mu 0\nu 0\rho 00} &= I^B_{\mu 0\rho\nu 000} = I^C_{\mu 0\nu 0\rho 00} = I^D_{00\rho\mu\nu 00},\\
I^A_{\mu 00\nu\rho\sigma 0} &= I^D_{\nu\sigma\rho\mu 000},\\
I^B_{\mu\nu\rho\sigma 000} &= I^C_{\mu\nu\sigma 0\rho 00},\\
I^C_{\mu\nu\rho 00\sigma 0} &= I^D_{\mu\nu 0\sigma 0\rho 0},\\
I^A_{\mu\nu\rho 0\sigma 00} &= I^B_{\mu\nu\sigma 0\rho 00} = I^C_{\mu\nu 0\rho\sigma 00},\\
I^A_{0\mu\nu\rho\sigma 00} &= I^C_{\mu 00\nu\sigma\rho 0} = I^D_{0\rho\sigma\mu\nu 00},\\
I^A_{\mu\nu\rho\sigma\kappa 00} &= I^C_{\mu\nu 0\rho\kappa\sigma 0},\\
I^B_{\mu\nu\rho\sigma\kappa 00} &= I^C_{\mu\nu\sigma\kappa\rho 00},\\
I^C_{\mu 0\nu\rho\sigma\kappa 0} &= I^D_{0\kappa\sigma\mu\nu\rho 0}.
\end{aligned}
\tag{6.2.5}
$$

The 39 master integrals are grouped into 25 blocks such that one block corresponds to one sub-topology. Some of the master integrals are taken as integrals in $D-2 = 2-2\epsilon$ space-time dimensions because of better UV behaviour apart from the ease of solving. We can express them in terms of a linear combination of master integrals in $D = 4-2\epsilon$ dimensions with the help of the DSR discussed in section ⟨4.1.1⟩.

6.3 The choice of coordinate system:

In our case, the master integrals depend on two dimensionless quantities

$$v = \frac{p^2}{m_t^2}, \quad w = \frac{m_W^2}{m_t^2},$$

with $p = p_1 + p_2$, after we set

$$\mu^2 \;=\; m_t^2.$$

The coordinate system v, w is the most obvious choice to start with. However, we soon realize that this is not a smart choice as we encounter multiple square roots in this coordinate.

In particular, we get the following square roots

$$\sqrt{-v(4-v)} \text{ and } \sqrt{\lambda(v,w,1)}.$$

The Källen function is defined by

$$\lambda(x,y,z) = x^2 + y^2 + z^2 - 2xy - 2yz - 2zx.$$

In order to rationalize the square roots, we introduce dimensionless quantities x and y through

$$\frac{p^2}{m_t^2} \;=\; v \;=\; -\frac{(1-x)^2}{x}, \quad \frac{m_W^2}{m_t^2} \;=\; w \;=\; \frac{(1-y+2xy)(x-2y+xy)}{x(1-y^2)}.$$

The first transformation very standard and has occurred in many places before, the second one is obtained using the algorithm mentioned in [101]. The Feynman integrals are then functions of x, y and the dimensional regularization parameter ϵ. The inverse transformations are given by

$$x \;=\; \frac{1}{2}\left(2 - v - \sqrt{-v(4-v)}\right), \quad y \;=\; \frac{\sqrt{\lambda(v,w,1)} - \sqrt{-v(4-v)}}{1-w+2v},$$

such that $x = 0$ corresponds to $v = \infty$ and $y = 0$ corresponds to $w = 1$.

6.4 The transformation for the master integrals

Let the canonical basis of master integrals [35] be denoted by $\vec{J} = (J_1, ..., J_{39})^T$. The system of differential equations is in ϵ-form in this basis:

$$d\vec{J} = \epsilon A \vec{J}, \tag{6.4.1}$$

where matrix A is independent of ϵ. An exmple of the transformation which gives us the vector in the eq. (6.4.1) is given by

$$\begin{aligned}
J_1 =& \epsilon^2\, \mathbf{D}^- I^A_{1001000},\\
J_2 =& \epsilon^2\, \mathbf{D}^- I^A_{1000100},\\
J_3 =& \epsilon^2 \frac{\left(1-x^2\right)}{2x}\, \mathbf{D}^- I^A_{1101000},\\
J_4 =& \epsilon^2 \frac{\left(1-x^2\right)}{2x}\, \mathbf{D}^- I^A_{1100100},\\
J_5 =& \frac{1}{2}\epsilon^2 v\, \mathbf{D}^- I^B_{1001010},\\
J_6 =& \frac{1}{2}\epsilon^2 v\, \mathbf{D}^- I^B_{0011010},\\
J_7 =& \epsilon^2 \frac{\left(1-x^2\right)}{2x}\, \mathbf{D}^- I^A_{0111000},
\end{aligned}$$

$$
\begin{aligned}
J_8 =& \epsilon^2\, \mathbf{D}^- I^A_{(-1)111000},\\
J_9 =& \epsilon^2 \frac{(1-x)\left(1+x-2y+y^2+2xy+xy^2\right)}{x(1-y^2)}\, \mathbf{D}^- I^B_{0111000},\\
J_{10} =& \epsilon^2 \left[\mathbf{D}^- I^B_{(-1)111000} - (1-w)\mathbf{D}^- I^B_{0111000}\right],\\
J_{11} =& 2\epsilon^2\, \mathbf{D}^- I^B_{0111(-1)00} - 2\epsilon^2\, \mathbf{D}^- I^B_{0110000},\\
J_{12} =& \epsilon^2 (1-w)\, \mathbf{D}^- I^A_{1010100},\\
J_{13} =& \epsilon^2 \frac{\left(1-x^2\right)^2}{4x^2}\, \mathbf{D}^- I^A_{1101010},\\
J_{14} =& \epsilon^2 \frac{(1-x)^3(1+x)}{4x^2}\, \mathbf{D}^- I^B_{1101010},\\
J_{15} =& \epsilon^3 (1-\epsilon) v\, I^A_{1001110},\\
J_{16} =& \epsilon^2 \frac{\left(1-x^2\right)}{x}\left[(1-w)\, \mathbf{D}^- I^B_{1111000} - \mathbf{D}^- I^B_{0111000}\right],\\
J_{17} =& \epsilon^3 v\, I^C_{1120010},\\
J_{18} =& \epsilon^3 v\, I^C_{1110020},\\
J_{19} =& \epsilon^2 \frac{\left(1-x^2\right)}{x}\left[(1-2\epsilon)\, I^C_{2110010} + \epsilon\, I^C_{1110020}\right],\\
J_{20} =& \epsilon^3 v\, I^A_{1120100},\\
J_{21} =& \epsilon^3 v\, I^A_{1110200},\\
J_{22} =& 2\epsilon^2 \frac{(1-x)}{x(1+w)}\left[(1-2\epsilon)(1+x)\, I^A_{2110100} - \epsilon(x-w)\, I^A_{1120100} + \epsilon(1-x+2w)\, I^A_{1110200}\right.\\
& \left. -\frac{1}{2}(1+x)\, \mathbf{D}^- I^A_{1100100}\right],\\
J_{23} =& 2\epsilon^3 v\, I^A_{0211100},\\
J_{24} =& 2\epsilon^3 v\, I^A_{0121100},\\
J_{25} =& 2\epsilon^3 v\, I^C_{0210110},\\
J_{26} =& 2\epsilon^3 v\, I^C_{0120110},\\
J_{27} =& \epsilon^3 \frac{(1-x)^2}{x(1+x)}\left[(1-2\epsilon)(1-x)\, I^A_{1101110} + 2(1-\epsilon)\, I^A_{1001110}\right],\\
J_{28} =& 2\epsilon^3 (1-2\epsilon) v\, I^B_{1111010},\\
J_{29} =& 2\epsilon^3 v(1-w)\, I^A_{1111200},\\
J_{30} =& 2\epsilon^3 v\left(I^A_{1112100} + I^A_{1111200}\right),\\
J_{31} =& 4\epsilon^3 \frac{(1-x)^2}{x(1+x^2)}\left[\left(1-x^2\right) I^A_{2111100} - (1+w) I^A_{1111200} - 2I^A_{1112100} + 2I^A_{1120100} + I^A_{1110200}\right.\\
& \left. - I^A_{0211100} - 2I^A_{0121100}\right],\\
J_{32} =& 4\epsilon^4 v\, I^B_{1111100},\\
J_{33} =& 2\epsilon^3 v(1-w)\, I^C_{1110120},\\
J_{34} =& 2\epsilon^3 vw\left(I^C_{1110210} + I^C_{1110120}\right),\\
J_{35} =& 2\epsilon^3 v(1-w)\, I^C_{1120110},
\end{aligned}
$$

$$
\begin{aligned}
J_{36} =& 4\epsilon^3 \frac{(1-x)^2}{x(1+x^2)} \Big[\left(1-x^2\right) I^C_{2110110} - (1+w)\, I^C_{1110120} - 2w\, I^C_{1110210} + 2(1-w)\, I^C_{1120110} \\
& + 2I^C_{1120010} + I^C_{1110020} - I^C_{0210110} - 2I^C_{0120110} \Big], \\
J_{37} =& 2\epsilon^4 v\, I^C_{1011110}, \\
J_{38} =& \epsilon^3 vw\, I^D_{1112010}, \\
J_{39} =& 4\epsilon^4 \frac{(1-x)^2 \left(1-x+x^2-xw\right)}{x^2}\, I^C_{1111110}.
\end{aligned} \tag{6.4.2}
$$

6.5 The one-forms of the system

Let us now discuss the singularities of the system of differential equations. The singularities are on hypersurfaces and each hypersurface is defined by a polynomial in x and y. The polynomials in our differential system are given by

$$
\begin{aligned}
p_1 =& x,\ \ p_2 = x-1,\ \ p_3 = x+1,\ \ p_4 = y,\ \ p_5 = y-1,\ \ p_6 = y+1,\ \ p_7 = xy+x-y+1, \\
p_8 =& xy+x-2y,\ \ p_9 = 2xy-y+1,\ \ p_{10} = xy^2+2xy-2y^2+x+2y, \\
p_{11} =& xy^2+2xy+y^2+x-2y+1,\ \ p_{12} = xy^2+2xy-y^2+x+2y-1,\ \ p_{13} = 2xy^2+2xy-y^2+2y-1, \\
p_{14} =& 2xy^2+2xy-3y^2+2y+1,\ \ p_{15} = 3xy^2+2xy-2y^2-x+2y,\ \ p_{16} = 3xy^2+2xy-3y^2-x+2y+1.
\end{aligned}
$$

In total we have 16 polynomials. We note that the polynomials p_k are maximally of degree 3 and the highest degree in the variable y is two, whereas the highest degree in the variable x is one. We observe that in our differential system the entries of matrix A are $\mathbb{Q}$-linear combinations of dlog-forms of these polynomials:

$$
A_{ij} = \sum_{k=1}^{16} \tilde{c}_{ijk}\, d\ln(p_k(x,y)), \qquad \tilde{c}_{ijk} \in \mathbb{Q}. \tag{6.5.1}
$$

and find that matrix A contains only fifteen $\mathbb{Q}$-independent linear combinations of dlog-forms. We can, therefore, consider a basis for these one forms as follows:

$$\omega_1 = \frac{ds}{s} = 2d\ln p_2 - d\ln p_1,\ \omega_2 = \frac{ds}{s-4m_t^2} = 2d\ln p_3 - d\ln p_1,\ \omega_3 = \frac{ds}{\sqrt{-s\left(4m_t^2-s\right)}} = d\ln p_1,$$

$$\omega_4 = \frac{dm_W^2}{m_W^2} = d\ln p_8 + d\ln p_9 - d\ln p_5 - d\ln p_6 - d\ln p_1,$$

$$\omega_5 = \frac{dm_W^2}{m_W^2-m_t^2} = d\ln p_7 - d\ln p_5 - d\ln p_6 + d\ln p_4 + d\ln p_2 - d\ln p_1,$$

$$\omega_6 = d\ln\left(s+m_W^2-m_t^2\right) = d\ln p_{16} - d\ln p_5 - d\ln p_6 + d\ln p_2 - d\ln p_1,$$

$$\omega_7 = d\ln\left(s-m_W^2+m_t^2\right) = d\ln p_{12} - d\ln p_5 - d\ln p_6 + d\ln p_2 - d\ln p_1,$$

$$\omega_8 = \frac{1}{2}d\ln\left(sm_W^2+\left(m_t^2-m_W^2\right)^2\right) = \frac{1}{2}d\ln p_{15} + \frac{1}{2}d\ln p_{14} - d\ln p_5 - d\ln p_6 + d\ln p_2 - d\ln p_1,$$

$$\omega_9 = \frac{1}{2}d\ln\left(\left(2m_t^2-m_W^2\right)s+\left(m_t^2-m_W^2\right)^2\right) = \frac{1}{2}d\ln p_{13} + \frac{1}{2}d\ln p_{10} - d\ln p_5 - d\ln p_6 + d\ln p_2 - d\ln p_1,$$

$$\omega_{10} = \frac{1}{2}d\ln\left(\lambda\left(s,m_W^2,m_t^2\right)\right) = d\ln p_{11} - d\ln p_5 - d\ln p_6 + d\ln p_2 - d\ln p_1,$$

$$\omega_{11} = \frac{1}{2}d\ln p_{15} - \frac{1}{2}d\ln p_{14},\ \omega_{12} = \frac{1}{2}d\ln p_{13} - \frac{1}{2}d\ln p_{10},\ \omega_{13} = \frac{1}{2}d\ln p_9 - \frac{1}{2}d\ln p_8,$$

$$\omega_{14} = \frac{1}{2}d\ln p_6 - \frac{1}{2}d\ln p_5,\ \omega_{15} = d\ln p_4 - \frac{1}{2}d\ln p_6 - \frac{1}{2}d\ln p_5.$$

The entries of A are therefore of the form

$$A_{ij} = \sum_{k=1}^{15} c_{ijk}\,\omega_k, \qquad c_{ijk} \in \mathbb{Q}.$$

We can also re-scaling the master integrals with constant factors such that we obtain only integer coefficients.

$$c_{ijk} \in \mathbb{Z}.$$

The basis of master integrals $\vec{J}$ presented in [108] has this form. We can also choose to express matrix A as

$$A = \sum_{k=1}^{15} C_k\,\omega_k,$$

where the entries of the 39×39-matrices C_k are integer numbers. This matrix can be obtained from the arXiv submission of [108].

In our choice of coordinate, the differential forms simplify considerably in the following cases:

1. On the hypersurface $y = 0$ (i.e. for the case $m_W = m_t$), i.e. for the case $p^2 \to \infty$, the differential forms reduce to a linear combination of
$$\frac{dx}{x},\ \frac{dx}{x-1},\ \frac{dx}{x+1}.$$

2. On the hypersurface $x = 0$, i.e. for the case $p^2 \to \infty$, the differential forms reduce to a linear combination of
$$\frac{dy}{y},\ \frac{dy}{y-1},\ \frac{dy}{y+1},\ \frac{dy}{y+\frac{1}{3}}.$$

3. On the hypersurface $x = 1$, i.e. for the case $p^2 = 0$ and $m_W^2 = m_t^2$, the differential forms reduce to a linear combination of

$$\frac{dy}{y}, \quad \frac{dy}{y-1}, \quad \frac{dy}{y+1}, \quad \frac{2ydy}{y^2+1}, \quad \frac{2(y-2)dy}{y^2-4y-1}, \quad \frac{2(y+2)dy}{y^2+4y-1}.$$

The derivative of the master integrals is given by the product of the matrix A with the vector $\vec{J}$:

$$d\vec{J} = \epsilon A \vec{J}.$$

On the hypersurface $x = 1$, $\vec{J}$ is in the kernel of A because

$$\left.\frac{\partial \vec{J}}{\partial y}\right|_{x=1} = 0,$$

even though $A \neq 0$. Therefore the master integrals are constant on the hypersurface $x = 1$. This motivates us to consider this as a boundary point while integrating the system of differential equations.

6.6 Boundary conditions and integration of the differential system for the master integrals

In order to obtain the analytic result for the master integrals at a point (x, y), we integrate the system from a boundary point (x_i, y_i) along a path (x_i, y_i) to (x, y). For our case, as already pointed out, we have several significant simplifications:

1. All master integrals are constant on the hypersurface $x = 1$ (corresponding to $p^2 = 0$ and $m_W^2 = m_t^2$) and therefore we take the values of the master integrals on this hypersurface as boundary values. We can refer to this as a boundary line.

2. Then we integrate the differential equation along a straight line from $(1, y)$ to (x, y) with $y = \text{const}$ (the result does not depend on the path chosen). The polynomials p_1-p_3 and p_7-p_{16} are all linear in x (the polynomials p_4-p_6 don't contribute along $y = \text{const}$), and thus we do not need to factorize higher-order polynomials in x.

3. We also notice that the boundary values on the hypersurface $x = 1$ are particularly simple as 35 out of the 39 master integrals vanish on this hypersurface and the only four master integrals which do not vanish are products of one-loop integrals.

We can see that all the integration kernels are dlog-forms and therefore the result can be expressed in terms of MPLs.

6.6.1 Boundary constants

As mentioned above all other master integrals vanish on the hypersurface $x = 1$. The only non-vanishing master integrals at $x = 1$ are J_1, J_2, J_5 and J_6. These are rather simple as they are

products of one-loop integrals. These are given by:

$$\begin{aligned}
J_1 =& e^{2\gamma_E\epsilon}\left(\Gamma(1+\epsilon)\right)^2,\\
J_2 =& e^{2\gamma_E\epsilon}\left(\Gamma(1+\epsilon)\right)^2 w^{-\epsilon},\\
J_5 =& e^{2\gamma_E\epsilon}\frac{\left(\Gamma(1+\epsilon)\right)^2\left(\Gamma(1-\epsilon)\right)^2}{\Gamma(1-2\epsilon)}(-v)^{-\epsilon},\\
J_6 =& e^{2\gamma_E\epsilon}\frac{\left(\Gamma(1+\epsilon)\right)^2\left(\Gamma(1-\epsilon)\right)^2}{\Gamma(1-2\epsilon)}(-v)^{-\epsilon}w^{-\epsilon}.
\end{aligned}$$

Therefore, we obtain the full set of boundary conditions required for our system, on the line $(x,y)=(1,y)$.

Since we are performing an integration in the (x,y)-space from $(1,y)$ to (x,y), it is better to change variables from x to $x'=1-x$. In (x',y)-space, we integrate the system from $(0,y)$ to (x',y), where y is treated as a parameter. This integration gives MPLs of the form

$$G\left(l'_1,...,l'_k;x'\right),$$

where the letters l'_1, ..., l'_k are from the alphabet

$$\mathcal{A}=\left\{0,1,2,x'_7,x'_8,x'_9,x'_{10},x'_{11},x'_{12},x'_{13},x'_{14},x'_{15},x'_{16}\right\}.$$

The non-trivial letters x'_7-x'_{16} are given by

$$\begin{aligned}
x'_7 &= \frac{2}{1+y}, & x'_8 &= \frac{1-y}{1+y}, & x'_9 &= \frac{1+y}{2y},\\
x'_{10} &= \frac{1+4y-y^2}{(1+y)^2}, & x'_{11} &= \frac{2\left(1+y^2\right)}{(1+y)^2}, & x'_{12} &= \frac{4y}{(1+y)^2},\\
x'_{13} &= -\frac{1-4y-y^2}{2y(1+y)}, & x'_{14} &= \frac{1+4y-y^2}{2y(1+y)}, & x'_{15} &= \frac{1-4y-y^2}{(1+y)(1-3y)},\\
x'_{16} &= -\frac{4y}{(1+y)(1-3y)}.
\end{aligned}$$

6.6.2 A peek at the results

For all the basis integrals in our case, we write

$$J_k=\sum_{j=0}^{\infty}\epsilon^j J_k^{(j)}.$$

To give an example, here we show the first non-vanishing term of the most complicated integral, the non-planar vertex correction J_{39}:

$$\begin{aligned}
J_{39}^{(3)} =& 8G(0,1,1;x') - 4G\left(0,1,x_8';x'\right) - 4G\left(0,x_8',1;x'\right) + 4G\left(0,x_8',x_9';x'\right) + 4G\left(0,x_9',x_8';x'\right) \\
& - 8G(1,2,1;x') + 8G\left(1,x_{15}',1;x'\right) - 4G\left(1,x_{15}',x_8';x'\right) - 4G\left(1,x_{15}',x_9';x'\right) \\
& - 16G\left(1,x_7',1;x'\right) + 8G\left(1,x_7',x_8';x'\right) + 12G\left(1,x_7',x_9';x'\right) + 4G\left(1,x_8',1;x'\right) \\
& - 4G\left(1,x_8',x_9';x'\right) - 4G\left(1,x_9',x_8';x'\right) + 8G\left(x_{14}',2,1;x'\right) - 8G\left(x_{14}',x_{15}',1;x'\right) \\
& + 4G\left(x_{14}',x_{15}',x_8';x'\right) + 4G\left(x_{14}',x_{15}',x_9';x'\right) + 16G\left(x_{14}',x_7',1;x'\right) - 8G\left(x_{14}',x_7',x_8';x'\right) \\
& - 12G\left(x_{14}',x_7',x_9';x'\right) - 4G\left(x_{14}',x_8',1;x'\right) + 4G\left(x_{14}',x_8',x_9';x'\right) + 4G\left(x_{14}',x_9',x_8';x'\right) \\
& + 8G\left(x_{15}',1,1;x'\right) + 4G\left(x_{15}',1,x_8';x'\right) - 8G\left(x_{15}',2,1;x'\right) + 4G\left(x_{15}',x_{14}',x_8';x'\right) \\
& + 4G\left(x_{15}',x_{14}',x_9';x'\right) + 4G\left(x_{15}',x_7',1;x'\right) - 12G\left(x_{15}',x_7',x_8';x'\right) - 8G\left(x_{15}',x_7',x_9';x'\right) \\
& - 4G\left(x_{15}',x_8',1;x'\right) + 4G\left(x_{15}',x_8',x_9';x'\right) + 4G\left(x_{15}',x_9',x_8';x'\right) - 8G\left(x_7',1,1;x'\right) \\
& + 4G\left(x_7',1,x_8';x'\right) + 4G\left(x_7',x_8',1;x'\right) - 4G\left(x_7',x_8',x_9';x'\right) - 4G\left(x_7',x_9',x_8';x'\right).
\end{aligned}$$

We can see that the results are expressible as Goncharov polylogarithms.

6.7 Numerical results

Numerical checks for any calculations are equally important and therefore we also discuss the numerical checks. The numerical results for

$$p^2 = m_H^2,$$

are particularly of interest. Since $p^2 > 0$, we are not in the Euclidean region. Feynman's $i0$-prescription instructs us to take a small imaginary part into account: $p^2 \to p^2 + i0$, which selects the correct branches for the two square roots $\sqrt{-v(4-v)}$ and $\sqrt{\lambda(v,w,1)}$. With

$$m_W = 80.38\,\text{GeV}, \quad m_H = 125.2\,\text{GeV}, \quad m_t = 173.1\,\text{GeV}$$

we obtain for the variables x and y

$$x = 0.7384 + 0.6743i, y = 0.3987i.$$

The values of the master integrals at this point are given to 8 digits in table 6.2. As explained in the previous chapter, these master integrals are easily computed to arbitrary precision by evaluating the MPLs with the help of `GiNaC` [67, 68]. In order to verify these results, we also calculated and matched the first few digits at various kinematic points with the help of the programs `sector_decomposition` [63] and `pySecDec` [69], for which we found a good agreement.

	ϵ^0	ϵ^1	ϵ^2	ϵ^3	ϵ^4
J_1	1	0	1.6449341	−0.80137127	1.8940657
J_2	1	1.5342081	2.8218314	2.3241685	2.8313617
J_3	0	$-0.74005414i$	$-0.069477641i$	$-1.2212434i$	$0.47861551i$
J_4	0	$-0.74005414i$	$-1.2048747i$	$-2.1988043i$	$-1.9222094i$
J_5	1	$0.64791401 + 3.1415927i$	$-4.7249059 + 2.0354819i$	$-6.357481 - 4.5083042i$	$-2.2935901 - 13.276148i$
J_6	1	$2.1821222 + 3.1415927i$	$-2.5539737 + 6.8553389i$	$-12.242073 + 2.3118807i$	$-16.987211 - 15.906447i$
J_7	0	$0.74005414i$	$-1.2490335i$	$4.0114542i$	$-7.931414i$
J_8	0	0	−0.54768013	0.47549335	−2.5261306
J_9	0	$1.4585842i$	$0.050868134i$	$6.4537259i$	$-4.1565512i$
J_{10}	0	1.5342081	−1.7502763	5.7981619	−12.790768
J_{11}	0	0	2.2406312	1.5008239	10.399293
J_{12}	0	−1.5342081	0.91070302	−5.9968338	8.8611857
J_{13}	0	0	−0.54768013	−0.10283443	−0.91150188
J_{14}	0	$0.74005414i$	$-2.3249487 + 0.54896908i$	$-1.7246372 - 3.4477675i$	$3.1827067 - 5.0304701i$
J_{15}	0	0	−0.40473314	−0.19458947	−0.73218618
J_{16}	0	$-1.4801083i$	$2.8153204i$	$-7.8872093i$	$15.843952i$
J_{17}	0	0	−0.27384007	0.25481947	−1.2423838
J_{18}	0	0	0	0.54349879	−0.505106
J_{19}	0	$-0.74005414i$	$1.3879888i$	$-3.8717735i$	$8.3164903i$
J_{20}	0	0	−0.40473314	−0.012836717	−1.766483
J_{21}	0	0	0	1.0679293	0.50513135
J_{22}	0	0	$0.40473314 + 2.8771124i$	$-2.1230218 - 1.197403i$	$0.75622025 + 11.086074i$
J_{23}	0	0	0	1.4266372	−0.44333884
J_{24}	0	0	−0.80946628	0.078302369	−3.4351805
J_{25}	0	0	0	1.447072	−0.3662879
J_{26}	0	0	−0.83957331	−0.038098053	−3.7104375
J_{27}	0	0	0.40473314	$0.19458947 - 0.29952444i$	$0.73218618 - 0.17212665i$
J_{28}	0	0	0	$2.4399925 + 2.5430133i$	$-6.9287969 + 2.8702957i$
J_{29}	0	0	0	0.69594214	1.4888349
J_{30}	0	0	0	1.3639124	2.6684304
J_{31}	0	0	0	$1.530613 - 0.59904887i$	$2.5899951 - 1.0224563i$
J_{32}	0	0	0	−1.6890882	−0.27250855
J_{33}	0	0	0	0.372767	0.60475274
J_{34}	0	0	0	0.30226015	0.61200492
J_{35}	0	0	−0.29189318	−0.65744728	−1.3431597
J_{36}	0	0	0	$1.5567823 - 0.61339819i$	$2.7076661 - 1.0872344i$
J_{37}	0	0	0	−0.78991058	0.12604664
J_{38}	0	0	0	0.050162573	0.077279399
J_{39}	0	0	0	0.18876826	0.41154739

Table 6.2. Numerical results for the first five terms of the ϵ-expansion of the master integrals J_1-J_{39} at the kinematic point $s = m_H^2$.

6.8 The total decay rate of the Higgs to two bottom quarks:

As already motivated at the beginning of this chapter, a precise measurement of the decay rate of the $H \to b\bar{b}$ process directly tests the Yukawa coupling of the Higgs boson to a down-type quark. This is necessary to solidify the Higgs boson as the only possible source of mass generation in the fermion sector of the SM. The Higgs boson decays most frequently in a pair of bottom quarks, which is a down-type quark. In the last part of this chapter, we briefly sketch the computation of the full decay rate using optical theorem mentioned in chapter 2. The scattering amplitudes, as a function of energy, has a branch cut on the positive real axis, and with the optical theorem, we can relate this imaginary part, of the forward scattering amplitude, to the total cross section.

In order to perform this calculation, we can parametrize the corrections to the decay rate as follows [98]:

$$\Gamma(H \to b\bar{b}) = \Gamma^{(0)}(1 + \Delta^{\alpha_s} + \Delta^{(\alpha)} + \Delta^{(\alpha\alpha_s)} + ...),$$

where the ellipses stand for higher-order corrections in α and α_s. We can split the EW corrections

into a weak and a QED contributions which are separately finite and gauge-invariant:

$$\begin{aligned}\Delta^{(\alpha)} &= \Delta^{(QED)} + \Delta^{(weak)},\\ \Delta^{(\alpha\alpha_s)} &= \Delta^{(QED,\alpha_s)} + \Delta^{(weak,\alpha_s)}.\end{aligned}$$

Here, $\Gamma^{(0)}$ denotes the Born decay rate given by

$$\Gamma^{(0)} = \frac{N_c \alpha m_b^2 M_H}{8 s_W^2 M_W^2} \beta_0^3,$$

where $N_c = 3$ is the number of colors and s_W is the sine of the weak mixing angle. $\beta_0 = \sqrt{1 - 4m_b^2/M_H^2}$ is the velocity of the produced bottom quarks, which we can approximate to 1. In section ⟨6.1.1⟩, we have used the Fermi constant G_F. It is useful to write down the relation between the two, which is given by,

$$\frac{G_F}{\sqrt{2}} = \frac{\pi\alpha}{2 s_W^2 M_W^2} \frac{1}{1 - \Delta r},$$

where Δr parametrizes the radiative corrections to the muon decay beyond QED corrections within the effective four-fermion theory. We need to renormalize all the quantities properly and take care of the counterterms.

The analytic expression for $\Delta^{(QED,\alpha_s)}$ can easily be obtained from the $O(\alpha_s^2)$ QCD corrections. In order to obtain the $\Delta^{(weak,\alpha_s)}$ corrections, we can use the following technique. We consider the imaginary part of the three-loop propagator-type diagrams which are obtained by dressing the $O(\alpha)$ diagrams in all possible ways with a coupling of top quark and Higgs. For the evaluation of the full decay rate $\Gamma(H \to b\bar{b})$, we use the optical theorem which for our case has the form

$$\Gamma(H \to b\bar{b}) = \frac{1}{M_H} \mathrm{Im}\left[\sum_H (q^2 = M_H^2 + i\epsilon)\right],$$

where $\sum_H(q^2)$ is the Higgs boson two-point function which is evaluated on the Higgs boson mass shell.

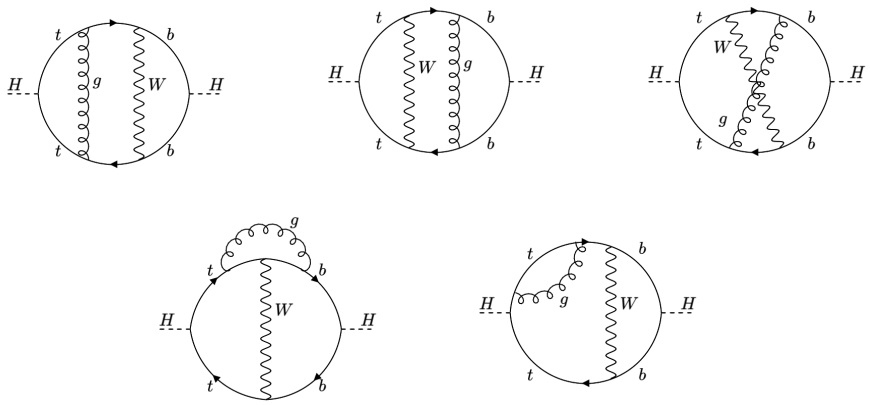

Figure 6.6. The propagator type diagrams needed to evaluate the decay rate of Higgs boson into a pair of b quarks using the optical theorem.

In figure 6.6, we show some examples of the type of diagrams needed in order to calculate the decay rate of the Higgs boson to a pair of bottom quarks using the optical theorem. Here t, b W and H denote the top quark, the bottom quark, the electroweak boson, and the Higgs boson respectively. All the diagrams symmetrical to these diagrams are not shown explicitly. The master integrals are also expected to be expressible in terms of MPLs.

6.9 Results

In this chapter, we discussed the two-loop master integrals relevant to the $O(\alpha\alpha_s)$-corrections to the decay $H \to b\bar{b}$ through a $Ht\bar{t}$-coupling. The master integrals depend exactly on the masses of the heavy particles (m_W and m_t) along with momentum p^2 of the Higgs boson. We found out that all the master integrals are expressed in terms of MPLs with an alphabet of 13 letters after we rationalize both the occurring square roots simultaneously. The integrals can be evaluated to arbitrary precision with the help of the `GiNaC`-library and we also had a look at the numerical values for the special case $p^2 = m_H^2$. These integrals are needed for computation of the partial width for the Higgs decay into a pair of bottom quarks. At the end, we also briefly looked at the full decay width computation for the process $H \to b\bar{b}$.

7 Conclusion and Outlook

The close coordination between experiments being carried out at the LHC and theoretical predictions by performing perturbative calculations is the need of the hour. We live in the time when mass corrections from electorweak bosons and top quarks are highly required. We therefore need to evaluate multi-loop scattering amplitudes which requires the evaluation of Feynman integrals with masses, which poses several theoretical challenges. In order to solve Feynman integrals we can use the method of differential equations. Bringing them to canonical form is often the easiest way to write down the solution immediately as iterated integrals when expanded as a Laurent series in the dimensional regulator ϵ. For most of the massless cases it is possible to write down the results in terms in MPLs. This is however not generally true when we start including masses in the diagram. The simplest example of an integral which cannot be written down in terms of MPLs is the sunrise diagram. This opens the door for Feynman integrals evaluating to functions 'beyond the MPLs'.

In this work we discussed various techniques which can be employed to solve such integrals. The case of the planar double box showed us an example of a diagram which contains three different elliptic curves, and hence was difficult to tackle. We showed explicitly how we can use the factorization properties of the Picard–Fuchs operator associated to the topologies, to construct a basis which decouples the system of differential equation in blocks of size 2×2, at order ϵ^0, at worst. For the system of linear differential equation, we used a special linear form to write down the results as iterated integrals of the kernels present in our differential system. The differential system simplifies in two particular limits, $t = m^2$ and $s = \infty$, where t and s are the Mandelstam variables in the system and m is the mass in the loop. At these special points we are able to write the result of our integrals as MPLs and iterated integrals of modular forms respectively.

We also discussed the computation of master integrals for the two-loop mixed QCD-EW corrections for the Higgs decay to two bottom quarks. This family of integral contains a hint of being associated to an elliptic curve. However we are able to find out that this is not the case, and once we rationalize all the occurring square roots in the differential system, we are able to write down the result of the master integrals entirely in terms of MPLs. Apart from performing the evaluation of the master integrals, we also had a look at how we can use these calculations to observe a physical observable, namely the full decay rate of Higgs boson to a pair of bottom quarks. The techniques discussed in this work are expected to be useful for tackling more complicated topologies in future.

8 Appendix

Contents

8.1 Feynman rules

In this section, we mention the Lagrangian for the SM for completeness and also show explicitly how to read off the rules from the Lagrangian in the case of QCD.

8.1.1 QCD lagrangian:

The $SU(N)$ gauge invariant classical Lagrangian density which governs the interaction between fermions and non-Abelian gauge fields is given as

$$\mathcal{L}_{classical} = -\frac{1}{4} F^a_{\mu\nu} F^{a,\mu\nu} + \sum_{f=1}^{n_f} \overline{\psi}^{(f)}_{\alpha,i} \left(i \not{D}_{\alpha\beta,ij} - m_f \delta_{\alpha\beta} \delta_{ij} \right) \psi^{(f)}_{\beta,j} ., \tag{8.1.1}$$

where,

$$\begin{aligned} F^a_{\mu\nu} &= \partial_\mu A^a_\nu - \partial_\nu A^a_\mu + g_s f^{abc} A^b_\mu A^c_\nu , \\ \not{D}_{\alpha\beta,ij} &\equiv \gamma^\mu_{\alpha\beta} D_{\mu,ij} = \gamma^\mu \left(\delta_{ij} \partial_\mu - i g_s T^a_{ij} A^a_\mu \right) \end{aligned} \tag{8.1.2}$$

and A^a_μ and $\psi^{(f)}_{\alpha,i}$ are the guage and fermionic quark fields, respectively. The indices in each case correspond to the following:

$$\begin{aligned}
a,b,\cdots: &\quad \text{color indices in the adjoint representation} \Rightarrow [1,N^2-1],\\
i,j,\cdots: &\quad \text{color indices in the fundamental representation} \Rightarrow [1,N],\\
\alpha,\beta,\cdots: &\quad \text{Dirac spinor indices} \Rightarrow [1,D],\\
\mu,\nu,\cdots: &\quad \text{Lorentz indices} \Rightarrow [1,D].
\end{aligned} \tag{8.1.3}$$

Here D is the space-time dimensions. The mass of the quark corresponding to $\psi^{(f)}$ is given by m_f and g_S stands for the strong coupling constant, respectively. The structure constants of SU(N) group is given by f^{abc}. The generators of the fundamental representations of SU(N) is related to the structure constant as

$$\left[T^a, T^b\right] = if^{abc}T^c\,. \tag{8.1.4}$$

T^a are traceless, Hermitian matrices and we can normalise them as

$$Tr\left(T^aT^b\right) = T_F\delta^{ab} \tag{8.1.5}$$

where, $T_F = \frac{1}{2}$. The completeness relation for these matrices are given as

$$\sum_a T^a_{ij}T^a_{kl} = \frac{1}{2}\left(\delta_{il}\delta_{kj} - \frac{1}{N}\delta_{ij}\delta_{kl}\right). \tag{8.1.6}$$

In addition, we also have the following relations for them.

$$\begin{aligned}
\sum_a (T^aT^a)_{ij} &= C_F\delta_{ij}\,,\\
f^{acd}f^{bcd} &= C_A\delta^{ab}\,,
\end{aligned} \tag{8.1.7}$$

where $C_A = N$ and $C_F = \frac{N^2-1}{2N}$ are the quadratic Casimirs of the SU(N) group in the adjoint and fundamental representations respectively. For QCD, the SU(N) group index, $N = 3$ and the flavor number $n_f = 6$.

In order to obtain the propagators unambiguously we need to add some terms in the Lagrangian to 'fix the gauge'. The gauge fixing in a covariant way, when done through the path integral formalism, generates new particles called Faddeev-Popov (FP) ghosts having spin-0 but obeying fermionic statistics. Perturbative gauge theories in certain non-covariant gauges, such as light-cone or axial gauges, are ghost free. However ghosts are unavoidable in order to maintain manifest Lorentz invariance in a perturbative gauge theory.

As a result we obtain the following full quantum Lagrangian density:

$$\mathcal{L}_{YM} = \mathcal{L}_{classical} + \mathcal{L}_{gauge-fix} + \mathcal{L}_{ghost} \tag{8.1.8}$$

where, the second and third terms on the right hand side correspond to the gauge fixing and FP contributions, respectively. These are obtained as

$$\begin{aligned}
\mathcal{L}_{gauge-fix} &= -\frac{1}{2\xi}\left(\partial^\mu A^a_\mu\right)^2\,,\\
\mathcal{L}_{ghost} &= (\partial^\mu\chi^{a*})\,D_{\mu,ab}\chi^b
\end{aligned} \tag{8.1.9}$$

with

$$D_{\mu,ab} \equiv \delta_{ab}\partial_\mu - g_s f_{abc} A^c_\mu \,. \tag{8.1.10}$$

The arbitrary gauge parameter ξ is introduced in order to specify the gauge in a covariant way. The prescription of fixing gauge in a covariant way is known as R_ξ gauge, the choice $\xi = 1$ is known as Feynman gauge. However, the physical result is independent of the choice of the gauges. The field χ^a and χ^{a*} are ghost and anti-ghost fields, respectively.

All the Feynman rules can be read off from the quantized Lagrangian $\mathcal{L}_{YM}$ in Eq. 8.1.8. Let us see how they are represented. The quarks are denoted through straight lines, gluons through curly and ghosts through dotted lines. We provide the rules in R_ξ gauge.

- The Feynman rules for the propagators for quarks, gluons and ghosts are given from this theory as:

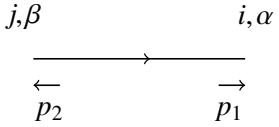

$$i\,(2\pi)^4\,\delta^{(4)}\,(p_1+p_2)\,\delta_{ij}\left(\frac{1}{\not{p}_1 - m_f + iO}\right)_{\alpha\beta}$$

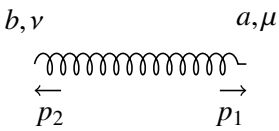

$$i\,(2\pi)^4\,\delta^{(4)}\,(p_1+p_2)\,\delta_{ab}\frac{1}{p_1^2}\left[-g_{\mu\nu} + (1-\xi)\frac{p_{1\mu}p_{1\nu}}{p_1^2}\right]$$

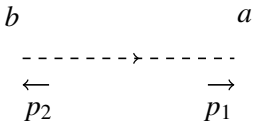

$$i\,(2\pi)^4\,\delta^{(4)}\,(p_1+p_2)\,\delta_{ab}\frac{1}{p_1^2}$$

- For the interacting vertices the rules are given by:

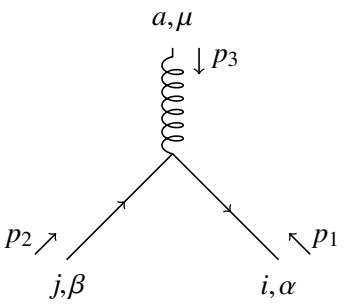

$$i g_s\,(2\pi)^4\,\delta^{(4)}\,(p_1+p_2+p_3)\,T^a_{ij}\,(\gamma^\mu)_{\alpha\beta}$$

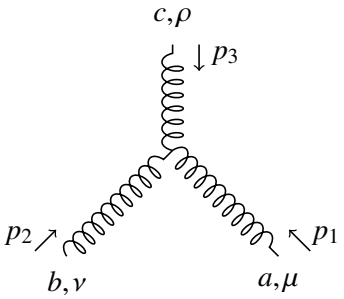

$$\frac{g_s}{3!}(2\pi)^4\delta^{(4)}(p_1+p_2+p_3)\,f^{abc}$$
$$\times\left[g^{\mu\nu}(p_1-p_2)^\rho+g^{\nu\rho}(p_2-p_3)^\mu+g^{\rho\mu}(p_3-p_1)^\nu\right]$$

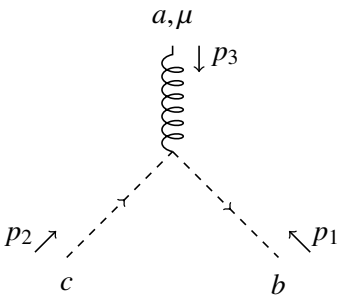

$$-g_s(2\pi)^4\delta^{(4)}(p_1+p_2+p_3)\,f^{abc}p_1^\mu$$

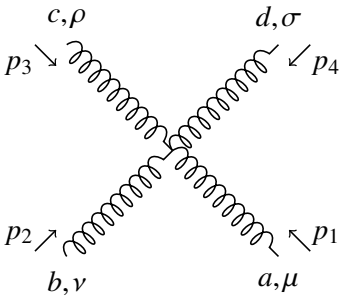

$$-\frac{g_s^2}{4!}(2\pi)^4\delta^{(4)}(p_1+p_2+p_3+p_4)$$
$$\left\{\left(f^{ac,bd}-f^{ad,cb}\right)g^{\mu\nu}g^{\rho\sigma}+\left(f^{ab,cd}-f^{ad,bc}\right)g^{\mu\rho}g^{\nu\sigma}\right.$$
$$\left.+\left(f^{ac,db}-f^{ab,cd}\right)g^{\mu\sigma}g^{\nu\rho}\right\}$$

with

$$f^{ab,cd}\equiv f^{abx}f^{cdx}$$

To be noted that we need to take care of the symmetry factor for any Feynman diagram, and for each quark/ghost loop, we need to multiply a factor of (-1).

8.1.2 Construction of the full standard model Lagrangian

Now we have a look at the different parts which contribute to the full SM Lagrangian [112]..

Gauge Group $SU(2)_L \times U(1)_Y$

The full gauge field (including the fermionic part) Lagrangian is

$$\mathcal{L}_{\text{gauge}} = -\frac{1}{4}F^a_{\mu\nu}F^{a\mu\nu} - \frac{1}{4}W^a_{\mu\nu}W^{a\mu\nu} - \frac{1}{4}B_{\mu\nu}B^{\mu\nu}, \tag{8.1.11}$$

where the field strength $F_{\mu\nu}$ was defined in the previous subsection. The covariant derivative for the $SU(2)_L$ group is given as

$$W^a_{\mu\nu} = \partial_\mu W^a_\nu - \partial_\nu W^a_\mu + g\epsilon^{abc}W^b_\mu W^c_\nu \quad (a=1,\ldots,3), \tag{8.1.12}$$

where, for the fundamental representation of $SU(2)_L$, $T^a = \tau^a/2$, where τ^a are the Pauli matrices, ϵ^{abc} is the completely anti-symmetric tensor in 3 dimensions. The covariant derivative for a field ψ_L transforming under this group non-trivially is given by,

$$D_\mu \psi_L = \left(\partial_\mu - i\, g\, W_\mu^a T^a\right)\psi_L. \tag{8.1.13}$$

As for the Abelian $U(1)_Y$ group, we have

$$B_{\mu\nu} = \partial_\mu B_\nu - \partial_\nu B_\mu, \tag{8.1.14}$$

with the covariant derivative given by

$$D_\mu \psi = \left(\partial_\mu - i\, g'\, \eta_Y Y\, B_\mu\right)\psi, \tag{8.1.15}$$

where Y is the hypercharge of the field and we put $\eta_Y = \pm$, connected to the electric charge through

$$Q = T_3 + \eta_Y Y\ . \tag{8.1.16}$$

We can write the covariant derivative in terms of the mass eigenstates A_μ and Z_μ, as follows:

$$\begin{cases} W_\mu^3 = \eta_Z Z_\mu \cos\theta_W + A_\mu \eta_\theta \sin\theta_W \\ B_\mu = -\eta_Z Z_\mu \eta_\theta \sin\theta_W + A_\mu \cos\theta_W \end{cases}, \quad \begin{cases} \eta_Z Z_\mu = W_\mu^3 \cos\theta_W - B_\mu \eta_\theta \sin\theta_W \\ A_\mu = W_\mu^3 \eta_\theta \sin\theta_W + B_\mu \cos\theta_W \end{cases}. \tag{8.1.17}$$

For a doublet field ψ_L, with hypercharge Y, we get,

$$\begin{aligned} D_\mu \psi_L &= \left[\partial_\mu - i\,\frac{g}{\sqrt{2}}\left(\tau^+ W_\mu^+ + \tau^- W_\mu^-\right) - i\,\frac{g}{2}\tau_3 W_\mu^3 - i\, g' \eta_Y Y B_\mu\right]\psi_L \\ &= \left[\partial_\mu - i\,\frac{g}{\sqrt{2}}\left(\tau^+ W_\mu^+ + \tau^- W_\mu^-\right) + i\,\eta_e e\, Q A_\mu - i\,\frac{g}{\cos\theta_W}\left(\frac{\tau_3}{2} - Q\sin^2\theta_W\right)\eta_Z Z_\mu\right]\psi_L, \end{aligned} \tag{8.1.18}$$

where

$$W_\mu^\pm = \frac{W_\mu^1 \mp i W_\mu^2}{\sqrt{2}}, \tag{8.1.19}$$

$$\tau_\pm = \frac{\tau_1 \pm i\tau_2}{\sqrt{2}}. \tag{8.1.20}$$

We can define the charge operator by

$$Q = \begin{bmatrix} \frac{1}{2} + \eta_Y Y & 0 \\ 0 & -\frac{1}{2} + \eta_Y Y \end{bmatrix}, \tag{8.1.21}$$

and we have used the relations,

$$\begin{aligned} \eta_e\, e &= -\eta_\theta\, g \sin\theta_W \\ &= -g' \cos\theta_W\,. \end{aligned} \tag{8.1.22}$$

For a singlet of $SU(2)_L$, ψ_R, we have,

$$\begin{aligned} D_\mu \psi_R &= \left[\partial_\mu - i\, g' \eta_Y Y B_\mu\right]\psi_R \\ &= \left[\partial_\mu + i\,\eta_e e\, Q A_\mu + i\,\frac{g}{\cos\theta_W} Q \sin^2\theta_W \eta_Z Z_\mu\right]\psi_R\,. \end{aligned} \tag{8.1.23}$$

For each fermion field ψ, we define the projection operator P by $\psi_{R,L} = P_{R,L}\psi$, where

$$P_{R,L} = \frac{1 \pm \gamma_5}{2}, \tag{8.1.24}$$

and $\psi = \psi_R + \psi_L$.

The Higgs Lagrangian

The SM includes a Higgs doublet which can be viewed as,

$$\Phi = \begin{bmatrix} \varphi^+ \\ \dfrac{v + H + i\varphi_Z}{\sqrt{2}} \end{bmatrix}. \tag{8.1.25}$$

Since $\eta_Y Y_\Phi = +1/2$, the covariant derivative reads

$$\begin{aligned} D_\mu \Phi &= \left[\partial_\mu - i\frac{g}{\sqrt{2}}\left(\tau^+ W_\mu^+ + \tau^- W_\mu^-\right) + i\eta\frac{g}{2}\tau_3 W_\mu^3 - i\frac{g'}{2}B_\mu\right]\Phi \\ &= \left[\partial_\mu - i\eta\frac{g}{\sqrt{2}}\left(\tau^+ W_\mu^+ + \tau^- W_\mu^-\right) + i\eta_e e Q A_\mu - i\frac{g}{\cos\theta_W}\left(\frac{\tau_3}{2} - Q\sin^2\theta_W\right)\eta_Z Z_\mu\right]\Phi, \end{aligned} \tag{8.1.26}$$

where, for the doublet field Φ,

$$Q = \begin{pmatrix} 1 & 0 \\ 0 & 0 \end{pmatrix}. \tag{8.1.27}$$

The Higgs Lagrangian is given as

$$\mathcal{L}_{\text{Higgs}} = \left(D_\mu\Phi\right)^\dagger D_\mu\Phi + \mu^2\Phi^\dagger\Phi - \lambda\left(\Phi^\dagger\Phi\right)^2, \tag{8.1.28}$$

from which we obtain the relation,

$$v^2 = \frac{\mu^2}{\lambda}, \quad m_h^2 = 2\mu^2, \quad \lambda = \frac{g^2}{8}\frac{m_h^2}{m_W^2}. \tag{8.1.29}$$

We expand this Lagrangian to find the following terms quadratic in the fields:

$$\begin{aligned} \mathcal{L}_{\text{Higgs}} \;=\; & \cdots + \frac{1}{8}g^2v^2W_\mu^3W^{\mu 3} + \frac{1}{8}g'^2v^2B_\mu B^\mu - \frac{1}{4}gg'v^2W_\mu^3B^\mu + \frac{1}{4}g^2v^2W_\mu^+W^{-\mu} \\ & + \frac{1}{2}v\partial^\mu\varphi_Z\left(-g'B_\mu + gW_\mu^3\right) + \frac{i}{2}gvW_\mu^-\partial^\mu\varphi^+ - \frac{i}{2}gvW_\mu^+\partial^\mu\varphi^- \,. \end{aligned} \tag{8.1.30}$$

After diagonalization, the first three terms give a massless field (the photon) and a massive one (the Z) while the fourth term gives mass to the charged $W_\mu^\pm$ bosons. The relations for the photon and the Z boson is given in Eq. (8.1.17), Using Eq. (8.1.17), we get

$$\begin{aligned} \mathcal{L}_{\text{Higgs}} \;=\; & \cdots + \frac{1}{2}m_Z^2Z_\mu Z^\mu + m_W^2W_\mu^+W^{-\mu} \\ & + \eta_Z m_Z Z_\mu\partial^\mu\varphi_Z + im_W\left(W_\mu^-\partial^\mu\varphi^+ - W_\mu^+\partial^\mu\varphi^-\right), \end{aligned} \tag{8.1.31}$$

where

$$m_W = \frac{1}{2}gv, \quad m_Z = \frac{1}{\cos\theta_W}\frac{1}{2}gv = \frac{1}{\cos\theta_W}m_W. \tag{8.1.32}$$

From this equation we find that the terms in the last line are quadratic in the fields, which complicates the definition of the propagators. We can again use gauge fixing to overcome this.

The Yukawa Lagrangian, fermion masses and the CKM matrix

The fermions and the Higgs doublet gain mass after the spontaneous symmetry breaking. For this, we have

$$\mathcal{L}_{\text{Yukawa}} = -\overline{L}_L\, Y_l\, \Phi\, \ell_R - \overline{Q}'_L\, Y_d\, \Phi\, d'_R - \overline{Q}'_L\, Y_u\, \widetilde{\Phi}\, u'_R + \text{h.c.}, \tag{8.1.33}$$

where L_L (Q'_L) are the left-handed lepton (quark) doublets and,

$$\widetilde{\Phi} = i\sigma_2 \Phi^* = \begin{bmatrix} \dfrac{v + H - i\varphi_Z}{\sqrt{2}} \\ -\varphi^- \end{bmatrix}. \tag{8.1.34}$$

Y_l, Y_d, and Y_u are general complex 3×3 matrices in the flavor spaces. We diagonalize Y_d and Y_u to bring the quarks into the mass basis. For this, we use the unitary transformations

$$\begin{aligned} \overline{u}'_L &= \overline{u}_L\, U^\dagger_{uL}, & \overline{d}'_L &= \overline{d}_L\, U^\dagger_{dL}, \\ u'_R &= U_{uR}\, u_R, & d'_R &= U_{dR}\, d_R, \end{aligned} \tag{8.1.35}$$

such that

$$\begin{aligned} \frac{v}{\sqrt{2}}\, U^\dagger_{uL}\, Y_u\, U_{uR} &= M_u = \text{diag}\,(m_u, m_c, m_t)\,, \\ \frac{v}{\sqrt{2}}\, U^\dagger_{dL}\, Y_d\, U_{dR} &= M_d = \text{diag}\,(m_d, m_s, m_b)\,. \end{aligned} \tag{8.1.36}$$

The Higgs couplings of the quarks become diagonal in this new basis,:

$$-\mathcal{L}_{\text{H}} = \left(1 + \frac{h^0}{v}\right)\left[\overline{u}\, M_u\, u + \overline{d}\, M_d\, d\right]. \tag{8.1.37}$$

The photon and the Z couplings remain diagonal, however, the couplings to the W mixes the upper and lower components of Q'_L, which transforms differently under the unitary transformations. Therefore, the couplings to $W^\pm$ become off-diagonal:

$$\mathcal{L}_{\text{W}} = \frac{g}{\sqrt{2}}\, \overline{u}_L\, V\, \gamma^\mu\, d_L\, W^\dagger_\mu + \text{h.c.}, \tag{8.1.38}$$

where we get the Cabibbo-Kobayashi-Maskawa (CKM) matrix,

$$V = U^\dagger_{uL} U_{dL}. \tag{8.1.39}$$

The complete SM Lagrangian

The complete Lagrangian for the Standard Model is obtained by summing all the contribution explained above.

$$\mathcal{L}_{\text{SM}} = \mathcal{L}_{\text{gauge}} + \mathcal{L}_{\text{Fermion}} + \mathcal{L}_{\text{Higgs}} + \mathcal{L}_{\text{Yukawa}} + \mathcal{L}_{\text{GF}} + \mathcal{L}_{\text{Ghost}}, \tag{8.1.40}$$

The Feynman rules can be read off from the Lagrangian as before. We do not mention the rules here explicitly and instead ask the reader to refer to [112].

8.2 Tensor reduction

In this section we have a look at the technique of reducing multi-loop tensor integrals to scalar integrals. We start with the one-loop case and then discuss the multi-loop case.

8.2.1 One-loop reduction

Let us discuss some features of the one-loop reduction. We first introduce the notation for integrals with one, two or three external legs, as follows:

$$\begin{aligned}
A_0(m) &= e^{\epsilon\gamma_E}\mu^{2\epsilon}\int\frac{d^Dk}{i\pi^{\frac{D}{2}}}\frac{1}{(-k^2+m^2)},\\
B_{0,\mu,\mu\nu(p,m_1,m_2)} &= e^{\epsilon\gamma_E}\mu^{2\epsilon}\int\frac{d^Dk}{i\pi^{D/2}}\frac{1,k_\mu,k_\mu k_\nu}{(-k^2+m_1^2)(-(k-p)^2+m_2^4)},\\
C_{0,\mu\mu\nu}(p_1,p_2,m_1,m_2,m_3) &= e^{\epsilon\gamma_E}\mu^{2\epsilon}\int\frac{d^Dk}{i\pi^{D/2}}\frac{1,k_\mu,k_\mu k_\nu}{(-k^2+m_1^2)(-(k-p_1)^2+m_2^2)(-(k-p_1-p_2)^2+m_3^2)},
\end{aligned} \tag{8.2.1}$$

where the notation for the numerator is quite self-explanatory. More legs and higher rank tensor can be easily generalized from the formulae shown above. The reduction technique in this case follows from the fact that the result can only depend on tensor structures which are built from external momenta p_j^μ and the metric tensor $g^{\mu\nu}$, due to Lorentz symmetry. Therefore, we can write a general form for the tensor integrals in terms of form factors times external momenta and/or the metric tensor, as shown below.

$$\begin{aligned}
B^\mu &= p^\mu B_1,\\
B^{\mu\nu} &= p^\mu p^\nu B_{21} + g^{\mu\nu}B_{22},\\
C^\mu &= p_1^\mu C_{11} + p_2^\mu C_{12},\\
C^{\mu\nu} &= p_1^\mu p_1^\nu C_{21} + p_2^\mu p_1^\nu C_{22} + (p_1^\mu p_2^\nu + p_1^\nu p_2^\mu)C_{23} + g^{\mu\nu}C_{24}.
\end{aligned} \tag{8.2.2}$$

We then solve for the form factors B_1, B_{21}, B_{22}, C_{11} etc by first contracting both the sides with the metric tensor and the external momenta. In this process, we re-write the resulting scalar products between the loop momenta k^μ and external momenta on the left hand side in terms of inverse propagators, so that the terms cancel with the propagators downstairs and we are left with integral with trivial numerical factors. Then the remaining step is just to invert the matrix which one obtains on the right hand side of the above equation.

This algorithm is based on the observation that for one-loop integrals a scalar product of the loop momentum with an external momentum can be expressed as a combination of inverse propagators, which does not hold true if one goes to two or more loops. Let us now look at the tensor reduction for multi-loop case.

8.2.2 Multi-loop reduction

For a general multi-loop tensor integrals let us start with integral which we obtain after Feynman or Schwinger parametrization and removal of the odd power of the loop momentum in the numerator. The integrals with an even power of the loop momentum can be related by Lorentz invariance to scalar integrals:

$$\begin{aligned}
\int\frac{d^Dk}{i\pi^{D/2}}k_\mu k^\nu f(k^2) &= -\frac{1}{D}g^{\mu\nu}\int\frac{d^Dk}{i\pi^{D/2}}(-k^2)f(k^2),\\
\int\frac{d^Dk}{i\pi^{D/2}}k^\mu k^\nu k^\rho k^\sigma f(k^2) &= \frac{1}{D(D+2)}(g^{\mu\nu}g^{\rho\sigma}+g^{\mu\rho}g^{\nu\sigma}+g^{\mu\sigma}g^{\nu\sigma}))\int\frac{d^Dk}{i\pi^{D/2}}(-k^2)^2f(k^2).
\end{aligned} \tag{8.2.3}$$

It is easy to generalize this to arbitrary higher tensor structures. Using the dimension shift operator introduced in section ⟨4.1.1⟩, we get

$$\mathbf{D}^{+}\int\frac{d^{D}k}{i\pi^{\frac{D}{2}}}f(k^{2}) \;=\; \int\frac{d^{(D+2)}k}{i\pi^{(D+2)/2}}f(k^{2}). \tag{8.2.4}$$

Shifting the dimension from D to $D+2$ is equivalent to introducing a factor $(-k^2)$ in the numerator. Therefore we can use the dimensional operator for example for the term

$$\int\frac{d^{D}k}{i\pi^{D/2}}k^{\mu}k^{\nu}f(k^{2}) = -\frac{1}{2}g^{\mu\nu}\mathbf{D}^{+}\int\frac{d^{D}k}{i\pi^{D/2}}f(k^{2}). \tag{8.2.5}$$

In addition we also get (Feynman or Schwinger) parameter x_j in the numerator when we shift the loop momentum like $k^{'} = k - xp$. For tensor reduction, it is more convenient to use the Schwinger parameters, which is given by

$$\frac{1}{-P^{\nu}} = \frac{1}{\Gamma(\nu)}\int_{0}^{\infty}dx x^{\nu-1}exp(xP). \tag{8.2.6}$$

A schwinger parameter x in the numerator is equivalent to raising the power of the original propagators by one. This is visualized as:

$$\nu_1\mathbf{i}^{+}\frac{1}{(-P_i)^{\nu_1}} = \nu_i\frac{1}{(-P_i)^{\nu_1}+1} = \frac{1}{\Gamma(\nu_i)}\int_{0}^{\infty}dx_i x_i^{\nu_i-1}x_i exp(x_iP_i), \tag{8.2.7}$$

where we used the same convention $\mathbf{i}$ for shifting the propagator by one unit, as introduced before. Therefore, we can consider an integral where a Schwinger parameter occurs in the numerator as a scalar integral and the corresponding propagator is raised to a higher power. In this way, we can express all tensor integrals in terms of scalar integrals by using an intermediate Schwinger parametrization. However, these scalar integrals involve higher power of the propagators and/or shifted dimensions, which is the price we pay for this technique.

8.3 The bubble graph

In other to use the techniques in the chapter of differential equations, we show an explicit example of the equal-mass bubble integral. This integral is given by

$$B_{\nu_1\nu_2}(D,p^2,m^2,\mu^2) = e^{\gamma_E\epsilon}(\mu^2)^{\nu_{12}-\frac{D}{2}}\int\frac{d^{D}k}{i\pi^{\frac{D}{2}}}\frac{1}{(-k_1^2+m^2)^{\nu_1}(-k_2^2+m^2)^{\nu_2}}, \tag{8.3.1}$$

where ν_{12} denotes the sum of the two propagator-powers. We recall that the tadpole integral T_1 is give by

$$T_{\nu}(D,m^2,\mu^2) = e^{\gamma_E\epsilon}\frac{\Gamma(\nu-\frac{D}{2})}{\Gamma(\nu)}\left(\frac{m^2}{\mu^2}\right)^{\frac{D}{2}-\nu}. \tag{8.3.2}$$

Generating and solving the IBP relations gives us the following reduction for the bubble integrals:

$$B_{21} = B_{12} = (D-3)\frac{\mu^2}{p^2-4m^2}B_{11} + \frac{1}{2}(D-2)\frac{\mu^4}{m^2(p^2-4m^2)}T_1. \tag{8.3.3}$$

Using the dimensional shift relation for B_{11}, we get

$$B_{11}(2-2\epsilon) = B_{21}(4-2\epsilon) + B_{12}(4-2\epsilon) = 2B_{21}(4-2\epsilon). \tag{8.3.4}$$

Combining eq. (8.3.3) and eq. (8.3.4) and putting $\mu = m$, we get

$$B_{11}(2-2\epsilon) = -\frac{2x}{(1+x)^2}((1-2\epsilon)B_{11}(4-2\epsilon) + (1-\epsilon)T_1(4-2\epsilon)). \tag{8.3.5}$$

If we substitute s by $-m^2\frac{(1-x)^2}{x}$, we can solve the equal mass bubble integral very easily if we consider

$$\tilde{B}_{11}(2-2\epsilon, x) = \epsilon\frac{(1-x)(1+x)}{2x}B_{11}(2-2\epsilon, s, m^2, m^2). \tag{8.3.6}$$

The differential equation for $\tilde{B}_{11}$ reads

$$\frac{d}{dx}\tilde{B}_{11}(2-2\epsilon, x) = \epsilon\left(\frac{1}{x} - \frac{2}{1+x}\right)\tilde{B}_{11}(2-2\epsilon, x) - \frac{\epsilon}{x}T_1(2-2\epsilon) \tag{8.3.7}$$

and the boundary condition

$$\tilde{B}_{11}(2-2\epsilon, 1) = 0.$$

This integral is easily written in terms of (harmonic) polylogs, after reading off the alphabet from eq. (8.3.7).

8.4 More results from the 'topbox'

As promised in chapter 5, we present here few more examples of the results for our master integrals with different dependencies.

The first example is an integral which only depends on t and is expressible as iterated integrals of modular forms $\{1, f_2, f_3, f_4, g_{2,1}\}$. The modular forms have been defined in eq. (5.5.2).

$$
\begin{aligned}
&J_6^{(0)} = 0,\\
&J_6^{(1)} = 0,\\
&J_6^{(2)} = F(1, f_3; q_6) + 3\zeta_2,\\
&J_6^{(3)} = -F(f_2, 1, f_3; q_6) - F(1, f_2, f_3; q_6) + 3\zeta_2 F(1; q_6) - 3\zeta_2 F(f_2; q_6) + \frac{21}{2}\zeta_3 - 18\zeta_2 \ln(2),\\
&J_6^{(4)} = F(f_2, f_2, 1, f_3; q_6) + F(f_2, 1, f_2, f_3; q_6) + F(1, f_2, f_2, f_3; q_6) + F(1, f_4, 1, f_3; q_6)\\
&+ 3\zeta_2 F(f_2, f_2; q_6) - 3\zeta_2 F(1, f_2; q_6) - 3\zeta_2 F(f_2, 1; q_6) + 3\zeta_2 F(1, f_4; q_6) + \zeta_2 F(1, f_3; q_6)\\
&+ \left(\frac{21}{2}\zeta_3 - 18\zeta_2 \ln(2)\right)(F(1; q_6) - F(f_2; q_6)) - 39\zeta_4 + 72\mathrm{Li}_4\left(\frac{1}{2}\right) + 36\zeta_2 \ln^2(2)\\
&+ 3\ln^4(2).
\end{aligned}
\tag{8.4.1}
$$

The next example is that of an integral which depends on both s and t.

$$
\begin{aligned}
J_{24}^{(0)} =& 0,\\
J_{24}^{(1)} =& 0,\\
J_{24}^{(2)} =& 0,\\
J_{24}^{(3)} =& I_\gamma\left(\eta_0^{(b)}, \eta_2^{(\frac{b}{a})}, f_3; \lambda\right) - \frac{3}{2} I_\gamma\left(\eta_0^{(b)}, \eta_{3,5}^{(b)}, \omega_{0,4}; \lambda\right) - 3 I_\gamma\left(\eta_{1,1}^{(b)}, \omega_{0,4}, \omega_{0,4}; \lambda\right)\\
&+ I_\gamma\left(\eta_2^{(\frac{a}{b})}, \eta_0^{(a)}, f_3; \lambda\right) + \frac{9}{2} I_\gamma\left(\eta_0^{(b)}, a_{3,2}^{(b)}, \omega_{0,4}, \omega_{0,4}; \lambda\right) + I_\gamma\left(\eta_0^{(b)}, a_{4,1}^{(a,b)}, \eta_0^{(a)}, f_3; \lambda\right)\\
&+ \frac{7}{4}\zeta_2 I_\gamma\left(\eta_0^{(b)}; \lambda\right) - 2\zeta_2 I_\gamma\left(\eta_{1,1}^{(b)}; \lambda\right) + 3\zeta_2 I_\gamma\left(\eta_2^{(\frac{a}{b})}; \lambda\right) + 3\zeta_2 I_\gamma\left(\eta_0^{(b)}, a_{3,2}^{(b)}; \lambda\right)\\
&+ 3\zeta_2 I_\gamma\left(\eta_0^{(b)}, a_{4,1}^{(a,b)}; \lambda\right) - 3\ln(2)\zeta_2 - \frac{7}{4}\zeta_3.
\end{aligned}
\tag{8.4.2}
$$

8.5 Topologies present in the two-loop planar double box

In this section we show diagrams of all master topologies for the case of topbox, discussed in chapter 5. In total there 27 master topologies.

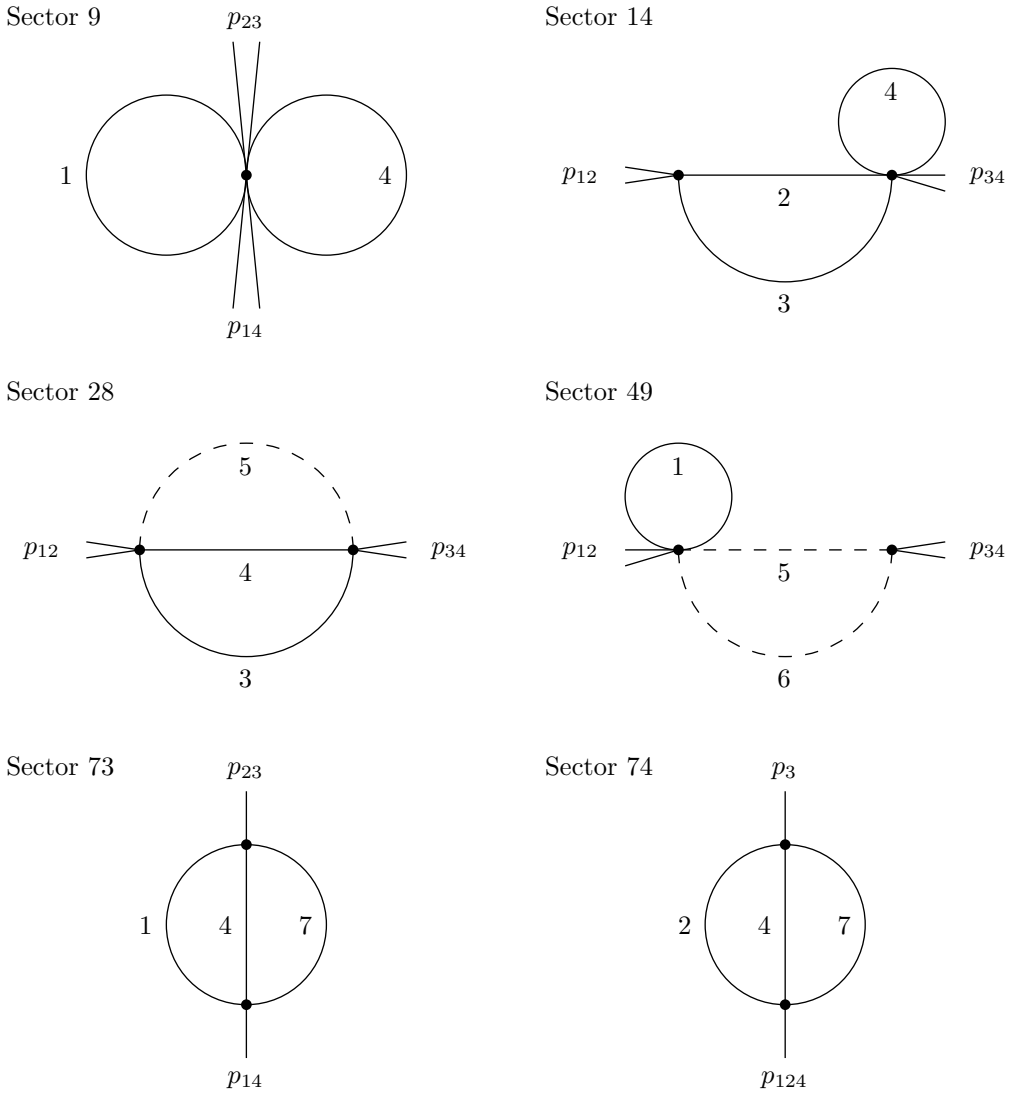

Figure 8.1. Master topologies (part 1).

Sector 15

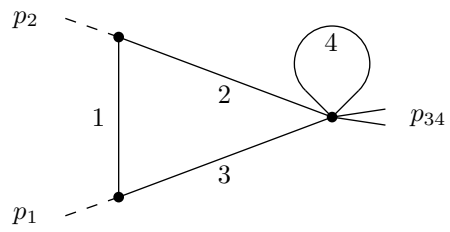

Sector 29

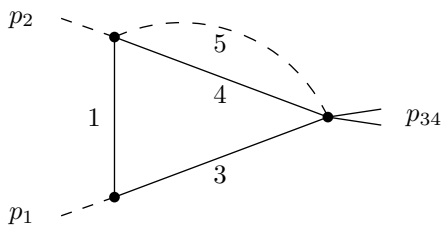

Sector 54

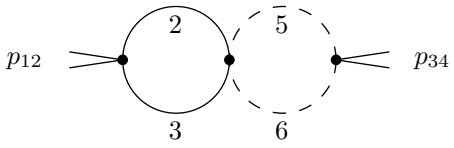

Sector 57

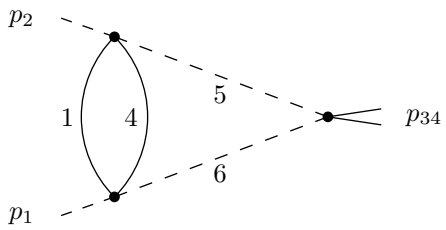

Sector 75

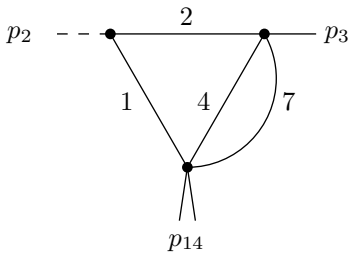

Sector 78

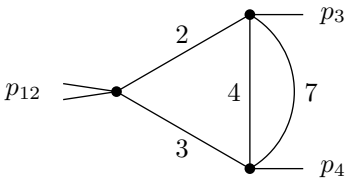

Sector 89

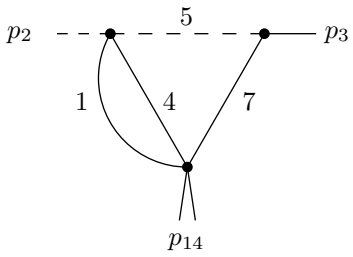

Sector 92

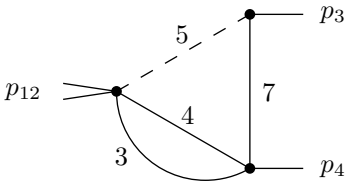

Figure 8.2. Master topologies (part 2).

Sector 113

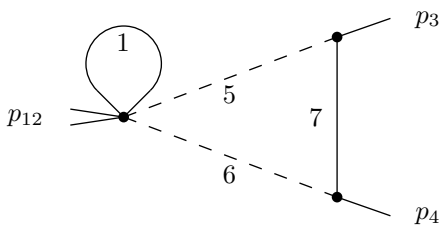

Sector 55

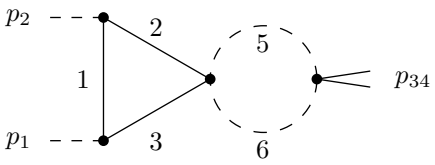

Sector 59

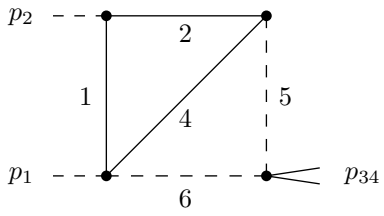

Sector 62

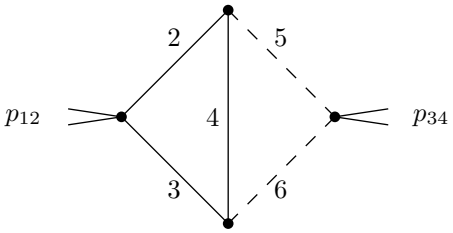

Sector 79

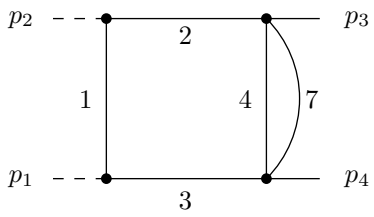

Sector 93

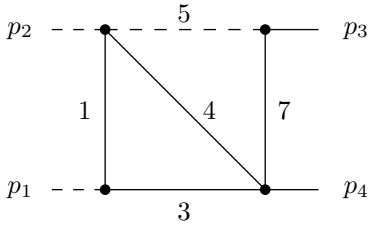

Sector 118

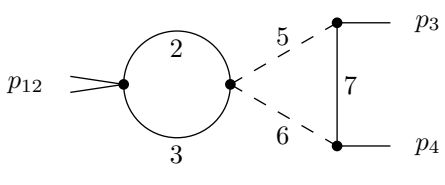

Sector 121

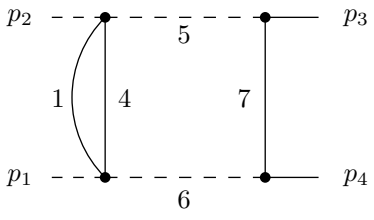

Figure 8.3. Master topologies (part 3).

Sector 63

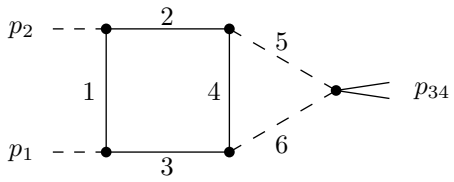

Sector 119

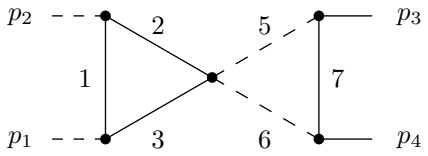

Sector 123

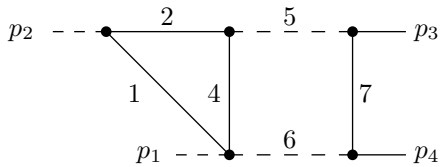

Sector 126

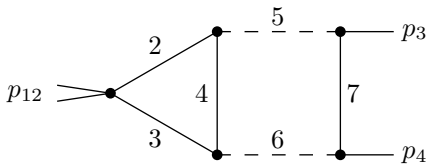

Sector 127

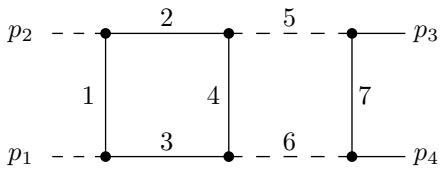

Figure 8.4. Master topologies (part 4).

8.6 Topologies for the two-loop mixed QCD-EW corrections for $H \to b\bar{b}$ through a $Ht\bar{t}$ coupling

In this section we show the diagrams of all master topologies relevant for the diagrams contributing to the two-loop mixed QCD-EW corrections for $H \to b\bar{b}$ through a $Ht\bar{t}$ coupling, discussed in chapter 6.

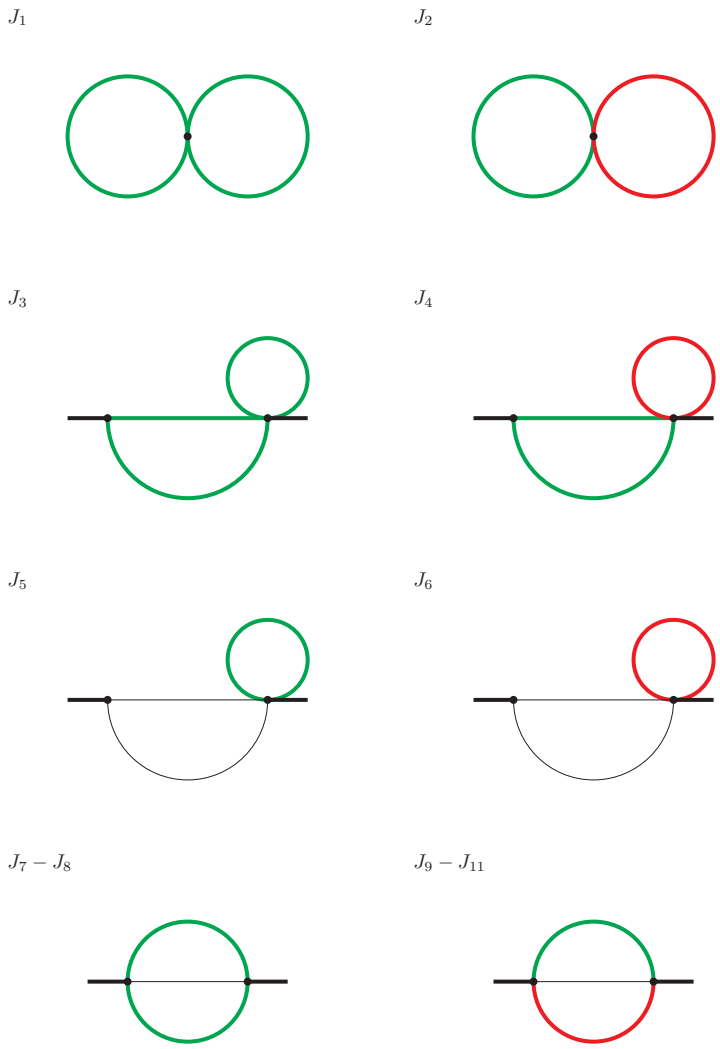

Figure 8.5. Master topologies (part 1).

J_{12}

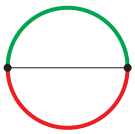

J_{13}

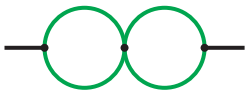

J_{14}

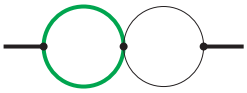

J_{15}

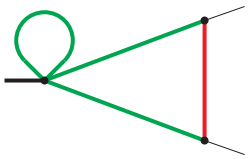

J_{16}

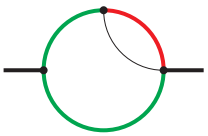

$J_{17} - J_{19}$

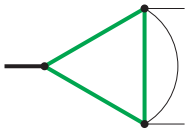

$J_{20} - J_{22}$

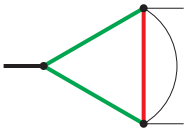

$J_{23} - J_{24}$

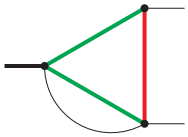

Figure 8.6. Master topologies (part 2).

$J_{25} - J_{26}$

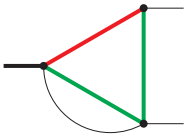

J_{27}

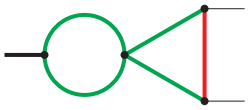

J_{28}

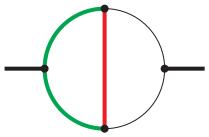

$J_{29} - J_{31}$

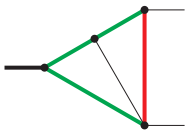

J_{32}

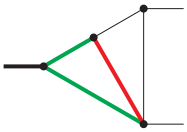

$J_{33} - J_{36}$

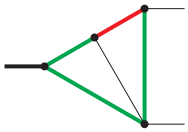

J_{37}

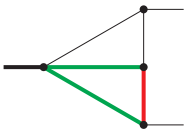

J_{38}

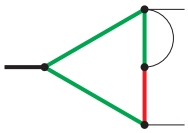

J_{39}

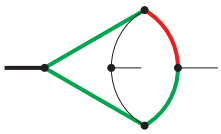

Figure 8.7. Master topologies (part 3).

ACKNOWLEDGMENTS

First of all, I would like to express my deepest gratitude to my supervisor Prof. for his unwavering support, collegiality, caring nature and extraordinary mentorship throughout my PhD life. I admire him as a person who has a very strong grasp on the physical, mathematical as well as computational knowledge about the world of Feynman integrals, which not only helped me to enhance my knowledge about the subject but it also always motivates me to try to become like him some day! I would also like to thank Prof. whose mentorship during my master's life and the QFT courses he taught helped and excited me about particle physics in the first place. I would also like to extend my gratitude to my collaborator Dr. , whose punctuality and dedication towards work was something I always admired.

I would like to take this opportunity to thank all the other awesome people I was surrounded and helped by during my PhD life. I want to thank Ms. for making my transition phase from India to Germany so smooth and hassle-free and Ms. for always smilingly helping me with any official problems I faced. I also want to thank THEP members for creating such an alive and working environment. I want to thank my friends for all those wonderful discussions I had which helped me a lot in my work. I want to thank for always being there for everything, be it having a discussion about physics, needing help with numerous language problems or just sharing all the stress-full moments that occurred during my PhD. I want to thank for making our group basically the best. I also want to thank for being so cute and helpful with almost everything. I want to convey my special thanks to for being amazingly critical about my work which motivated me to always try better the next time and to never loose hope.

Finally, I am thankful to my beloved parents and my brothers for their unconditional love, supports and sacrifices.

Ekta

Bibliography

[1] **ATLAS** Collaboration, G. Aad *et al.*, *Observation of a new particle in the search for the Standard Model Higgs boson with the ATLAS detector at the LHC*, *Phys. Lett.* **B716** (2012) 1–29, arXiv:1207.7214 [hep-ex].

[2] **CMS** Collaboration, S. Chatrchyan *et al.*, *Observation of a new boson at a mass of 125 GeV with the CMS experiment at the LHC*, *Phys. Lett.* **B716** (2012) 30–61, arXiv:1207.7235 [hep-ex].

[3] D. J. Gross and F. Wilczek, *Ultraviolet Behavior of Nonabelian Gauge Theories*, *Phys. Rev. Lett.* **30** (1973) 1343–1346.

[4] G. 't Hooft and M. Veltman, *Regularization and renormalization of gauge fields*, *Nuclear Physics B* **44** (1972) 189 - 213.

[5] T. D. Lee and M. Nauenberg, *Degenerate Systems and Mass Singularities*, *Phys. Rev.* **133 6B**(1964)B1549–B1562.

[6] Kinoshita,Toichiro, *Mass Singularities of Feynman Amplitudes*, *Journal of Mathematical Physics*, **3**,(1962) {4} 650-677.

[7] G. Passarino and M. J. G. Veltman, *One Loop Corrections for e^+e^- Annihilation Into $\mu^+\mu-$ in the Weinberg Model*, *Nucl. Phys.* **B160** (1979) 151.

[8] S. Pincherle, *Sulle funzioni ipergeometriche generalizzate*, *Atti R. Accad. Lincei, Rend. Cl. Sci. Fis. Mat. Natur.* **(Ser 4) 4 (1888)**, 694-700, 792-799 .

[9] E. E. Kummer, *Über die Transcendenten, welche aus wiederholten Integrationen rationaler Formeln entstehen*, *J. reine ang. Mathematik* **21** (1840) 74-90; 193-225; 328-371.

[10] N. Nielsen, *Der Eulersche Dilogarithmus und seine Verallgemeinerungen*, *Nova Acta Leopoldina (Halle) 9* **90** (1909) no. 123.

[11] A. B. Goncharov, *Multiple polylogarithms, cyclotomy and modular complexes*, Math. Res. Lett. **5**, 497 (1998).

[12] A. B. Goncharov, *Multiple polylogarithms and mixed Tate motives*, *math.AG* **(2001)**.

[13] D. J. Broadhurst, *The Master Two Loop Diagram With Masses*, *Z. Phys.* **C47** (1990) 115-124.

[14] S. Bauberger, F. A. Berends, M. Bohm and M. Buza, *Analytical and numerical methods for massive two loop self energy diagrams*, *Nucl. Phys. B* **434** (1995) 383.

[15] S. Laporta and E. Remiddi, *Analytic treatment of the two loop equal mass sunrise graph*, *Nucl. Phys. B* **704** (2005) 349.

[16] S. Bloch and P. Vanhove, *The elliptic dilogarithm for the sunset graph*, *J. Number Theor.* **148** (2015) 328.

[17] L. Adams, C. Bogner and S. Weinzierl, *The two-loop sunrise graph with arbitrary masses*, *J. Math. Phys.* **54** (2013) 052303.

[18] L. Adams, C. Bogner and S. Weinzierl, *The two-loop sunrise graph in two space-time dimensions with arbitrary masses in terms of elliptic dilogarithms*, *J. Math. Phys.***55** (2014) no.10, 102301.

[19] L. Adams, C. Bogner and S. Weinzierl, *The iterated structure of the all-order result for the two-loop sunrise integral*, *J. Math. Phys.* **57** (2016) no.3, 032304.

[20] J. L. Bourjaily, A. J. McLeod, M. Spradlin, M. von Hippel and M. Wilhelm, *Elliptic Double-Box Integrals: Massless Scattering Amplitudes beyond Polylogarithms*, *Phys. Rev. Lett.***120** (2018) no.12, 121603.

[21] A. Primo and L. Tancredi, *On the maximal cut of Feynman integrals and the solution of their differential equations*, *Nucl. Phys. B* **916** (2017) 94.

[22] L. Adams, E. Chaubey and S. Weinzierl, *Planar Double Box Integral for Top Pair Production with a Closed Top Loop to all orders in the Dimensional Regularization Parameter*, *Phys. Rev. Lett.* **121** (2018) no.14, 142001

[23] J. Broedel, C. Duhr, F. Dulat, R. Marzucca, B. Penante and L. Tancredi, *An analytic solution for the equal-mass banana graph*, `arXiv:1907.03787 [hep-th]`.

[24] L. Adams, C. Bogner and S. Weinzierl, *The two-loop sunrise integral around four space-time dimensions and generalisations of the Clausen and Glaisher functions towards the elliptic case*, *J. Math. Phys.* **56** (2015) no.7, 072303.

[25] R. Bonciani, V. Del Duca, H. Frellesvig, J. M. Henn, F. Moriello and V. A. Smirnov, *Two-loop planar master integrals for Higgs→ 3 partons with full heavy-quark mass dependence*, JHEP **1612** (2016) 096.

[26] A. von Manteuffel and L. Tancredi, *A non-planar two-loop three-point function beyond multiple polylogarithms*, *JHEP* **1706** (2017) 127.

[27] L. Adams, C. Bogner, A. Schweitzer and S. Weinzierl, *The kite integral to all orders in terms of elliptic polylogarithms*, *J. Math. Phys.* **57** (2016) no.12, 122302.

[28] E. Remiddi and L. Tancredi, *Differential equations and dispersion relations for Feynman amplitudes. The two-loop massive sunrise and the kite integral*, *Nucl. Phys. B* **907** (2016) 400.

[29] A. V. Kotikov, *Differential equations method. New technique for massive Feynman diagram calculation*, *Physics Letters B* **B254** (1991) 158–164.

[30] A.V. Kotikov, *Differential equation method. The calculation of N-point Feynman diagrams*, *Physics Letters B* **B267** (1991) 123–127.

[31] E. Remiddi, *Differential equations for Feynman graph amplitudes*, *Nuovo Cim.* **A110** (1997) 1435-1452 .

[32] K.G. Chetyrkin and F.V. Tkachov, *Integration by parts: The algorithm to calculate β-functions in 4 loops*, *Nuclear Physics B* **B 192** (1981) 159.

[33] F.V. Tkachov, *A theorem on analytical calculability of 4-loop renormalization group functions*, *Physics Letters B* **100** (1981) 65.

[34] S. Laporta, *High precision calculation of multiloop Feynman integrals by difference equations*, *Int. J. Mod. Phys. A* **15** (2000) 5087.

[35] J. M. Henn, *Multiloop integrals in dimensional regularization made simple*, Phys. Rev. Lett. **110** (2013) 251601.

[36] A. V. Smirnov, *Algorithm FIRE – Feynman Integral REduction*, *JHEP* **0810** (2008) 107.

[37] A. von Manteuffel and C. Studerus, *Reduze 2 - Distributed Feynman Integral Reduction*, arXiv:1201.4330[hep-ph].

[38] P. Maierhöfer, J. Usovitsch and P. Uwer, *Kira- A Feynman integral reduction program*, *Comput. Phys. Commun.* **230** (2018) 99.

[39] A. V. Smirnov, *FIRE5: a C++ implementation of Feynman Integral REduction*, *Comput. Phys. Commun.* **189** (2015) 182.

[40] R. N. Lee, *Presenting LiteRed: a tool for the Loop InTEgrals REDuction*, arXiv:1212.2685 [hep-ph].

[41] O. V. Tarasov, *Connection between Feynman integrals having different values of the space-time dimension*, Phys. Rev. D **54** (1996) 6479.

[42] P. A. Baikov, *Explicit solutions of the multiloop integral recurrence relations and its application*, *Nucl. Instrum. Meth. A* **389** (1997) 347.

[43] H. Frellesvig and C. G. Papadopoulos, *Cuts of Feynman Integrals in Baikov representation*, *JHEP* **1704** (2017) 083.

[44] A. Primo and L. Tancredi, *Maximal cuts and differential equations for Feynman integrals. An application to the three-loop massive banana graph*, *Nucl. Phys. B* **921** (2017) 316

[45] O. V. Tarasov, *Generalized recurrence relations for two loop propagator integrals with arbitrary masses*, *Nucl. Phys. B* **502** (1997) 455

[46] T. Binoth, E. W. N. Glover, P. Marquard and J. J. van der Bij, *Two loop corrections to light by light scattering in supersymmetric QED*, *JHEP* **0205** (2002) 060.

[47] R. N. Lee, *LiteRed 1.4: a powerful tool for reduction of multiloop integrals*, *J. Phys. Conf. Ser.* **523** (2014) 012059

[48] L. Adams, E. Chaubey and S. Weinzierl, *Analytic results for the planar double box integral relevant to top-pair production with a closed top loop*, *Journal of High Energy Physics.* **1810** (2018) 206, arXiv:1806.04981[hep-ph].

[49] L. Adams, E. Chaubey and S. Weinzierl,*Simplifying Differential Equations for Multiscale Feynman Integrals beyond Multiple Polylogarithms*, *Phys. Rev. Lett.* **118** (2017) no.14, 141602.

[50] M. Czakon, P. Fiedler and A. Mitov, *Total Top-Quark Pair-Production Cross Section at Hadron Colliders Through $O(\alpha_S^4)$*, Phys. Rev. Lett. **110** (2013) 252004.

[51] P. Bärnreuther, M. Czakon and P. Fiedler, *Virtual amplitudes and threshold behaviour of hadronic top-quark pair-production cross sections*, JHEP **1402** (2014) 078.

[52] M. Czakon, *Tops from Light Quarks: Full Mass Dependence at Two-Loops in QCD*, Phys. Rev. Lett. B **664** (2008) 307.

[53] M. Czakon, A. Mitov and S. Moch, *Heavy-quark production in gluon fusion at two loops in QCD*, Nucl. Phys. B **798** (2008) 210.

[54] S. Di Vita, T. Gehrmann, S. Laporta, P. Mastrolia, A. Primo and U. Schubert, *Master integrals for the NNLO virtual corrections to $q\bar{q} \to t\bar{t}$ scattering in QCD: the non-planar graphs*, JHEP **1906** (2019) 117.

[55] S. Catani, S. Devoto, M. Grazzini, S. Kallweit, J. Mazzitelli and H. Sargsyan, *Top-quark pair hadroproduction at next-to-next-to-leading order in QCD*, Phys. Rev. D **99** (2019) no.5, 051501.

[56] L. B. Chen and J. Wang, *Master integrals of a planar double-box family for top-quark pair production*, Phys. Lett. B **792** (2019) 50.

[57] S. Bloch, M. Kerr and P. Vanhove, *A Feynman integral via higher normal functions*, Compos. Math. **151** (2015) no.12, 2329.

[58] C. Bogner, A. Schweitzer and S. Weinzierl, *Analytic continuation and numerical evaluation of the kite integral and the equal mass sunrise integral*, Nucl. Phys. B **922** (2017) 528.

[59] L. Adams and S. Weinzierl, *The ε-form of the differential equations for Feynman integrals in the elliptic case*, Phys. Lett. B **781** (2018) 270.

[60] D. de Florian *et al.* [LHC Higgs Cross Section Working Group], *Handbook of LHC Higgs Cross Sections: 4. Deciphering the Nature of the Higgs Sector*, CERN Yellow Reports: Monographs

[61] C. Bogner and S. Weinzierl, *Feynman graph polynomials*, Int. J. Mod. Phys. A **25** (2010) 2585.

[62] G. Heinrich, *Sector Decomposition*, Int. J. Mod. Phys. A **23** (2008) 1457.

[63] C. Bogner and S. Weinzierl, *Resolution of singularities for multi-loop integrals*, Comput. Phys. Commun. **178** (2008) 596.

[64] A. V. Smirnov and M. N. Tentyukov, *Feynman Integral Evaluation by a Sector decomposiTion Approach (FIESTA)*, Comput. Phys. Commun. **180** (2009) 735.

[65] T. Kaneko and T. Ueda, *A Geometric method of sector decomposition*, Comput. Phys. Commun. **181** (2010) 1352.

[66] J. Vollinga, *GiNaC: Symbolic computation with C++*, Nucl. Instrum. Meth. A **559** (2006) 282.

[67] J. Vollinga and S. Weinzierl, *Numerical evaluation of multiple polylogarithms*, Comput. Phys. Commun. **167** (2005) 177.

[68] C. Bauer, A. Frink and R. Kreckel, *Introduction to the GiNaC Framework for Symbolic Computation within the C++ Programming Language*, *J. Symb. Comput.* bfseries 33, 1 (2002).

[69] S. Borowka, G. Heinrich, S. Jahn, S. P. Jones, M. Kerner, J. Schlenk and T. Zirke, *pySecDec: a toolbox for the numerical evaluation of multi-scale integrals*, *Comput. Phys. Commun.* **222** (2018) 313.

[70] D. H. Bailey and H. R. P. Ferguson, *A polynomial time, numerically stable integer relation algorithm SRC Technical Report SRC-TR-92-066; RNR Technical Report RNR-91-032* (16 December 1991; 14 July 1992), 1-14.

[71] Bailey, David H. and Broadhurst, David J.,*Parallel Integer Relation Detection: Techniques and Applications*, *Math. Comput.*, **70 (236)** (2001) 1719-1736.

[72] R. Britto, F. Cachazo, B. Feng and E. Witten, *Direct proof of tree-level recursion relation in Yang-Mills theory*, *Phys. Rev. Lett.* **94** (2005) 181602.

[73] L. Adams and S. Weinzierl, *Feynman integrals and iterated integrals of modular forms*, *Commun. Num. Theor. Phys.* **12** (2018) 193.

[74] Wikipedia contributors, *Complex torus — Wikipedia, The Free Encyclopedia*, Wikipedia.

[75] Washington, Lawrence C., Book on *Elliptic Curves Number, Theory and Cryptography Second Edition*, Taylor & Francis Group, LLC(2018).

[76] Husemöller, Dale, Book on *Elliptic curves*, Springer-Verlag New York **111**(2004).

[77] F. Brown, Mutilple Modular Values and the relative completion of the fundamental group of $M_{1,1}$, `arXiv:1407.5167 (2014).[math-NT]`.

[78] T. Hahn, *Generating Feynman diagrams and amplitudes with FeynArts 3*, *Comput. Phys. Commun.* **140** (2001) 418.

[79] P. Nogueira, *Automatic Feynman graph generation*, *J. Comput. Phys.* **105** (1993) 279.

[80] T. Hahn, S. Paßehr and C. Schappacher, *FormCalc 9 and Extensions*, J. Phys. Conf. Ser. **762** (2016) no.1, 012065.

[81] G. Cullen, N. Greiner, G. Heinrich, G. Luisoni, P. Mastrolia, G. Ossola, T. Reiter and F. Tramontano, *Automated One-Loop Calculations with GoSam*, *Eur. Phys. J. C* **72** (2012) 1889.

[82] F. Cascioli, P. Maierhofer and S. Pozzorini, *Scattering Amplitudes with Open Loops*, Phys. Rev. Lett. **108** (2012) 111601.

[83] C. F. Berger, Z. Bern, L. J. Dixon, F. Febres Cordero, D. Forde, H. Ita, D. A. Kosower and D. Maitre, *An Automated Implementation of On-Shell Methods for One-Loop Amplitudes*, *Phys. Rev. D* **78** (2008) 036003.

[84] J. Kuipers, T. Ueda, J. A. M. Vermaseren and J. Vollinga, *FORM version 4.0*, *Comput. Phys. Commun.* **184** (2013) 1453.

[85] I. Bierenbaum and S. Weinzierl, *The Massless two loop two point function*, Eur. Phys. J. C **32** (2003) 67.

[86] C. Bogner and S. Weinzierl, *Periods and Feynman integrals*, *J. Math. Phys.* **50** (2009) 042302.

[87] M. Kontsevich, D. Zagier, *Periods, in:Mathematics - 20101 and beyond*, .

[88] J. R. Andersen *et al.*, *Les Houches 2017: Physics at TeV Colliders Standard Model Working Group Report*, [hep-ph].

[89] R. E. Cutkosky, *Singularities and discontinuities of Feynman amplitudes*, *J. Math. Phys.* **1** (1960) 429-433.

[90] Z. Bern, L. J. Dixon, D. C. Dunbar and D. A. Kosower, *One loop n point gauge theory amplitudes, unitarity and collinear limits*, *Nucl. Phys. B* **425** (1994) 217.

[91] R. Britto, F. Cachazo and B. Feng, *New recursion relations for tree amplitudes of gluons*, *Nucl. Phys. B* **715** (2005) 499.

[92] G. Ossola, C. G. Papadopoulos and R. Pittau, *Reducing full one-loop amplitudes to scalar integrals at the integrand level*, *Nucl. Phys. B* **763** (2007) 147.

[93] R. K. Ellis, W. T. Giele, Z. Kunszt, and K. Melnikov, *Masses, fermions and generalized D-dimensional unitarity*, *Nucl. Phys.* bfseries B822 (2009) 270-282.

[94] S. Badger, G. Mogull, A. Ochirov and D. O'Connell, *A Complete Two-Loop, Five-Gluon Helicity Amplitude in Yang-Mills Theory*, *JHEP* **1510** (2015) 064.

[95] S. Abreu, F. Febres Cordero, H. Ita, M. Jaquier, B. Page and M. Zeng, *Two-Loop Four-Gluon Amplitudes from Numerical Unitarity*, *Phys. Rev. Lett.* **119** (2017) no.14, 142001.

[96] CMS Collaboration *Observation of Higgs boson decay to bottom quarks*, **CMS-PAS-HIG-18-016** 2018.

[97] M. Aaboud *et al.* [ATLAS Collaboration], *Observation of $H \to b\bar{b}$ decays and VH production with the ATLAS detector*, *Phys. Lett. B* **786** (2018) 59.

[98] L. Mihaila, B. Schmidt and M. Steinhauser, *$\Gamma(H \to b\bar{b})$ to order $\alpha\alpha_s$*, *Phys. Lett. B* **751** (2015) 442.

[99] A. V. Smirnov and A. V. Petukhov,*The Number of Master Integrals is Finite*, *Lett. Math. Phys.* **97** (2011) 37.

[100] S. Müfller-Stach, S. Weinzierl and R. Zayadeh, *Picard-Fuchs equations for Feynman integrals*, *Commun. Math. Phys.* **326** (2014) 237.

[101] M. Besier, D. Van Straten and S. Weinzierl, *Rationalizing roots: an algorithmic approach*, *Commun. Num. Theor. Phys.* **13** (2019) 253.

[102] R. N. Lee, *Reducing differential equations for multiloop master integrals*, *JHEP* **1504** (2015) 108.

[103] O. Gituliar and V. Magerya, *Fuchsia and master integrals for splitting functions from differential equations in QCD*, *PoS LL* **2016** (2016) 030.

[104] M. Prausa, *epsilon: A tool to find a canonical basis of master integrals*, *Comput. Phys. Commun.* **219** (2017) 361.

[105] C. Meyer, *Transforming differential equations of multi-loop Feynman integrals into canonical form*, *JHEP* **1704** (2017) 006.

[106] M. Argeri, S. Di Vita, P. Mastrolia, E. Mirabella, J. Schlenk, U. Schubert and L. Tancredi, *Magnus and Dyson Series for Master Integrals*, *JHEP* **1403** (2014) 082.

[107] A. Blondel *et al.*, *Theory report on the 11th FCC-ee workshop*, arXiv:1905.05078 [hep-ph].

[108] E. Chaubey and S. Weinzierl, *Two-loop master integrals for the mixed QCD-electroweak corrections for $H \to b\bar{b}$ through a $Ht\bar{t}$-coupling*, *JHEP* **1905** (2019) 185.

[109] J. Blumlein, D. J. Broadhurst and J. A. M. Vermaseren, *The Multiple Zeta Value Data Mine*, *Comput. Phys. Commun.* **181** (2010) 582.

[110] Afaf Sabry, *Fourth order spectral functions for the electron propagator*, *Nuclear Physics* **33** (1962) 401-430.

[111] R. N. Lee, *Group structure of the integration-by-part identities and its application to the reduction of multiloop integrals*, *JHEP* **0807** (2008) 031.

[112] J. C. Romao and J. P. Silva,*A resource for signs and Feynman diagrams of the Standard Model*, *Int. J. Mod. Phys. A* **27** (2012) 1230025.